

THE ROAD TO THE HYDROGEN FUTURE: RESEARCH & DEVELOPMENT IN THE HYDROGEN PROGRAM

Catherine E. Gregoire Padró
National Renewable Energy Laboratory
1617 Cole Blvd.
Golden, CO 80401

KEYWORDS: hydrogen research; renewable energy; sustainable energy systems

INTRODUCTION

The U. S. Department of Energy (DOE) conducts R&D for the development of safe, cost-effective hydrogen energy technologies that support and foster the transition to a hydrogen economy. Of particular interest is the innovative research supported by the DOE's Hydrogen Program, focused primarily on exploration of long-term, high-risk concepts that have the potential to address large-scale energy needs.

Hydrogen can be produced directly from sunlight and water by biological organisms and using semiconductor-based systems similar to photovoltaics (PV), or indirectly, via thermal processing of biomass. These production technologies have the potential to produce essentially unlimited quantities of hydrogen in a sustainable manner.

Storage of hydrogen is an important area for research, particularly when considering transportation as a major user, and the need for efficient energy storage for intermittent renewable power systems. Although compressed gas and liquid hydrogen storage systems have been used in vehicle demonstrations worldwide, the issues of safety, capacity, and energy consumption have resulted in a broadening of the storage possibilities to include metal hydrides and carbon nanostructures. Stationary storage systems that are high efficiency with quick response times will be important for incorporating large amounts of intermittent PV and wind into the grid as base load power.

In addition to the extensive fuel cell development programs in other offices within DOE, the Hydrogen Program conducts fuel cell research focused on development of inexpensive, membrane electrode assemblies, and the development of reversible fuel cells for stationary applications. The Program also supports research in the development of hydrogen/methane blends and hydrogen-fueled internal combustion engines and generator sets.

A large hurdle to expanded use of hydrogen is public perception. Widespread hydrogen use represents an extraordinary educational challenge, as well as the absolute requirement that safety be intrinsic to all processes and systems. The development of reliable, low-cost hydrogen sensors is an important aspect of the Program, as is the development of codes and standards for the safe use of hydrogen.

DIRECT HYDROGEN PRODUCTION TECHNOLOGIES

The use of solar energy to split water into oxygen and hydrogen is an attractive means to directly convert solar energy to chemical energy. Biological, chemical, and electrochemical systems are being investigated within DOE as long-term (>10 years), high-risk, high-payoff technologies for the sustainable production of hydrogen.

Biological Systems

In nature, algae absorb light and utilize water and CO₂ to produce cell mass and oxygen. A complex model referred to as the "Z-scheme" has been identified to describe the charge separation and electron transfer steps associated with this process that ultimately drives photosynthesis. A number of enzymatic side pathways that can also accept electrons have been identified. Of interest is a class of enzymes known as hydrogenases that can combine protons and electrons obtained from the water oxidation process to release molecular hydrogen. These algal hydrogenases are quickly deactivated by oxygen. Researchers have identified mutant algal strains that evolve hydrogen at a rate that is 4 times that of the wild type, and are 3-4 times more oxygen tolerant [1,2].

Photosynthetic organisms also contain light harvesting, chlorophyll-protein complexes that effectively concentrate light and funnel energy for photosynthesis. These antenna complexes also dissipate excess incident sunlight as a protective mechanism. The amount of chlorophyll antennae in each cell is directly related to the amount of "shading"

experienced by subsequent layers of microorganisms in a mass culture. In a recent set of experiments, researchers have observed that green alga grown under high light intensities exhibit lower pigment content and a highly truncated chlorophyll antennae size. These cells showed photosynthetic productivity (on a per chlorophyll basis) that was 6-7 times greater than the normally pigmented cells [3], a phenomenon that could lead to significant improvements in the efficiency of hydrogen production on a surface-area basis.

These technical challenges are being addressed by a team of scientists from Oak Ridge National Laboratory (ORNL), the University of California Berkeley, and the National Renewable Energy Laboratory (NREL). Various reactor designs are under development for photobiological hydrogen production processes (single-stage vs two-stage, single organism vs dual organism). At the University of Hawaii's Natural Energy Institute (HNEI), a new, potentially low cost, outdoor tubular photobioreactor is under development to test a sustainable system for the production of hydrogen [4].

In addition to the photosynthetic production of hydrogen from water, the Program supports the development of systems to convert CO (found in synthesis gas) to hydrogen via the so-called water-gas shift reaction ($\text{CO} + \text{H}_2\text{O} = \text{CO}_2 + \text{H}_2$). This reaction is essential to the widely-used commercial steam methane reforming process for the production of hydrogen. In the industrial process in use today, high-temperature (450°C) and low-temperature (230°C) shift reactors are required to increase the overall hydrogen production efficiency and to reduce the CO content to acceptable levels. In this project, microorganisms isolated from nature are used to reduce the level of CO to below detectable levels (0.1 ppm) at temperatures of around 25-50°C in a single reactor [5,6]. This process, under development at NREL, has significant potential to improve the economics of hydrogen production when combined with the thermal processing of biomass or other carbon-containing feeds.

Photochemical Systems

Among the technologies that have been investigated, photocatalytic water splitting systems using relatively inexpensive, durable, and nontoxic semiconductor photocatalysts show promise. Supported catalysts such as Pt-RuO₂/TiO₂ have sufficient band gaps for water splitting, although the current rate of hydrogen production from these systems is too low for commercial processes. Modifications to the system are required to address issues such as the narrow range of solar wavelengths absorbed by TiO₂, the efficiency of subsequent catalytic steps for formation of hydrogen and oxygen, and the need for high surface areas. Binding of catalyst complexes that absorb light in the visible range to the TiO₂ should improve the absorption characteristics. Aerogels of TiO₂ as a semiconductor support for the photocatalysts have potential for addressing reaction efficiency and surface area issues. The University of Oklahoma is investigating these systems.

The Florida Solar Energy Center (FSEC), in conjunction with the University of Geneva, is investigating tandem/dual bed photosystems using sol/gel-deposited WO₃ films as the oxygen-evolving photocatalyst, rather than TiO₂. In this configuration, the dispersion containing the wider band gap photocatalyst must have minimal light scattering losses so that the lower band gap photocatalyst behind it can also be illuminated.

Photoelectrochemical Systems

Multijunction cell technology developed by the PV industry is being used to develop photoelectrochemical (PEC) light harvesting systems that generate sufficient voltage to split water and are stable in a water/electrolyte environment. The cascade structure of these devices results in greater utilization of the solar spectrum, resulting in the highest theoretical efficiency for any photoconversion device. In order to develop cost effective systems, a number of technical challenges must be overcome. These include identification and characterization of semiconductors with appropriate band gaps; development of techniques for preparation and application of transparent catalytic coatings; evaluation of effects of pH, ionic strength, and solution composition on semiconductor energetics and stability, and on catalyst properties; and development of novel PV/PEC system designs. NREL's approach to solving these challenges is to use the most efficient semiconductor materials available, consistent with the energy requirements for a water splitting system that is stable in an aqueous environment. To date, a PV/PEC water splitting system with a solar-to-hydrogen efficiency of 12.4% (lower heating value, LHV) using concentrated light, has operated for over 20 hours [7]. HNEI is pursuing a low-cost amorphous silicon-based tandem cell design with appropriate stability and performance, and is developing protective coatings and effective catalysts. An outdoor test of the a-Si cells resulted in a solar-to-hydrogen efficiency of 7.8% LHV under natural sunlight [8].

INDIRECT HYDROGEN PRODUCTION TECHNOLOGIES

These systems offer the opportunity to produce hydrogen from renewable resources in the mid-term (5-10 years). Using agricultural residues and wastes, or biomass specifically grown for energy uses, hydrogen can be produced using a variety of processes.

Biomass pyrolysis produces a bio-oil that, like petroleum, contains a wide spectrum of components. Unlike petroleum, bio-oil contains a significant number of highly reactive oxygenated components derived mainly from constitutive carbohydrates and lignin. These components can be transformed into hydrogen via catalytic steam reforming using Ni-based catalysts. By using high heat transfer rates and appropriate reactor configurations that facilitate contact with the catalyst, the formation of carbonaceous deposits (char) can be minimized. The resulting products from the thermal cracking of the bio-oils are steam reformed at temperatures ranging from 750-850°C. At these conditions, any char formed will also be gasified. At NREL and the Jet Propulsion Laboratory, research and modeling are underway to develop processing technologies that take advantage of the wide spectrum of components in the bio-oil, and address reactivity and reactor design issues [9, 10]. Evaluation of co-product strategies indicates that high value chemicals, such as phenolic resins, can be economically produced in conjunction with hydrogen [11].

Biomass is typically 50 weight % (wt%) moisture (as received); biomass gasification and pyrolysis processes require drying of the feed to about 15 wt% moisture for efficient and sustained operation, in addition to requiring size reduction (particle size of ~1 cm). In supercritical gasification processes, feed drying is not required, although particle size reduction requirements are more severe. A slurry containing approximately 15 wt% biomass (required size reduction ~1 mm) is pumped at high pressure (>22 MPa, the critical pressure of water) into a reactor, where hydrothermolysis occurs, leading to extensive solubilization of the lignocellulosics at just above the supercritical conditions. If heat transfer rates to the slurry are sufficiently high, little char is formed, and the constituents of biomass are hydrolyzed and solubilized in the supercritical medium. Increasing the temperature to ~700°C in the presence of catalysts results in the reforming of the hydrolysis products. Catalysts have been identified that are suitable for the steam reforming operation [12]. HNEL, Combustion Systems Inc., and General Atomics are investigating appropriate slurry compositions, reactor configurations, and operating parameters for supercritical water gasification of wet biomass.

HYDROGEN STORAGE, TRANSPORT, AND DELIVERY

The storage, transport, and delivery of hydrogen are important elements in a hydrogen energy system. With keen interest in mobile applications of hydrogen systems, and as intermittent renewables penetration of the electric grid increases, storage becomes essential to a sustainable energy economy. Light weight and high energy density storage will enable the use of hydrogen as a transportation fuel. Efficient and cost effective stationary hydrogen storage will permit PV and wind to serve as base load power systems.

Compressed Gas Storage Tanks

Currently, compressed gas is the only commercially available method for ambient-temperature hydrogen storage on a vehicle. Compressed hydrogen stored at 24.8 MPa in a conventional fiberglass-wrapped aluminum cylinder results in a volumetric storage density of 12 kg of hydrogen per m³ of storage volume and a gravimetric density of 2 wt% (grams of hydrogen per gram of system weight). Carbon fiber-wrapped polymer cylinders achieve higher densities (15 kg/m³ and 5 wt%), but are significantly below target values required for hydrogen to make major inroads in the transportation sector (62 kg/m³ and 6.5 wt%). Advanced lightweight pressure vessels have been designed and fabricated by Lawrence Livermore National Laboratory [13]. These vessels use lightweight bladder liners that act as inflatable mandrels for composite overwrap and as permeation barriers for gas storage. These tank systems are expected to exceed 12 wt% hydrogen storage (at 33.8 MPa) when fully developed.

Carbon-based Storage Systems

Carbon-based hydrogen storage materials that can store significant amounts of hydrogen at room temperature are under investigation. Carbon nanostructures could provide the needed technological breakthrough that makes hydrogen powered vehicles practical. Two carbon nanostructures are of interest – single-walled nanotubes and graphite nanofibers. Single-walled carbon nanotubes, elongated pores with diameters of molecular dimensions

(12 Å), adsorb hydrogen by capillary action at non-cryogenic temperatures. Single-walled nanotubes have recently been produced and tested at NREL in high yields using a number of production techniques, and have demonstrated hydrogen uptake at 5-10 wt% at room temperature [14]. Graphite nanofibers are a set of materials that are generated from the metal catalyzed decomposition of hydrocarbon-containing mixtures. The structure of the nanofibers is controlled by the selection of catalytic species, reactant composition, and temperature. The solid consists of an ordered stack of nanocrystals that are evenly spaced at 0.34-0.37 nanometers (depending on preparation conditions). These are bonded together by van der Waals forces to form a "flexible wall" nanopore structure. Northeastern University estimates that excellent hydrogen storage capacities are possible in these structures.

Metal Hydride Storage and Delivery Systems

Conventional high capacity metal hydrides require high temperatures (300-350°C) to liberate hydrogen, but sufficient heat is not generally available in fuel cell transportation applications. Low temperature hydrides, however, suffer from low gravimetric energy densities and require too much space on board or add significant weight to the vehicle. Sandia National Laboratories (SNL) and Energy Conversion Devices (ECD) are developing low-temperature metal hydride systems that can store 3-5 wt% hydrogen. Alloying techniques have been developed by ECD that result in high-capacity, multi-component alloys with excellent kinetics, albeit at high temperatures. Additional research is required to identify alloys with appropriate kinetics at low temperatures.

A new approach for the production, transmission, and storage of hydrogen using a chemical hydride slurry as the hydrogen carrier and storage medium is under investigation by Thermo Power Corporation. The slurry protects the hydride from unanticipated contact with moisture and makes the hydride pumpable. At the point of storage and use, a chemical hydride/water reaction is used to produce high purity hydrogen. An essential feature of the process is recovery and reuse of spent hydride at a centralized processing plant. Research issues include the identification of safe, stable and pumpable slurries and the design of an appropriate high temperature reactor for regeneration of spent slurry.

END USE TECHNOLOGIES

Proton exchange membrane (PEM) fuel cells could provide low-cost, high-efficiency electric power, and be operated "in reverse" as electrolyzers to generate hydrogen. There has been a significant increase in industry activity for the development of PEM fuel cells for vehicular applications, with a number of active demonstration projects. Improvements in catalyst loading requirements, water management, and temperature control have helped move these power units from mere curiosities to legitimate market successes. In order to increase the market penetration in both the transportation and utility sectors, additional improvements are required. Los Alamos National Laboratory is developing non-machined stainless steel hardware and membrane electrode assemblies with low catalyst loadings to achieve cost reductions and efficiency improvements [16]. The most important barriers to implementation of low-cost PEM fuel cells are susceptibility of the metal or alloy to corrosion, water management using metal screens as flow fields, and effective stack sealing. Operating the PEM fuel cell "in reverse" as an electrolyzer is possible, but optimum operating conditions for the power production mode and for the hydrogen production mode are significantly different. Design issues for the reversible fuel cell system include thermal management, humidification, and catalyst type and loading.

In an effort to promote near-term use of hydrogen as a transportation fuel, the Program is investigating the development of cost effective, highly efficient, and ultra-low emission internal combustion engines (ICE) operating on pure hydrogen and hydrogen-blended fuels. Research at SNL is focused on the development of a hydrogen fueled ICE/generator set with an overall efficiency of >40% while maintaining near zero NO_x emissions [15].

SAFETY

Hydrogen leak detection is an essential element of safe systems. The development of low-cost fiber optic and thick film sensors by NREL and ORNL, respectively, will provide affordable and reliable options for hydrogen safety systems. NREL is using optical fibers with a thin film coating on the end that changes optic properties upon reversible reaction with hydrogen. Changes in the reflected light signal is an indication of the presence of hydrogen. Sensitivity and selectivity are important research issues. ORNL is focused on the development of monolithic, resistive thick film sensors that are inherently robust,

selective to hydrogen, and easy to manufacture. Research issues include developing appropriate techniques for active (versus traditional passive) thick film applications.

Recognizing the importance of safe use of hydrogen, the DOE, in conjunction with Natural Resources Canada, has compiled a comprehensive document of prevailing practices and applicable codes, standards, guidelines, and regulations for the safe use of hydrogen. The *Sourcebook for Hydrogen Applications* is intended to be a "living document" that can be updated to reflect the current state of knowledge about, and experience with, safely using hydrogen in emerging applications. DOE also supports the development of codes and standards under the auspices of the International Standards Organization.

CONCLUSIONS

The DOE Hydrogen Program conducts R&D in the areas of production, storage, and utilization, for the purpose of making hydrogen a cost-effective energy carrier for utility, buildings, and transportation applications. Research is focused on the introduction of renewable-based options to produce hydrogen; development of hydrogen-based electricity storage and generation systems that enhance the use of distributed renewable-based utility systems; development of low-cost technologies that produce hydrogen directly from sunlight and water; and support of the introduction of safe and dependable hydrogen systems including the development of codes and standards for hydrogen technologies.

REFERENCES

- [1] Ghirardi, M.L., R.K. Togasaki, and M. Seibert, 1997, "Oxygen Sensitivity of Algal Hydrogen Production," *Appl. Biochem. Biotechnol.*, 63-65, 141-151.
- [2] Seibert, M., T. Flynn, D. Benson, E. Tracy, and M. Ghirardi, 1998, "Development of Selection/Screening Procedures for Rapid Identification of Hydrogen-Producing Algal Mutants with Increased Oxygen Tolerance," International Conference on Biological Hydrogen Production, Plenum, NY, in press.
- [3] Melis, A., J. Neidhardt, I. Baroli, and J.R. Benemann, 1998, "Maximizing Photosynthetic Productivity and Light Utilization in Microalgal by Minimizing the Light-Harvesting Chlorophyll Antenna Size of the Photosystems," International Conference on Biological Hydrogen Production, Plenum, NY, in press.
- [4] Szyper, J.P., B.A. Yoza, J.R. Benemann, M.R. Tredici, and O.R. Zaborsky, 1998, "Internal Gas Exchange Photobioreactor: Development and Testing in Hawaii," International Conference on Biological Hydrogen Production, Plenum, NY, in press.
- [5] Maness, P.-C. and P.F. Weaver, 1997, "Variant O₂-Resistant Hydrogenase from Photosynthetic Bacteria Oxidizing CO," Proceedings of the Fifth International Conference on the Molecular Biology of Hydrogenase, Albertville, France.
- [6] Weaver, P.F., P.-C. Maness, and S. Markov, 1998, "Anaerobic Dark Conversion of CO into H₂ by Photosynthetic Bacteria," International Conference on Biological Hydrogen Production, Plenum, NY, in press.
- [7] Khaselev, O. and J.A. Turner, 1998, "A Monolithic Photovoltaic-Photoelectrochemical Device for Hydrogen Production via Water Splitting," *Science*, 280, 425.
- [8] Rocheleau, R., 1998, "High Efficiency Photoelectrochemical H₂ Production using Multijunction Amorphous Silicon Photoelectrodes," *Energy & Fuels*, 12 (1), 3-10.
- [9] Wang, D., S. Czernik, and E. Chomet, 1998, "Production of Hydrogen from Biomass by Catalytic Steam Reforming of Fast Pyrolysis Oil," *Energy & Fuels*, 12 (1), 19-24.
- [10] Miller, R.S. and J. Bellan, 1997, "A Generalized Biomass Pyrolysis Model Based on Superimposed Cellulose, Hemicellulose and Lignin Kinetics," *Comb. Sci. and Techn.*, 126, 97-137.
- [11] Wang, D., S. Czernik, D. Montane, M.K. Mann, and E. Chomet, 1997, "Hydrogen Production via Catalytic Steam Reforming of Fast Pyrolysis Oil Fractions," Proceedings of the Third Biomass Conference of the Americas, Montreal, 845-854.
- [12] Matsunaga, Y., X. Xu, and M.J. Antal, 1997, "Gasification Characteristics of an Activated Carbon in Supercritical Water," *Carbon*, 35, 819-824.
- [13] Miltitsky, F., and B. Myers, and A.H. Weisberg, 1998, "Regenerative Fuel Cell Systems," *Energy & Fuels*, 12 (1), 56-71.
- [14] Dillon, A.C., K.M. Jones, T.A. Bekkedahl, C.H. Kiang, D.S. Bethune, and M.J. Heben, 1997, "Storage of Hydrogen in Single-Walled Carbon Nanotubes," *Nature*, 386, 377-279.
- [15] Van Blarigan, P., 1998, "Advanced Hydrogen Fueled Internal Combustion Engines," *Energy & Fuels*, 12 (1), 72-77.
- [16] Cleghorn, S., X. Ren, T. Springer, M. Wilson, C. Zawodzinski, T. Zawodzinski, and S. Gottesfeld, 1997, "PEM Fuel Cells for Transportation and Stationary Power Generation Applications," *Int. J. Hydrogen Energy*, 23, 1137-1144.

HYDROGEN ENERGY: THE GOOD, THE BAD, AND THE ENVIRONMENTALLY ACCEPTABLE

Clovis A. Linkous
Florida Solar Energy Center
1679 Clearlake Road
Cocoa, FL 32922-5703

ABSTRACT

Hydrogen is in many respects the ultimate fuel: it is the most abundant element in the universe; as a molecular species it possesses the highest gravimetric energy density of any chemical substance; it can be burned cleanly to produce only water as a reaction product; and its simple and rapid electrode kinetics open the possibility of high efficiency fuel cell-driven power trains. On the other hand, as a gaseous substance under standard conditions, it is inconvenient to use as an on-board fuel without severe compromises with respect to distance between refueling stops; rapid rates of effusion and wide combustibility range limits give rise to safety concerns; and finally, under terrestrial conditions, H₂ is seldom found in Nature—it must be derived from other compounds, often at considerable expense. The various aspects of hydrogen energy combine to paint a picture that is compelling but also technologically challenging.

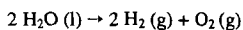
INTRODUCTION

Hydrogen is in many respects the ultimate fuel. First off, it is the most abundant element in the universe. It is estimated that hydrogen makes up 90% of all the atoms or 75% of the mass of the universe. While this fact has little bearing on our current energy economy on Earth, the recent revelation that abundant frozen water deposits may lie below the polar regions of the Moon has galvanized the space technology community over the possibility of producing hydrogen fuel from extraterrestrial sources [1]. While the elemental abundance of hydrogen on earth is also great, almost none of it is found in diatomic molecular form. Free H₂ can be found in the atmosphere at the 0.5 ppm level [2,3], but otherwise it exists principally in combined form with water, biomass, and fossil fuels. H₂ must then be derived from other materials; depending on the source, the energy cost of liberating the hydrogen as H₂ can be quite high, and becomes a major cost component in its manufacture.

For example, H₂ can be had from methane by reaction with steam at 500° C over a Ni catalyst:



The enthalpy of this process per mole of H₂ is only 10.33 kcal, and can be performed with a 65-75% energy efficiency (H₂ heating value out compared to energy input) [4]. In contrast, there is great interest in economically obtaining H₂ directly from liquid water:



Here one is essentially inputting the entire heat of combustion with the hope of getting the free energy back at a later time. The standard enthalpy per mole of H₂ here is 68.3 kcal, a more energetically challenging proposition. Nevertheless, the use of solar based, renewable energy sources to drive the reaction is conceptually very attractive, both from an environmental preservation and a long term sustainability point of view.

While H₂ as a fuel today seems relegated only to certain types of space travel, its energetic nature is in fact greatly in demand as a chemical commodity. US H₂ consumption is already something on the order of 9×10^6 tons/year [5]. Most of this represents internal consumption: the oil refineries account for half of the total, employing it for hydrocracking and hydrodesulfurization; another third is used for ammonia production; much of the remainder is used in methanol production, hydrogenation of polyolefins, and various other chemical and manufacturing processes. The electrolytic production of Cl₂ also yields an equimolar amount of by-product H₂ that is usually used internally for brine concentration or other process heat applications.

Only a few percent of the total is actually sold as a market commodity. Of that, NASA is by far the largest single consumer, requiring some 7000 tons of liquified H₂ per year [5]. Despite its major position in certain industries, annual non-refinery H₂ production (6.7×10^{12} l) represents only 2 day's US gasoline consumption [6].

In Table I, a comparison of relevant fuel properties of H₂ are compared to those of methane, methanol, and gasoline. Many of the superlative characteristics of H₂ are apparent. With the LHV heat of combustion of -57.8 kcal/mol (LHV= lower heating value: product water is left in the vapor state, so that the latent heat of vaporization is not included in the total reaction enthalpy), H₂ is certainly not an exceptional energy producer on a molar basis. However, because it is the lightest element in the Periodic Table, it has a gravimetric energy density of 1.20 x 10⁵ kJ/kg, or 51,590 Btu/lb. This can be compared to jet fuel at about 18,400 Btu/lb, or coal and biomass at 7500 Btu/lb. H₂ has indeed been considered as a substitute for jet fuel: the US Air Force ran Project Bee from 1955-57, where a B-578 twin engine bomber containing a Curtis Wright J-65 turbo-jet engine ran on liquid H₂ [7].

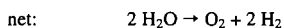
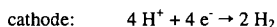
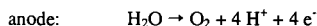
H₂ ELECTROCHEMISTRY

Another asset of H₂ lies in the simplicity of its chemistry. With relatively few bonds being broken and formed, its energy is quickly released. The high intrinsic rate constants enables one to consider the possibility of electrochemically releasing its energy. The exchange current density, or fundamental dynamic charge transfer rate at zero applied voltage, for H₂ discharge on a Pt electrode is 1.0 x 10⁻³ A/cm² [8]. One can operate a continuous flow hydrogen-air electrochemical cell, or fuel cell, by introducing H₂ to the anode or fuel compartment, and air or O₂ to the cathode or oxidant compartment. Product water is exhausted from the cathode compartment. By utilizing gas diffusion electrodes, where the reactant gases penetrate a thin, finely porous, hydrophobic matrix of fluorocarbon polymer, carbon fiber, and supported noble metal catalyst, current densities in the 100's of mA/cm² can be obtained. This translates to a specific power on order of 100 W/kg.

The free energy of reaction is manifested as a voltage that can be used to power an external load. One is then freed from the Carnot efficiency limitations of combustion engines. Fuel cells offer the possibility of obtaining operating fuel efficiencies of 40-50% for vehicular applications. This represents on order of a 50% improvement in fuel efficiency over internal combustion engines. As an example, to match the range of an average-sized vehicle equipped with an IC engine rated at 19 mpg and carrying 111 lb (18 gal) of gasoline, its H₂ fuel cell counterpart would only need to carry 15 lb of H₂ [9].

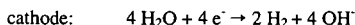
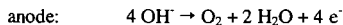
By the same token, one can electrolyze water and produce H₂ by application of a voltage sufficient to exceed its free energy of formation, or 1.23 V:

acidic electrolyte



The mechanism written above assumes an acidic electrolyte. While electrolysis using simple mineral acids is indeed possible, the leading technology at low pH is based on solid polymer electrolytes [10]. Alkaline electrolysis is also possible, and in fact is the most longstanding and least expensive electrolytic technology. The respective half cell reactions then become:

alkaline electrolyte



The energy efficiency of electrolysis is generally taken as 60-80%. These are practical, as opposed to theoretical, values. The basic relationship between current and applied voltage enables one to operate the cell at any desired efficiency. The determining factor is the relationship between current density and capital cost. Smaller voltages make for less energy per volume unit of H₂, but the current density (H₂ evolution rate per unit area) is also less, and so the electrolyzer must be made larger and more costly for a given H₂ production capacity. An can be run at 99% efficiency, but the H₂ output would be so low as to be impractical.

While generally not as economical as steam reforming of natural gas, electrolysis has already carved out various market niches for H₂ production where the cost of electricity is low, the

availability of natural gas is poor, the required H₂ purity is high, or the required production rate is modest (< 10,000 scf/day).

H₂ STORAGE

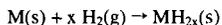
As a gaseous substance under standard conditions, it is inconvenient to use H₂ as an on-board fuel without severe compromises with respect to distance between refueling stops. This is perhaps its greatest limitation, and a large segment of the hydrogen community is committed to increasing the range limits of H₂-fueled travel by reducing the volumetric energy density of the stored material.

The simplest answer is to carry the H₂ as a pressurized gas; unfortunately, the H-content of a standard 2200 psi cast iron vessel is less than one percent [11]. It has been estimated that tank pressure must be increased to >10,000 psi using carbon fiber-reinforced cylinders in order for a H₂-powered vehicle to have the same range as a gasoline-powered one [12].

One can then consider liquifaction as a means of carrying H₂. As a liquid, it has one-tenth the weight of an equal volume of gasoline, but only one-quarter the energy as well. While this represents a tremendous improvement in volumetric energy density over the gaseous state, one should consider that the liquid must be stored at 20.3 K. As a result, vacuum-insulated, stainless steel storage tanks must be used. For vehicles such as NASA's space shuttle, the low surface-to-volume ratio of its 10⁵ plus gallon tanks minimize boil off losses. For domestic transportation, boil-off would be a greater problem, although it is estimated that boil-off could be held to 2% per day [13]. The resulting H-content of an insulated LH₂ storage system would be on order of 20%.

Since the freezing point of H₂ is only 6.5 degrees less than its liquifaction temperature, engineers have sought to increase the LH₂ density by about 15% by mixing solid and liquid to make a slurry, or "slush H₂". It is typically mixed as 50% solids at the triple point of H₂ (13.8 K, 52.8 torr). A further advantage of this approach is that the refrigeration heat capacity is increased by 82.7 kJ/kg, resulting in a 24% increase in the effective heat of vaporization [14,15].

Another way of storing H₂ in the solid state is to combine it with various electropositive metals to form metal hydrides:



There are a number of low molecular weight metal hydrides whose H-contents lie in the 4-7% range, such as CaH₂ and MgH₂. While the numbers may appear low, as noted above, they are well in excess of what can be obtained with conventional pressurized gas cylinder technology. These hydriding reactions are typically exothermic, so that to recover the stored H₂, the hydride must be heated to overcome the enthalpy of formation and shift the equilibrium back toward the free gas. This becomes a problem when the heat of formation of the hydride becomes comparable to the heat of combustion of H₂.

There are some metal alloys for which the hydride heat of formation is low enough that the equilibrium can be controlled at ambient temperature simply by pumping H₂ into and out of the hydride storage bed. Two families of metal alloys that have received much attention are the AB₂'s and the AB₃'s. The former group consists of some combination of low valency first row transition metals, such as Ti, V, and Fe. The latter group is represented by LaNi₅. With H-contents on order of 3%, they represent only a modest improvement over compressed gas. Nevertheless, because of their stability under negative potential in alkaline electrolyte, these materials have attracted great attention in the battery business, where Ni-metal hydride batteries are rapidly replacing Ni-Cd secondaries in high cost portable devices, such as laptop computers.

THE ENVIRONMENTAL IMPERATIVE

The idea of hydrogen energy has been with us since the days of Jules Verne, but events in recent years have begun to stimulate serious public discussion.

One was the push in California to mandate the used of zero emission vehicles. In 1991, California enacted legislation creating a market for clean vehicles that will require significant changes in the automobile of today. A series of categories defining progressively more stringent emissions standards were defined: Transitional Low Emission Vehicles (TLEV); Low Emission Vehicles (LEV); Ultra-Low emission Vehicles (ULEV); and Zero Emission Vehicles (ZEV) [16]. The TLEV will allow hydrocarbon emissions of 0.18 g/mile, 3.4 g/mile of CO, and 0.4 g/mile of NO_x. The ZEV is exactly what it says: 0.0 g/mile for the above pollutants. A H₂-powered fuel

cell vehicle is one of the few that could meet these standards. While the original legislation mandated that by 1998, 2% of all vehicles sold by major automakers must be ZEV's, the California Air Resources Board has since relaxed that requirement until 2003, at which time 10% of sales must qualify [17].

Another recent event is the signing of the Kyoto Protocol. This treaty requires industrialized countries to reduce greenhouse gas emissions on average by 5.2 percent below 1990 levels during the first "commitment period" between 2008 and 2012. There are differentiated targets ranging from 92 and 110 percent of 1990 levels. The US must reduce emissions by 7%. US greenhouse gas emissions in 1990 were estimated at 1.46×10^9 metric tons in carbon equivalent [18].

With the likelihood of future carbon tax assessments, clean burning H_2 is a clear advantage. In truth, H_2 does make for some NO_x formation, as does any fuel using air as oxidant in a combustion process. However, the extent of NO_x formation per energy unit is estimated to be some 80% less than for petroleum-based fuels [19].

SAFE H_2 ?

The H_2 flammability limits vary from 4 to 75% in air, the widest of any fuel. From a safety point of view this is thought to be a negative attribute: leaks that contain H_2 may ignite while other fuels would be too concentrated or too dilute. H_2 detectors should alarm when $[H_2] > 1\%$, at 20-25% lower flammability limit. On the other hand, a plume of H_2 gas leaking into the air quickly rises and dissipates because of its lower density. Engine tolerances must be made more precise to prevent significant blow-by during compression; pronounced "flashback" effects (engine backfire through intake system) require direct cylinder injection.

Just as with natural gas, safety codes will undoubtedly require that an odorant be added to H_2 to alert consumers to leakage. This is a matter of concern to fuel cell manufacturers, who need ultrapure H_2 to prevent poisoning of their noble metal electrocatalysts.

Regardless of the advances made in H_2 energy technology, to achieve widespread acceptance the public image of H_2 must change. Few public conversations on H_2 can go for very long without mention of the either the Challenger space shuttle or Hindenburg disasters. Recently, research by A. Bain has shown that the shell material of the Hindenburg was sufficiently flammable that it would have burned even if the dirigible had been filled with helium [20]. Indeed, there have been less publicized instances where He-filled balloons have caught fire. Burning H_2 produces a largely transparent flame, so that hydrogen's role in the enormous conflagration caught on film in 1937 could only have been indirect.

The economics of H_2 transport basically follow that of natural gas: for many users at close distance, pipeline is the preferred way of transporting H_2 ; for few users at longer distance, liquifaction is cheaper. Much effort has gone into determining whether the existing natural gas pipeline network could some day be used for transporting H_2 . The ability of H_2 to penetrate and embrittle metallic parts is a matter of concern. Carbon steel is embrittled by H_2 , making it more susceptible to stress fractures. The general view is that at modest pressures (< 700 psi) H_2 would be compatible; at higher pressure, seamless stainless steel piping would be necessary [4]. Actually, some 500 miles of pipelines dedicated to H_2 transport currently exist worldwide, with major concentrations in Germany's Ruhr Valley and near LaPorte, Texas [21].

CONCLUSION

While most consider H_2 to be a fuel of the future, it is actually all around us today as a basic chemical commodity. It will always be there when we need it, first from fossil fuels, then biomass, and finally from water. The obvious gravimetric advantage is tempered by its gaseous state. A number of storage technologies offer trade-offs between weight and volume. The simplicity of its chemistry invites the more efficient electrochemical option. Its widespread implementation may ultimately hinge on what levels of air quality our society is willing to accept.

ACKNOWLEDGEMENT

The author would like to thank the many co-workers at the Florida Solar Energy Center who assisted in the preparation of this report, as well as the U.S. Department of Energy, Office of Solar Thermal, Biomass Power, and Hydrogen Technologies, for their financial support.

REFERENCES

- 1- R.A. Kerr, Science, 1998, Vol. 279, 1628.
- 2- W. Zittel and M. Altmann, "Molecular Hydrogen and Water Vapour Emissions in a Global Hydrogen Energy Economy," Hydrogen Energy Progress XI, proceedings of the 11th World Hydrogen Energy Conference, T.N. Veziroglu, C.-J. Winter, J.P. Baselt, and G. Kreysa, eds, Schön and Weitzel GmbH, Frankfurt am Main, 1996, p. 71-81.
- 3- D.R. Lide, ed., CRC Handbook of Chemistry and Physics, 74th edn, CRC Press, Boca Raton, 1974, p. 4-14.
- 4- R.L. Mauro, "The Hydrogen Technology Assessment, Phase I," National Hydrogen Association, Washington, DC, 1994.
- 5- J.R. Birk, B. Mehta, A. Fickett, R. Mauro, and F. Serfass, Hydrogen Energy Progress IX, additive, proceedings of the 9th World Hydrogen Energy Conference, International Association of Hydrogen Energy, p. 101.
- 6- R.L. Bechtold, Alternative Fuels Guidebook. Properties, Storage, Dispensing, and Vehicle Facility Modifications, Society of Automotive Engineers, Warrendale, PA, 1997.
- 7- J.L. Sloop, "Liquid H₂ as a Propulsion Fuel," NASA report SP4404, 1978.
- 8- J.O'M. Bockris and S. Srinivasan, "Electroodic Reactions of Oxygen," ch. 8 in Fuel Cells, McGraw-Hill, New York, 1968.
- 9- "Feasibility Study of Onboard Hydrogen Storage for Fuel Cell Vehicles," US Department of Energy, Office of Transportation Technologies, January, 1993.
- 10- A.B. LaConti, A.R. Fragala, and D.L Smith, in "Proceedings of the Symposium on Electrode Materials and Processes for Energy Conversion and Storage," J.D.E. McIntyre, S. Srinivasan, and F.G. Will, eds., The Electrochemical Society, Inc., Pennington, NJ, 1977.
- 11- A.J. Appleby, "Fuel Cells and Hydrogen Fuel," Hydrogen Energy Progress IX, proceedings of the 9th World Hydrogen Energy Conference, Paris, France, June 22-25, 1992, T.N. Veziroglu, C. Derive, and J. Pottier, eds, MCI, Paris, 1992, p. 1375-1383.
- 12- D.L. Block, S. Dutta, and A. T-Raissi, "Storage of Hydrogen in Solid, Liquid, and Gaseous Forms," Florida Solar Energy Center, FSEC-CR-204-88, June, 1988.
- 13- W. Strobl and W. Peschka, "Liquid Hydrogen as a Fuel of the Future for Individual Transport," BMW AG Presse, Munich, Germany.
- 14- Fujiwara, M. Yatabe, H. Tamura, M. Takahashi, J. Miyazaki, and Y. Tsuruta, Int. J. Hydrogen Energy, Vol 23, (1998) 333-338.
- 15- R.L. Mauro, "The Hydrogen Technology Assessment, Phase III," National Hydrogen Association, Washington, DC, 1994.
- 16- D.L. Smith, "Strategy for Fuel Cells in Vehicles," National Hydrogen Association, Washington D.C., March 4, 1994, p. 1.
- 17- "Guide to Alternative Fuel Vehicle Incentives and Laws," 2nd edition, November, 1996, U.S. Department of Energy, Clean Cities Program.
- 18- B. Hileman, Chemical and Engineering News, Vol. 74, Jan. 15, 1996.
- 19- "Liquid Hydrogen Powers Third EQHPPP Demonstration Bus," Hydrogen and Fuel Cell Letter, P. Hoffmann, ed., Vol. 11, No. 5, May 1996, p. 4.
- 20- M. DiChristina, Popular Science, November 1997, p 71-76.
- 21- "Direct-Hydrogen-Fueled Proton-Exchange-Membrane Fuel Cell System for Transportation Applications," C.E. Thomas, Directed Technologies, Inc., Department of Energy, DOE/CE/50389-502.

Table I. Selected Fuel Properties of Hydrogen, Methanol, and Gasoline

property	hydrogen	methane	methanol	gasoline
molecular weight (g/mol)	2.018	16.043	32.042	100-105
carbon content (wt %)	0	75	37.5	85-88
specific gravity	0.0838 g/l (g) 0.070 g/cm ³ (l)	0.6512 g/l (g) 0.466 g/cm ³ (l)	0.796	0.69-0.79
boiling point (°C)	-252.87	-162	65	27-225
heat of combustion (HHV, kcal/mol)	68.3	212.9	173.5	1307
lower flammability limit (vol %)	4.1	5	7.3	1.4
upper flammability limit (vol %)	75	15	36	7.6
diffusion coefficient (cm ² /s) STP in air	0.61	0.16	-	0.05

HYDROGEN PRODUCTION FROM HIGH MOISTURE CONTENT BIOMASS IN SUPERCRITICAL WATER

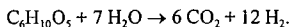
Michael Jerry Antal, Jr. and Xiaodong Xu

Hawaii Natural Energy Institute

University of Hawaii at Manoa, Honolulu, HI 96822

INTRODUCTION

The goal of this work is to define conditions which enable the steam reforming of biomass (represented below as cellulose $C_6H_{10}O_5$) to produce hydrogen:



Earlier work has shown that when biomass is heated quickly in water above its critical pressure, no char is formed. Instead, the biomass decomposes into simple organic molecules dissolved in the water, which further decompose to hydrogen, carbon dioxide, and some methane when exposed to a carbon catalyst at temperatures above 600 °C. In this paper we detail the conditions which evoke the biomass steam reforming chemistry, and we offer insight into the influence of the reactor's wall on the product distribution.

APPARATUS AND EXPERIMENTAL PROCEDURES

The two flow reactors (see Figures 1 and 2) used in this work are fabricated from Hastelloy C276 tubing with 9.53 mm OD x 6.22 mm ID x 1.016 m length. The reactant flow is quickly heated by an annulus heater (located along the reactor's centerline) and an entrance heater outside the reactor to temperatures as high as 800 °C. The annulus heater (3.18 mm OD x 15.2 cm heated length) delivers all its heat directly to the feed. The entrance heater is made from a split stainless steel tube that is held in good thermal contact with the reactor, and an electrical heater which is coiled around the outer surface of the stainless steel tube. Downstream of the entrance heater, the reactor's temperature is maintained in an isothermal condition by the furnace. The chief purpose of the furnace is to prevent heat loss. In fact, in some experiments the temperature setpoint of the furnace was below the lowest temperature measured along the reactor wall. Carbon catalyst is usually packed in about 60% of the heated zone of the reactor, as well as the downstream cold section of the reactor. The reactor's temperature profile is monitored by 12 fixed, type K thermocouples held in good thermal contact with the reactor along its outer wall. Also, in reactor #1 the reactant temperature is measured by a fixed, internal, annulus thermocouple which is located 5.08 cm upstream of the furnace (see Figure 1). Pressure in the reactor is measured by an Omega PX302 pressure transducer. A Grove Mity-Mite model 91 back-pressure regulator reduces the pressure of the cold, two phase, product effluent from 28 to 0.1 MPa. After leaving the back-pressure regulator, the reaction products pass through a gas-liquid separator. The liquid product is collected over a measured time period to calculate the liquid outlet flow rate. The gas flow rate is measured using a wet test meter.

The feeder consists of a cylinder, a movable piston, and two end-caps (High Pressure Equipment). The cylinder is first filled with the feedstock, then the piston is placed on top of the feed, and the two end-caps are installed. Both the feeder and the reactor are pressurized separately to 28 MPa at the beginning of a run. During the time that the system is being brought up to temperature, water is pumped into the reactor by a Waters 510 HPLC pump. When the main body of the reactor reaches the desired temperature (usually about 650 °C), the feeder is connected to the reactor. Thereafter, water flow to the reactor is terminated, and water flow to the feeder is initiated, displacing the sawdust paste feedstock into the reactor. Because the thermophysical properties of the paste are considerably different than those of water, and possibly also because of exothermic pyrolysis reactions associated with the decomposition of the paste, the temperature of the feed rises very rapidly in the entrance region of the reactor. To avoid excessively high temperatures, usually it is necessary to reduce the heat input to the feed from the annulus heater and the entrance heater.

RESULTS

In earlier work we reported the ease of gasification of glycerol in supercritical water. Table 1 confirms the earlier result. In it we see that the hydrogen content of the gas increases from 38% to 51% after 3.45 hr, while the methane content decreases from 20% to 11%. During this time the total gas yield increased from 1.18 to 1.6 L/g and all the carbon in the feedstock was converted to gas. The increasing gas yield is due to the consumption of water and methane by the steam reforming reaction. Evidently this reaction is catalyzed by the reactor's wall and/or the carbon catalyst, which become more active (i.e. "seasoned") as time passes. When the gas yield reached a steady state, the feed was switched and sawdust paste was fed to the reactor for 4

hours. After this, glycerol was again fed to the reactor. Table 1 shows that the sawdust paste causes the reactor's wall and/or the carbon catalyst to lose some activity towards the steam reforming reaction.

The waste product generated by the commercial production of biodiesel fuel contains glycerol and methanol. We prepared a mixture of these two alcohols with a composition identical to that of the industrial waste. The gas produced from this mixture (see Table 2) is very rich in hydrogen, and the yield (2.05 L/g) is high. The water leaving the reactor was clean with a pH of 4-5. Evidently, this waste product is a perfect feedstock for hydrogen production.

As mentioned earlier, we prepare a sawdust paste by mixing wood sawdust into a starch gel, and this paste is easily fed to our reactors. Large quantities of wood sawdust are available at \$30 per dry ton, and the quoted price of corn starch in bulk is \$0.12 per pound. Using these values, the price of a 10 wt % sawdust, 3.65 wt % starch paste is \$0.043 per pound. Similarly, the price of a 20 wt % sawdust, 3.65 wt % starch paste is \$0.031 per pound. For comparison, the price of low sulfur coal is about \$0.025 per pound.

Sawdust paste gasification results from three consecutive runs (no intervening experiments) on different days are displayed in Table 3. In all 3 cases, the reactor plugged after 2 to 3 hours on stream. Although the measured temperatures were similar on 3 and 10 July, the gas yield increased from 1.61 to 2.18 L/g, and the hydrogen content of the gas increased from 43 to 57%. Because fresh carbon catalyst was employed with each experiment, we assumed that the increase in gas yield was due to a seasoning effect of the high temperature in the entrance region on the reactor's wall. To see if the seasoned wall would provide a high gas yield at lower temperatures, we employed a lower entrance temperature in the next experiment (21 July). Remarkably, the results were effectively identical to those of the first experiment. This result, and others indicate that high temperatures are requisite to achieve high gas yields with high hydrogen concentrations from wood sawdust.

CONCLUSIONS

1. A semi-solid gel can be made from 4 wt % (or less) corn starch in water. Wood sawdust and other particulate biomass can be mixed into this gel and suspended therein, forming a thick paste. This paste is easily delivered to a supercritical flow reactor by a cement pump.
2. Above the critical pressure of water, wood sawdust can be steam reformed over a carbon catalyst to a gas composed entirely of hydrogen, carbon dioxide, methane, and a trace of carbon monoxide. There are effectively no tar or char byproducts. The liquid water effluent from the reactor has a low TOC value, a neutral pH, and no color. This water can be recycled to the reactor.
3. The wall affects the gasification chemistry. Products from wood sawdust paste gasification decrease the activity of the wall towards hydrogen production by improving methane yields. These wall effects are strongly temperature dependent. High entrance temperatures strongly favor the methane steam reforming reaction and result in the production of a hydrogen rich gas.

ACKNOWLEDGMENTS

This work was supported by NREL/DOE under cooperative agreement DE-FG36-94AL85804, and the Coral Industries Endowment of the University of Hawaii at Manoa. We thank for useful advice, and Neil Rosmeissl (DOE), Dr. Patrick Takahashi, and Dr. Richard Rocheleau (UH) for their interest in this work. We also thank Jose Arteiro (UH) for assistance with the experiments, Prof. Don Scott (U. Waterloo), Prof. Esteban Chomet (U. Sherbrooke), Prof. Jefferson Tester (MIT), Dave Nahmias, and William Hauserman, Prof. Angela Garcia (University of Alicante), and Professor Galen J. Suppes (University of Kansas) for useful advice.

Table 1. Gas composition from glycerol gasification in supercritical water at 28 MPa with coconut shell activated carbon catalyst using reactor #2 (exp. date: 2/19/98).

Feedstock	18.72 wt% glycerol in water				
Reactor peak temp / Catalyst bed temp	560°C/ 665°C				
Flow rate (g/min)	2.0				
Time on stream (hr)	Before paste ¹				After paste ²
	1.32	2.08	2.55	3.45	5.48
Product	Mole fraction				
H ₂	0.38	0.46	0.51	0.51	0.48
CO	0.02	0.03	0.03	0.03	0.03
CO ₂	0.35	0.33	0.31	0.32	0.32
CH ₄	0.20	0.13	0.12	0.11	0.16
C ₂ H ₆	0.05	0.04	0.04	0.03	0.01
Total gas yield (L gas / g of organics)	1.18	1.40	1.49	1.60	1.60
(g gas / g of organics)	1.01	1.11	1.13	1.18	1.17
C efficiency	0.96	1.00	1.00	1.01	1.01
Global mass balance	0.99	1.01	1.01	1.02	1.02

1. Poplar wood sawdust/corn starch paste was fed to the reactor for 4 hours after the gas generation from glycerol reached a steady state.
2. Glycerol was fed to the reactor again after the reactor plugged with the sawdust/corn starch paste.

Table 2. Gas composition from gasification of glycerol/methanol mixture in supercritical water at 28 MPa with coconut shell activated carbon catalyst using reactor #2 (exp. date: 3/13/98).

Feedstocks	Simulated biodiesel waste product			
Reactor peak temp / Catalyst bed temp	730°C/ 720°C			
Flow rate (g/min)	2.0			
Time on stream (hr)	0.42	0.73	1.25	1.68
Product	Mole fraction			
H ₂	0.64	0.64	0.65	0.64
CO	0.05	0.05	0.05	0.05
CO ₂	0.21	0.21	0.21	0.21
CH ₄	0.10	0.10	0.10	0.10
Total gas yield (L gas / g of organics)	2.05	2.05	2.05	2.05
(g gas / g of organics)	1.25	1.22	1.24	1.20
C efficiency	1.05	1.03	1.04	1.01
H efficiency	1.43	1.41	1.44	1.38
O efficiency	1.36	1.32	1.35	1.31
H balance	1.04	1.03	1.04	1.03
O balance	0.99	0.98	0.99	0.98
Global mass balance	0.98	0.97	0.98	0.97

Table 3. Gas composition from poplar wood sawdust / corn starch gasification in supercritical water at 28 MPa with coconut shell activated carbon catalyst on different dates using reactor #1.

Experiment date	7/3/97	7/10/97	7/21/97
Feedstocks (dry basis)	10.72 wt% sawdust/ 4.01 wt% corn starch	11.17 wt% sawdust/ 4.19 wt% corn starch	11.1 wt% sawdust/ 4.15 wt% corn starch
Reactor peak temp / Catalyst bed temp	790°C/ 685°C	790°C/ 700°C	732°C/ 690°C
Flow rate (g/min)	2.0		
Time on stream (hr)	1.62	1.52	1.42
Product	Mole fraction		
H ₂	0.43	0.57	0.45
CO	0.03	0.04	0.03
CO ₂	0.38	0.33	0.38
CH ₄	0.17	0.06	0.15
C ₂ H ₆	0.001	0.001	0.0
Total gas yield (L gas / g of organics)	1.61	2.18	1.57
(g gas/ g of organics)	1.37	1.65	1.48
C efficiency	0.96	1.01	1.01
Global mass balance	1.01	1.00	0.99

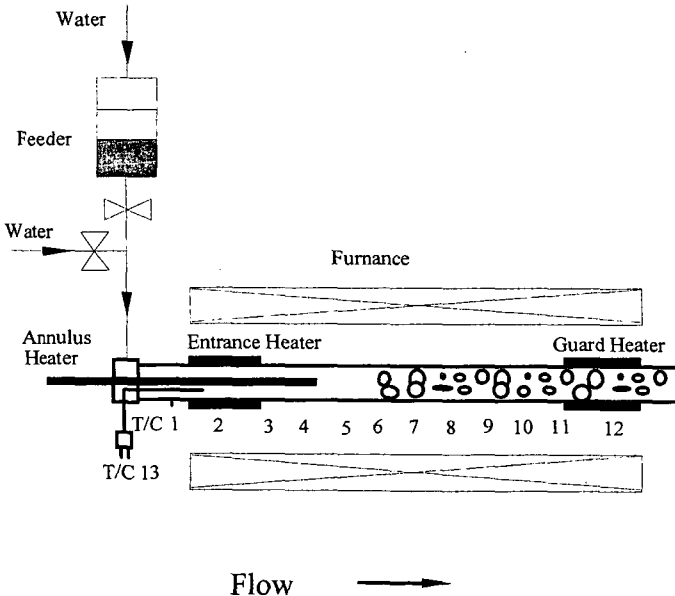


Figure 1. Reactor #1.

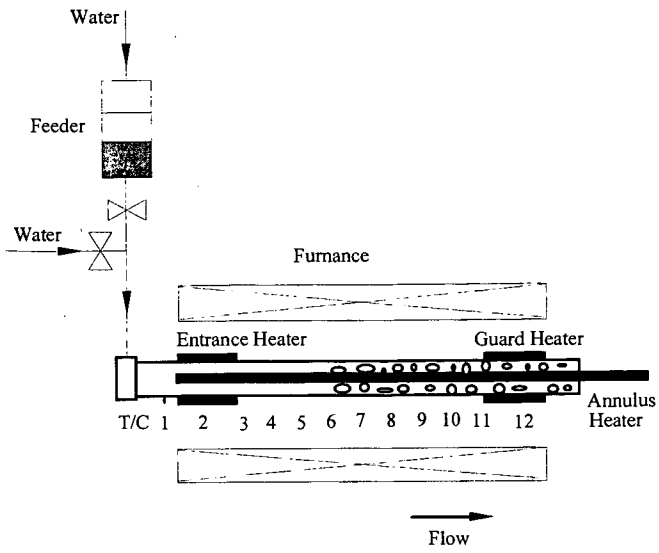


Figure 2. Reactor #2.

DEVELOPMENT OF HYDROGEN STORAGE SYSTEMS BASED ON GRAPHITE NANOFIBERS

C. D. Tan, R. Hidalgo, C. Park and N. M. Rodriguez
Chemistry Department, Hurtig Hall,
Northeastern University, Boston, MA 02115

KEYWORDS: HYDROGEN STORAGE, GRAPHITE NANOFIBERS, CARBON NANOSTRUCTURES

INTRODUCTION

The ever growing demand for energy, as well as the increase in environmental concerns, are exerting pressure for the development of cleaner fuels and more efficient engines. The conventional internal combustion engine currently used in most automobiles produces an array of pollutants including, particulate materials, nitrogen oxides, sulfur oxides, hydrocarbons and carbon monoxide as well as large amounts of carbon dioxide. Although reduction of toxic emissions has been achieved to some degree by the use of the catalytic converter unit, this approach puts great demands on supported noble metal systems, which are required to operate with maximum efficiency over extreme temperature ranges (1).

It has been predicted that oil reserves will peak in about 15 years and therefore, in order to sustain the energy demand it is necessary to find new fuels and more efficient processes. A new technology that is becoming the subject of increasing research effort, is that of fuel cells. In this method, direct conversion from chemical into electrical energy is realized, and consequently, the efficiency of the process is enhanced by almost a factor of three over that of the conventional internal combustion engine, where most of the energy is wasted as heat. Hydrogen and oxygen are the essential reactants for the PEM fuel cells that are being developed for electric vehicles (2,3). A number of factors contribute to the choice of hydrogen as a fuel, not least being the fact that it is one of the most abundant elements found in nature and during its reaction with oxygen the only product is water. Unfortunately, due to the lack of a suitable storage system and a combination of both volume and weight limitations, the driving range of electric vehicles is restricted to about 100 miles. This is one of the shortcomings that has prevented this very promising technology from reaching the commercial arena.

Currently, four methods are being considered for hydrogen storage in commercial applications; pressurized gas storage, liquefied hydrogen, selected metal hydrides and refrigerated super-activated carbon. Pressurized gas offers the advantage of being simple, however, in mobile applications the large volume coupled with the small capacity (8.7 wt. % at 5,000 psi and 7.6 wt. % at 10,000 psi) will limit its practicality. Liquefied hydrogen is expensive since it requires constant refrigeration and loss of the gas by evaporation is inevitable. While the latter two approaches may offer benefits over the other technologies with regard to safety aspects, they do however, have their own set of associated drawbacks. Metal hydrides are heavy, expensive, release heat during the hydrogen absorption process (4) and require the use of about one third of the stored energy during the release of the hydrogen fuel.

Because of their extremely high surface area, active carbons constitute without any doubt the preferred adsorbent in many processes (5-8). Carbon molecular sieves have been known for several decades (9-15) and present an alternative choice for many commercial gas separation processes. These structures are produced from a variety of carbonaceous solids of different origins, including active carbons, cokes, and chars. Activated carbons possess a wide pore size distribution, where the fraction of micro- and nanopores is rather small. While these materials are very effective for the adsorption of a variety of molecules, one has to consider that the interaction between the adsorbent and the adsorbate is only of a physical nature, and as a consequence, the retention of gases is only achieved at extremely low temperatures. The use of activated carbons for gas storage at high temperatures has been found to be ineffective since the solid takes up storage volume without appearing to add any substantial benefits to the overall capacity.

In more recent years there has been a growing interest in the effects of confinement and the influence of the walls of the solid on the gas adsorption process. Indeed, theoretical studies carried out by Gubbins (16-18) using modern statistical mechanic fluids theory indicate that when fluids are restricted within narrow pores, their behavior does not conform to that predicted by classical thermodynamic methods. Non local density functional theory method calculations and molecular simulations have been employed to determine the optimum pore size of carbons for gas adsorption and it was concluded that the ideal system consisted of slit pores bounded by parallel single layers of graphite (16). One of the reasons for this requirement is that in such a configuration, the solid will exhibit the highest ratio of nanopore volume to total volume and as a consequence void space will be eliminated.

In addition, since adsorption of gas molecules on the wall of the pore can cause profound perturbations in the system it is perhaps this aspect that might allow retention of the adsorbate at higher temperatures and at low pressures. It is well known that certain solids, particularly metals, chemisorb gases at room temperature and indeed, this property is routinely used to determine the metal surface area in supported catalyst systems (19). In contrast to physical adsorption, chemisorption requires energy in order to release the adsorbed molecules.

Graphite, is a layered solid in which the various planes are bonded by van der Waals forces where the minimum distance possible between the carbon layers for single crystal graphite is 0.335 nm. In this crystalline structure delocalized π -electrons form a cloud above and below the basal plane and it is this arrangement that imparts a certain degree of metallic character to the solid that results in a relatively high electrical conductivity across each carbon layer. The interlayer spacing in graphitic materials is a property dependent on a number of parameters including, the nature and the thermal history of the precursor, and can vary between 0.335 and 0.342 nm, which by appropriate intercalation procedures can be expanded up to values of 0.9 nm (20,21). Unfortunately, in its conventional form of flat sheets, graphite has an extremely low surface area (~ 0.5 m²/g) resulting from the very small number of edges that are exposed and this aspect has tended to limit its usefulness as a practical selective adsorption agent for small diameter molecules due to diffusion restrictions.

Graphite nanofibers, GNF, are a novel material that has been developed in our laboratory from the metal catalyzed decomposition of certain hydrocarbons (22,23). These structures possess a cross-sectional area that varies between 5 to 100 nm and have lengths ranging from 5 to 100 μ m (24). High-resolution transmission electron microscopy studies have revealed that the nanofibers consist of extremely well-ordered graphite platelets (25), which are oriented in various directions with respect to the fiber axis. The arrangement of the graphene layers can be tailored to a desired geometry by choice of the correct catalyst system and reaction conditions, and it is therefore possible to generate structures where the layers are stacked in a "ribbon", "herringbone", or "parallel" orientation.

EXPERIMENTAL

Synthesis and Characterization of Graphite Nanofibers

GNF were prepared from the decomposition of ethylene, carbon monoxide and hydrogen mixtures over selected metal powders at temperatures between 500 and 700°C as described in previous publications (22,23). The solids were demineralized by immersing them in a mineral acid solution for a period of a week, washed and dried before testing. GNF were examined by high resolution transmission electron microscopy, temperature programmed oxidation, X-ray diffraction and nitrogen adsorption techniques.

Hydrogen Adsorption/Desorption

Hydrogen adsorption experiments were performed in a custom built unit that consists of two stainless steel vessels. The sample vessel, which is 100 cm³ in volume is connected to the hydrogen reservoir vessel via a high pressure bellows valve. GNF are loaded in the sample container and the entire system evacuated in an oil free

environment for about 5 hours at 150°C. The connecting valve is then closed and the sample cooled to room temperature for several hours. Hydrogen is permitted to enter the reservoir vessel and the pressure allowed to reach thermal equilibrium over a two hour period. The connecting valve is then opened and hydrogen immediately gains access to the sample and undergoes adsorption at room temperature. Blank experiments to determine the various parameters involved during gas expansion were conducted in the absence of GNF and also in the presence of other solids. Approximately 1 gram of GNF was placed in the adsorption unit and allowed to react with hydrogen at 1800 psi at room temperature for a several hours. Changes in pressure were carefully monitored as a function of time. Following adsorption hydrogen was allowed to exit the system and the volume carefully measured by displacement of water. Throughout these processes the adsorption unit was continuously monitored with a high sensitivity H₂ detector to ensure a complete absence of leaks in the system.

RESULTS

TEM examinations of the carbon deposited during the catalytic formation of GNF indicated that under the conditions described above, nanofibers were the only product of the reaction, with no other forms of carbon being present. A high resolution transmission micrograph of the typical appearance of the nanofibers is presented in Figure 1a, where the graphene layers that are separated at a distance of ~ 0.34 nm can be observed. A schematic rendition illustrating the arrangement of graphite platelets within the structure is shown in Figure 1b.

When samples of catalytically grown GNF were placed in the adsorption unit, hydrogen uptake to unprecedented levels was obtained. Certain types of graphite nanofibers were found to be capable of adsorbing and storing extremely high quantities of hydrogen at room temperatures in amounts that were over an order of magnitude higher than that found with conventional materials such as metal hydrides (26). Figure 2 shows two typical isotherms for the adsorption of the hydrogen over a selected sample of GNF. Following the first adsorption, hydrogen was released from the sample and a second adsorption was carried out. Based on the pressure drop of the second uptake it is estimated that this sample of GNF adsorbs over 40 wt % of hydrogen.

DISCUSSION

The extraordinary hydrogen adsorption behavior exhibited by GNF is believed to be due to the unique structure of this molecularly designed solid. The material consists of graphite platelets possessing a small cross-sectional area, which is estimated to be on average 20 nm, combined with an abundance of exposed edges. In addition, since hydrogen possesses a kinetic diameter of 0.289 nm, a value slightly smaller than that of the interlayer spacing in graphite nanofibers, 0.342 nm as measured by X-ray diffraction, adsorption occurs due to the gas being able to readily gain access to the inner regions of the solid. Another aspect of significance in this regard is that the solid consists entirely of non-rigid wall nanopores that extend across the nanofiber.

Following adsorption we found that a significant amount of hydrogen was still retained within the structure and the presence of this stored gas caused the lattice to expand as determined by X-ray diffraction. This finding leads us to conclude that during the adsorption process, the GNF lattice expands in order to accommodate a multi-layer configuration of H₂.

The interaction of hydrogen with graphite surfaces has been investigated using various techniques including neutron scattering (27). It has been concluded that a commensurate $\sqrt{3} \times \sqrt{3}$ structure is achieved at low coverage and an incommensurate layer is observed at monolayer coverage. Following the formation of a second monolayer, a lattice parameter of 0.35 nm is observed. This value is smaller than the measured bulk hexagonal closed packed of 0.376 nm, which suggests that the presence of graphite causes hydrogen to adopt an unusually highly packed structure, thus accounting for the high storage levels measured in the current experiments.

ACKNOWLEDGMENTS

Financial support was provided by the United States Department of Energy, Grant number DE-FC36-97GO10235

REFERENCES

1. K. C. Taylor, in *Automobile Catalytic Converters*, Springer-Verlag, New York, p. 120 (1984).
2. A. J. Appleby and F. R. Foulkes, *Fuel Cell Handbook*, (Van Nostrand) 1989.
3. K. V. Kordesch and G. R. Simader, *Cgem. Rev.* 25, 191 (1995)
4. F. E. Lynch, *J. Less Common Metals* 172, 943 (1991).
5. J. S. Noh, R. K. Agarwal and J. A. Schwarz, *Int. J. Hydrogen Energy*, 12, 693 (1987).
US Patent 4,960,450 (1990).
6. J. S. Mattson and H. B. Mark, Jr., "Activated Carbons" Dekker, New York, 1971.
7. B. R. Puri, in "Chemistry and Physics of Carbon" (P. L. Walker, Jr., Ed.) Dekker, New York, 8, 191 (1970).
8. T. Wigmans, in "Carbon and Coal Gasification" (J. L. Figueiredo and J. A. Moulijn, Eds.) NATO ASI Series No.105, Martinus Nijhoff Publ. Dordrecht, p. 559 (1986).
9. Walker, P. L., Jr., Austin, L. G., and Nandi, S. P., in "Chemistry and Physics of Carbon", (P. L. Walker, Jr., ed.) Vol. 2, p. 257, Marcel Dekker, New York (1966).
10. Koresh, J., and Soffer, A., *J. C. S. Faraday 1*, 76, 2457, 2472 (1980).
11. Koresh, J., and Soffer, A., *J. C. S. Faraday 1*, 77, 3005 (1981).
12. Kapoor, A., and Yang, R. T., *Chem. Eng. Sci.* 44, 1723 (1989).
13. Walker P. L., Jr., *Carbon* 28, 261 (1990).
14. Cabrera, A. L. Zehner J. E., Coe, C. G., Gaffney, T. R., Farris, T. S. and Armor, J. N., *Carbon* 31, 969 (1993).
15. Hynek, S, Fuller, W. and Bentley, J. *Int. J. Hydrogen Energy*, 22, 601 (1997)
16. R. F. Cracknell, K. E. Gubbins, M. Maddox and D. Nicholson, *Accounts of Chemical Research*, 28, 281 (1995)
17. C. Rhykerd, Z. Tan L. A. Pozzhar and K. E. Gubbins, *J. Chem. Soc. Faraday Trans*, 87 2011 (1991)
18. P. B. Balbuena, and K. E. Gubbins, *Langmuir*, 8 1801 (1993)
19. J. R. Anderson, "Structure of Metallic Catalysts" Academic Press, New York, 1975.
20. M. S. Dresselhaus, G. Dresselhaus, K. Suguhara, I. L. Spain, and H. A. Goldberg, "Graphite Fibers and Filaments", Springer-Verlag, Berlin, 1993.
21. M. S. Dresselhaus, and G. Dresselhaus, *Adv. Phys.* 30, 139 (1981).
22. R. T. K. Baker and N. M. Rodriguez, U.S. Patent 5,149,584.
23. M. S. Kim, N. M., Rodriguez and R. T. K. Baker, *J. Catal.* 131, 60 (1991).
24. N. M. Rodriguez, *J. Mater. Res.* 8, 3233 (1993).
25. N. M. Rodriguez, A. Chambers and R. T. K. Baker, *Langmuir* 11, 3862 (1995).
26. C. Park, A. Chambers, R. T. K. Baker and N. M. Rodriguez, *J. Phys. Chem.* in press.
27. M. Nielsen in "Phase Transitions in Surface Films" edited by J.G. Dash and J. Ruvalds. Plenum Press, NY 1980.

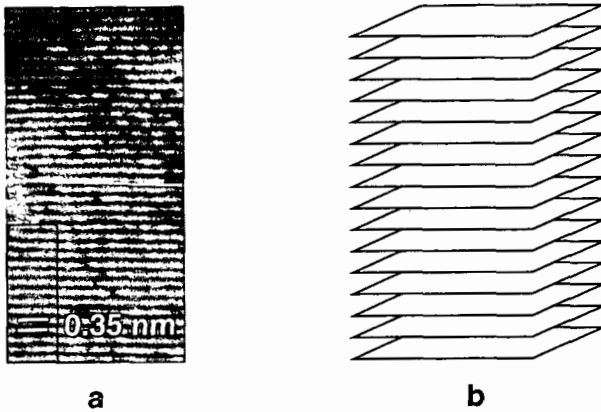


Figure 1. (a) Transmission electron micrograph showing the appearance of a graphite nanofiber produced from the interaction of an iron-based catalyst with carbon containing gases; (b) schematic representation of the arrangement of graphite platelets within GNF marked in a.

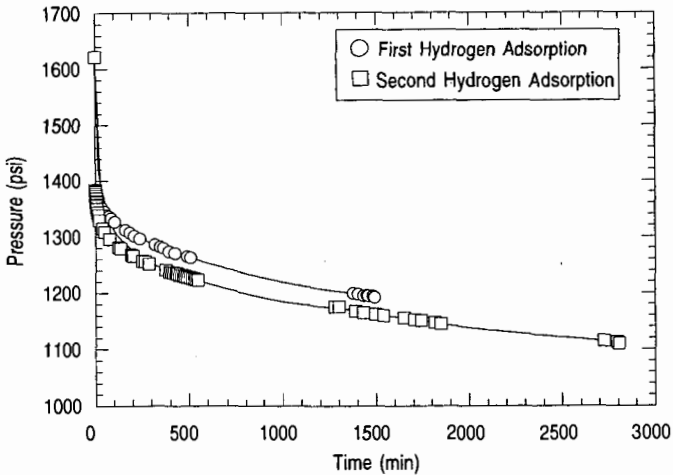


Figure 2. Change in hydrogen pressure as a function of time in the presence of 1.1285 g of GNF at room temperature.

AN OPTIMIZED ALTERNATIVE MOTOR FUEL FORMULATION:
NATURAL GAS LIQUIDS, ETHANOL, AND A BIOMASS-DERIVED ETHER

Stephen F. Paul
Plasma Physics Laboratory
Princeton University
Princeton, New Jersey 08543

ABSTRACT

A multi-component, liquid, non-petroleum, alternative motor fuel for spark ignition engines has been developed. The fuel is composed of approximately equal volumes of: (1) medium-molecular weight alkanes, isoalkanes, and cycloalkanes (C₅ - C₈) which are extracted in the course of coalbed gas or natural gas production and/or processing, (2) anhydrous fermentation ethanol, and (3) 2-methylTHF, a biomass-derived heterocyclic ether. The ether serves as a co-solvent that reduces the volatility of the ethanol/hydrocarbon blend. The formulation can be adjusted to vary the fuel characteristics over a range similar to winter/summer and regular/premium gasoline grades: 87 - 94 octane; 0.74 - 0.78 specific gravity; and a 6.5 - 13.5 psi Reid vapor pressure. This fuel contains little or no sulfur, phosphorous, aromatics, olefins, or high-boiling-point hydrocarbons, but does contain 11 - 19% oxygen (by weight), with a corresponding reduction in heat content (100,000 - 106,000 BTU/gal). This fuel has been tested in 1996 and 1997 Ford Taurus ethanol-Flexible Fuel Vehicles which automatically adjust the air/fuel ratio over a wide range. Emissions testing (USEPA's FTP protocol) show the following differences in the tailpipe exhaust characteristics (compared to conventional gasoline): 40 - 50% less unburned hydrocarbons, 20% less CO, no significant change in NO_x, 4% less CO₂, 40% less ozone-forming potential, and 2 - 3 times less toxicity.

BACKGROUND

Natural gas liquids (NGL's) and coalbed gas liquids (CGL's) are underutilized alternatives to crude oil as hydrocarbon sources for spark ignition engine motor fuels. NGL's are recovered from natural gas wells as a gas-saturated liquid condensate.[1] The quantity of hydrocarbons with higher molecular weight is typically about 4 - 5%. Coalbed gases have long been recognized because of explosions that have occurring in the course of coal mining. In New Mexico and Europe, coalbed gas can contain significant amounts of heavier hydrocarbons, with C₂₊ fractions as high as 70%.[2] The liquids are classified by the Gas Processors Association [3] and the American Society for Testing and Materials (ASTM) according to carbon chain length as ethane, propane, n-butane, isobutane and "pentanes plus." Pentanes plus is further subdivided into iso-pentane and "natural gasoline". Pentanes plus are not generally desirable as gasoline is because they have low (65 - 70) octane and a 10 - 13 psi Reid Vapor Pressure (RVP) [4] which results in high evaporative losses and, in severe cases, engine vapor lock in warm weather.

Ethanol (EtOH) is a biomass-derived, octane-increasing motor fuel additive. While neat ethanol has a 2.3 psi RVP, when blended alone with gasoline, the resulting fuel has an RVP much higher than the ideal linear blending-RVP of gasoline ethanol mixtures.[5] This has been analyzed and explained as being a result of the strong dipole moment of ethanol.[6] EtOH's hydrogen bonding reduces its vapor pressure far below that expected from its molecular weight. But when mostly diluted in a non-polar substance such as gasoline, the attractive van der Waals force between the EtOH and the hydrocarbon dominates and is much weaker than the attraction due to hydrogen bonding. The maximum RVP is reached at 5-10% EtOH and is typically 1 psi above the base gasoline.

The situation is considerably more severe in NGL's. The high partial pressures of the low-carbon-number species in gasoline are the main contributors to the RVP. However, the deviation from ideal mixing is a function of the heavy hydrocarbons contained in the fuel.[7] The ideal vapor liquid equilibrium ratio is largely determined by the individual vapor pressure of the diluents and the vapor-phase fugacity coefficient. Non-ideal mixing effects alter the ideal vapor-liquid equilibrium and are parameterized in the activity coefficient. For EtOH, the activity coefficient is a stronger function of the composition of the heavy hydrocarbons than of carbon number. For a carbon number of 7, the activity coefficient for paraffins and naphthenes ranges from 25 - 35, for olefins it is ≈ 18 , and for aromatics, ≈ 11 . For pentanes, the primary constituent in pentanes-plus, it is ≈ 40 . Therefore the aromatic content, absent in NGL's, serves as a co-solvent for mixing EtOH in gasoline.

In the search for a non-toxic, renewable solubilizing agent to replace the aromatics, the solubility of the proposed solvent in both hydrocarbons and EtOH was considered. In general, hydrocarbons are more tolerant of ethers that contain non-polar groups. And ethers are quite tolerant of EtOH: the activity coefficients of EtOH in TAME, ETBE and MTBE are 10, 6.5 and 3.7 respectively. Because of its high density, low solubility in water, and low flashpoint, 2-methyl-tetrahydrofuran (MTHF) was selected as the primary candidate. It is produced from waste cellulosic biomass materials such as corn husks, corn cobs, straw, oat/rice hulls, sugar cane stocks, low-grade waste paper, paper mill waste sludge and wood wastes. It has been considered as a fuel additive to gasoline [8,9]. MTHF has been proposed as a low-cost, low-octane alternative oxygenate to EtOH in conventional gasoline [10]

METHODOLOGY

A fuel composition was prepared by blending 32.5% pentanes-plus, 35% 200 proof anhydrous EtOH, and 32.5% MTHF. The EtOH was pre-blended in the MTHF in order to avoid evaporative loss of the EtOH upon contact with the natural gasoline. The EtOH and MTHF were cooled to 40 °F prior to blending to further minimize evaporative losses. The pentanes-plus were cooled to 40 °F to minimize evaporative losses was poured into a cooled steel mixing tank. The blend of ethanol and MTHF was then added to the pentanes-plus while gently stirring for 5 seconds until a uniform, homogeneous blend was obtained.

The fuel characteristics were obtained in accordance with ASTM Standards.[6] To maintain the ability to test for exhaust emissions on both gasoline, E85 and/or this fuel without any manual engine adjustment, a 1996 Ford Taurus Flexible Fuel Vehicle (ethanol calibration) was used as the test vehicle. This engine includes a fuel sensor that, by measuring the dielectric constant of the fuel, enables it to calculate the concentration of ethanol. The vehicle was not modified between tests.

RESULTS

Hydrocarbon speciation of the NGL's (supplied as C₅⁺ from a natural gas processing plant) was measured using a gas chromatograph shows that the composition of the NGL's was $\approx 46\%$ pentanes, $\approx 33\%$ hexanes, $\approx 14\%$ heptanes, and $\approx 3\%$ octanes. The vapor pressure resulting from diluting EtOH in NGL's is shown in Figure 1. Unlike when blending with gasoline, the concentration of EtOH must exceed 50% to return the RVP down to 10.8 psi, the RVP the NGL's alone. The non-ideal mixing is very apparent in the curvature of the RVP plot. To achieve the 7 - 8 psi requirements of reformulated gasoline, 80- 85% EtOH would have to be blended. This is in distinct contrast to blending MTHF in NGL's, also shown in Figure 1. The RVP decreases in a nearly ideal fashion from the 10.8 psi RVP of the NGL's to the neat RVP of MTHF at 3.2 psi. Also, the MTHF blends with the EtOH, but there is a

stronger decline when the EtOH concentration exceeds 60%. While the solubility seems good, MTHF alone could not be a substitute for the aromatics, because the measured research octane number (RON) is only 86. The motor octane number (MON) is 72, 10 points below the minimum standard for regular fuel and the $(R+M)/2$ anti-knock index is 79, 9 points below the minimum standard. The low octane of the NGL's (67 measured in this case), means that substantial quantities of EtOH with a RON of 112 and a MON of 96 need be included.

After repeated experimentation, a blend of roughly equal parts of NGL's, EtOH, and MTHF was formulated as described in the methods section. The resulting fuel characteristics are shown in Table 1. The specific gravity, octane, RVP, and heat content are all within ranges detailed by ASTM specification for gasoline, D439-86. However, the distillation properties are quite different. The T90 value indicates the amount of "heavy-end" components (polyaromatics, etc.) fuels. These components are considered to be a source of unburned hydrocarbons during the cold start phase of engine operation. The lower values for the EtOH/MTHF/NGL blends compared to gasoline (T90 is $\approx 350^\circ\text{F}$ for gasoline) should reduce HC emissions.

After having been operated for 5,000 miles to age the vehicle's catalyst, the car was tested using the Federal Test Protocol (FTP), the transient driving cycle developed by the USEPA as specified in 40 CFR 86. The vehicle's engine block heater was not used to preheat the engine in any of these tests. The composite weighted results averaged over several (3-10) tests are shown in Table 2. For all the controlled pollutants, all the fuels emit 25-75% less than present federal standards (Tier I) allow at 50,000 miles.

Both the NGL/EtOH/MTHF blend and the CA RFG meet TLEV standards for NMHC. The CA RFG had the lowest NMHC emissions, and nearly met LEV standards, but in one of the three tests, .080 g/mi of NMHC was emitted. E85 emitted nearly 50% more NMHC than indolene, but all of the increase was during the cold-start phase. The low combustion temperature and high heat of vaporization of ethanol results in a longer warm-up period. Despite the 35% ethanol content of the NGL/EtOH/MTHF blend, it showed a 30% reduction in NMHC compared to indolene. reduction in adiabatic flame temperature. During the hot-stabilized portion (phase II) of the FTP, NMHC emissions from the NGL/EtOH/MTHF blend were 78% less than that of indolene.

Carbon monoxide emission was much more comparable among the fuels and was less than Tier I/TLEV/LEV standard of 3.4 g/mi. The NGL/EtOH/MTHF blend, Fed RFG and CA RFG emitted less than the 1.75 g/mi ULEV standard. The NGL/EtOH/MTHF blend emitted 7% less CO than indolene but the measurement error showed that this was not significant. In the stabilized portion (phase II) of the FTP, CO emissions from the summer blend were 49% less than that of indolene.

NO_x emissions for all fuels were less than half the Tier I/TLEV 0.4 g/mi standard and easily met the LEV/ULEV standards at 0.2 g/mile. The fuels containing ethanol had the higher NO_x emissions, though the increase was not proportional to the ethanol content. E85 exhibited an 7% increase in NO_x over indolene. The NGL/Et/MTHF blend showed a 30% increase and Federal RFG showed a 27% increase. During the stabilized portion of the FTP, NO_x emissions from the summer blend showed no change from indolene.

REFERENCES

- [1] N. P. Lieberman, Troubleshooting Natural Gas Processing. Tulsa: PenWell, 1987.
- [2] Dudley D. Rice, "Composition and Origins of Coalbed Gas", Hydrocarbons from Coal, Am. Assoc. of Petroleum Geologists Stud. in Geology #38, 1993, p. 159.
- [3] S.L. Montgomery, Editor, "Coalbed Methane: An Old Hazard Becomes a New Resource", Petroleum Frontiers, 3, (1986), Petroleum Information Corp. p. 8.
- [4] Annual Book of ASTM Standards, section 5, American Society for Testing and Materials. Easton, Maryland: ASTM, 1987.
- [5] "Industrial Uses of Agricultural Materials", USDA Economic Research Service, June 1993.
- [6] Ted R. Aulich, Xinming He, Ames A. Grisanti, and Curtis L. Knudson, "Gasoline Evaporation -- Ethanol and Nonethanol Blends", Journal of Air & Waste Management Association, 1994, 44:1004-1009.
- [7] D. Zudkevitch, A.K.S. Murthy, J. Gmehling, "Thermodynamics of reformulated automotive fuels", Hydrocarbon Processing, June 1995, p. 93.
- [8] Rudolph et al., Biomass, 16, 33-49 (1988).
- [9] Lucas et al., SAE Technical Paper Series, No. 932675 (1993).
- [10] S. Fitzpatrick, J Jarnefeld, "Biofine's Voyage from the Lab to the Plant . . .", Proceedings of the Seventh National Bioenergy Conference, SE Regional Biomass Energy Program, 1996, vol. 2, p 1083.

FIGURE 1.

Variation of RVP in 3 mixtures: EtOH in NGL's, MTHF in NGL's, EtOH in MTHF.

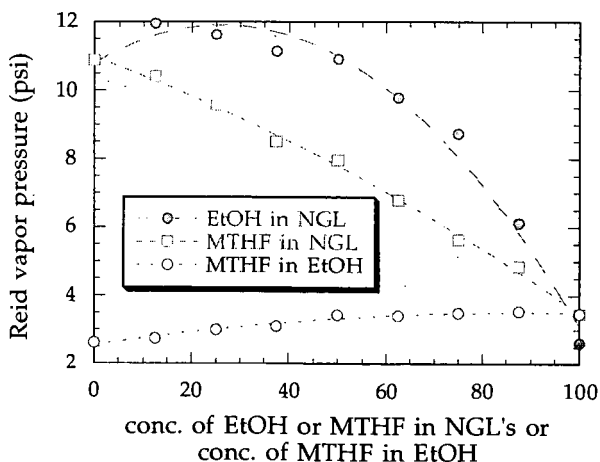


TABLE 1.
ASTM test results for NGL/EtOH/MTHF alternative fuel:

TEST	METHOD	RESULT	UNITS
API GRAVITY	ASTM D4052	52.1	60 DEGS F
COLOR	VISUAL	UNDYED	
DISTILLATION	ASTM D86		DEGS F
IBP		107.0	
10 PCT EVAPORATED		133.2	
50 PCT EVAPORATED		161.8	
90 PCT EVAPORATED		166.9	
FBP		195.5	
PCT RECOVERED		99.5	WT. %
PCT RESIDUE		0.3	WT. %
PCT LOSS		0.2	WT. %
RVP, PSI	ASTM D5191	8.10	
LEAD	ASTM D3237	<0.01	gm/gal
RESEARCH OCTANE NO.	ASTM D2699	96.8	
MOTOR OCTANE NO.	ASTM D2700	82.6	
R+M/2	ASTM D4814	89.7	
COPPER CORROSION	ASTM D130	1A	3 HRS @ 122I
GUM, (AFTER WASH)	ASTM D381	2.2	mg/100 ml
SULFUR	ASTM D2622	3	PPM
PHOSPHOROUS	ASTM D3231	<0.004	gm/gal
OXIDATION STABILITY	ASTM D525	165	minutes
OXYGENATES -- ETHANOL	ASTM D4815	34.87	PCT VOL
OXYGEN	ASTM D4815	12.48	PCT WT
BENZENE	ASTM D3606	0.15	PCT VOL
V/L 20	CALCULATED	135	DEGS F
DOCTOR TEST	ASTM D4952	POSITIVE	
APPEARANCE	VISUAL	BRIGHT/CLEAR	
AROMATICS	ASTM D1319	0.17/.41	PCT VOL
OLEFINS	ASTM D1319	0.09	PCT VOL
MERCAPTAN SULFUR	ASTM D3227	.0010	PCT WT
WATER TOLERANCE	ASTM D4814	<-65°C	
HEAT CONTENT	ASTM D3338	18,663 BTU/lb	

TABLE 2.

FTP weighted exhaust emissions for several fuels (all figures in grams per mile):

	Tier I Fed Standards	Et/MTHF alt. fuel	indolene	E85	Fed RFG	CA RFG Phase II
NMHC:	0.25	0.085	0.122	0.142	0.136	0.071
CO:	3.40	1.66	1.78	1.82	1.70	1.47
NO _x :	0.40	0.161	0.124	0.132	0.157	0.097

notes:

- 1) *indolene* is EPA certified emissions testing gasoline (40 CFR 86)
- 2) RFG is reformulated gasoline
- 3) NMHC is non-methane hydrocarbons
- 4) CO is carbon monoxide
- 5) NO_x is oxides of nitrogen
- 6) Fed Winter RFG is blended from 92.5% indolene and 7.5% 200-proof ethanol. It is a premium grade (92 octane) winter fuel.
- 7) E85 is blended from 20% indolene and 80% 200-proof ethanol
- 8) CA RFG Phase II is a premium grade (93 octane) reformulated fuel
- 9) NGL/Et/MTHF is an 89 octane, 8.1 psi fuel alt. fuel with the following composition: 35% EtOH, 32.5% MTHF, 32.5% NGL's

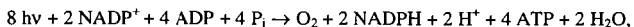
SOLAR HYDROGEN VIA A PHOTOSYNTHETIC Z-SCHEME ANALOGUE BASED ON SEMICONDUCTOR POWDERS

Clovis A. Linkous
Darlene K. Slattery
Florida Solar Energy Center
1679 Clearlake Road
Cocoa, FL 32922-5703

ABSTRACT

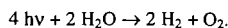
Mother Nature uses solar energy to oxidize water to O₂ and reduce protons onto NADP⁺ via dual photosystems connected by a string of redox agents. By splitting the energetically challenging task of decomposing water between two separate photochemical reactions, more abundant and lower energy solar photons can be employed. This same approach can be utilized with semiconductor powders. Based upon their electronic band structure, semiconductors can be chosen that selectively oxidize or reduce water. One can then select O₂-evolving and H₂-evolving photocatalysts, disperse or immobilize them in separate containers, and use an appropriate reversible redox agent as an electron shuttle between them. We have had some success with this photosynthetic Z-scheme analogue using an alkaline iodate redox electrolyte and a variety of semiconductor compounds, such as TiO₂ and InP. Proof of concept has been demonstrated, but various materials problems underscore the need to identify other photocatalysts.

The scientific community has long marveled at Nature's ability to perform kinetically and/or thermodynamically challenging reactions such as O₂ reduction and N₂ fixation under ambient conditions. In particular, with the rise of mankind's consciousness toward environmental preservation and the need for a sustainable energy supply, we have sought ways to emulate Nature and develop our own approach to the light reaction of photosynthesis, where solar energy is stored by photo-oxidatively decomposing water to O₂ and synthesizing adenosine triphosphate, ATP, and reduced nicotinamide adenine dinucleotide phosphate, NADPH:



where hv refers to light quanta and P_i is a phosphate oxyanion, HPO_4^{2-} .

In particular, we would like to skip the various phosphorylations and nicotinamide reductions and simply photo-decompose water to its constituent elements:



This energy-storing reaction would become the basis of the "Solar-Hydrogen Economy."

Even though the water-splitting reaction is mechanistically less ambitious than the overall photosynthetic reaction, the challenge is the same: how to use abundant, relatively low energy photons to drive a chemical system thermodynamically uphill.

Because the water decomposition process can be described in terms of a redox reaction or half cell reactions, it is convenient to look at the free energy relationships in terms of its voltage equivalent. The cell voltage corresponding the standard Gibbs free energy change for water decomposition is:

$$\begin{aligned} \Delta E^0 &= -\Delta G^0 / nF = -(-56.6 \times 10^3 \text{ cal/mol})(4.184 \text{ J/cal}) / (2 \text{ equiv/mol})(96485 \text{ Coul/equiv}) \\ &= 1.23 \text{ V.} \end{aligned}$$

The various photosynthetic reactions can also be viewed in terms of their redox potentials. The general trend is shown in Figure 1a. Mother Nature has developed two photosystems; one for oxidative water splitting, one for reducing NADP⁺. An electron transfer chain of redox reactions connects them. Note that the redox potential is shifted by an amount corresponding to the energy of the photon that was absorbed. The zigzag shifting of redox potential energy as an electron courses through the photosynthetic light reaction has engendered the appellation "Z-scheme" [1].

To enable water oxidation to occur, a ground state electron must be promoted from an energy level positive of +0.82 V at neutral pH (the standard state value calculated above assumes unit protonic activity, or approximately 1.0 M acid). To reduce the first acceptor state in the electron transfer chain (plastoquinone), one needs a redox potential of about 0.0 V. An excited state electron in chlorophyll *a* at 680 nm has an energy of 1.83 eV; therefore, in analogy to overpotentials in electrolysis, Nature is putting an extra eV of energy into the redox system to make sure there is a driving force on the reaction.

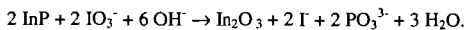
We have been attempting to put together our own water-splitting Z-scheme utilizing immobilized semiconductor powders, or photocatalysts, as our photosystem elements. We needed one material that would be O₂-evolving under illumination, and another that would be H₂-evolving. For this purpose we were able to draw from the wealth of photoelectrochemical work done over the last 25 years. Mainly because of the requirement to exhibit long term aqueous stability, most semiconductor materials are eliminated and only a few choices remain. For the water-oxidizing photocatalyst, there are a number of transition metal oxides that have been used as photoanodes, such as SnO₂, ZnO, WO₃, Fe₂O₃, and TiO₂. For the H₂-evolving photocatalyst, one can consider various photocathode materials; most of these have been metalloid phosphides and arsenides, such as GaP, InP, and GaAs. We chose TiO₂ and InP as the initial photosystem pairing.

To provide an electron transfer chain between our two photosystems, we needed to identify a "redox mediator", a reversible redox couple that would be highly soluble, optically transparent, allow facile charge transfer kinetics between the TiO₂ and InP dispersions. After testing many possible redox couples [2], it was decided to concentrate on the I/IO₃⁻ and Br⁻/BrO₃⁻ systems in alkaline solution. In particular, the IO₃⁻ couple best facilitated an even split of the energy-storing requirement between the two photosystems.

In Figure 1b, the corresponding energy level diagram for the photocatalytic system is shown. The valence band edge of TiO₂ becomes the ground state electronic energy for the reaction center in Photosystem II. The photogenerated hole is easily capable of performing water oxidation. The conduction band is the excited state donor level that injects electrons into the electron transfer chain, which in our case is simply IO₃⁻ ion. Having been reduced to I, the redox mediator migrates to the InP dispersion, or Photosystem I, where it is reoxidized by valence band holes in the InP photocatalyst. Photogenerated electrons in the conduction band of InP are energetically capable of reducing water to H₂.

We have studied each photocatalytic system separately and confirmed that the TiO₂/IO₃⁻ system evolved O₂ and only O₂, and that the InP/I system evolved H₂ and only H₂. Data for O₂-evolution from various TiO₂ particle dispersions are shown in Table I. The positive effect of adding a 1.0% by weight coating of noble metal co-catalyst is clearly evident. It is also clear that IO₃⁻ or some other electron acceptor must be present to achieve a reasonable photoreaction rate. While TiO₂ is satisfactory in terms of showing proof of concept, with a band gap of 3.0 eV, it is not an effective absorber of solar radiation. Narrower band gap materials need to be identified.

The InP, while showing initial H₂ evolution, would slow to virtually nothing after about an hour of photolysis. This was initially thought to be a form of photocorrosion, but after some control experiments, it became clear that the InP was being attacked by photogenerated IO₃⁻:



Thus alternatives to the H₂-evolving photocatalyst also need to be identified.

In both the natural photosynthetic and photocatalytic schemes, there needs to be some type of ordered, spatial arrangement of the photosystems and the electron transport chain to enable efficient charge and product separation. The photosynthetic organelle is the chloroplast. In higher plants, they appear as discs or flat ellipsoids 3-10 μm across. Within the chloroplast are many stacked arrays of flattened, sac-like membranes or thylakoids. Each stack, or granum, is about 500 nm in diameter. Both photosystems are embedded in the thylakoid membrane. They consist of bundles of several hundred chlorophyll molecules and associated species forming a 175 Å particle, as shown in Figure 2.

With a formal redox potential of -0.32 V (vs NHE) at pH 7.0, NADPH would be easily oxidized by O₂. However, this reaction is prevented because they are generated on opposite sides of the thylakoid membrane. The thylakoid membrane could be thought of as a semiconductor electrode, with a directed flow of charge carriers through it.

For the photocatalytic system, we have opted to disperse the two semiconductor powders in separate modules, or beds, as shown in Figure 3. A pump circulates a working fluid containing the redox mediator between them. The product gases are thus evolved at the macro scale in separate containers. This avoids the issue of how to safely separate the H₂ and O₂ co-evolved in a 2:1 ratio, well within the combustibility range.

Theoretical studies on the solar spectrum versus photovoltaic efficiency have shown that the optimum band gap for a single material is 1.3 eV. Efficiency can be improved upon by using multiple semiconductor materials in a tandem arrangement. By carefully lining up the band edges, so that the hole current in one layer feeds the electron current in the next, one can achieve a summation of individual voltages that can have a much higher efficiency. This comes from minimizing the energy lost in thermalizing a high energy charge carrier inside a wide energy band. In particular for water-splitting, the more efficient semiconductor materials, when used as a photoelectrode, cannot generate sufficient voltage to drive the electrolysis. The use of tandem electrodes, however, has made this possible. Work by Rocheleau on triple junction a-Si pin cells [3] and by Turner on GaAs/GaInP₂ cells [4] have demonstrated water decomposition using a single photoelectrode. Reported efficiencies have recently exceeded 12.8% [5].

The dual bed photocatalytic system can be "tandemized" as well by folding one bed underneath the other as shown in Figure 4. This would be feasible as long as: 1) the top layer photocatalyst has a wider band gap than the lower layer, so that light not absorbed in the first layer is transmitted underneath; and 2) the upper photocatalyst is finely dispersed, minimizing scattering losses. One may further be able to minimize mass transport problems by finely perforating the support membrane. The redox mediator would then travel through micro-channels instead of across the top face of the membrane in one direction and then back underneath. The resulting perforated, photocatalytic tandem membrane would then no longer require a circulating fluid, eliminating that parasitic loss.

It is interesting to note that Nature decided not to tandemize her photosynthetic apparatus, i.e., Photosystems I and II have nearly the same, instead of complementary, absorption spectra. Instead, the spectral gaps between the chlorophyll maxima at 650-700 and 430-470 nm are filled by secondary pigments, such as the carotenes, phycobilins, and xanthophylls. Perhaps the lesson here is that if solar power conversion efficiency percentages in the single digit range are acceptable, then concentrating on absorbing as much light as possible and then letting all the charge carriers thermalize to an energy band edge that can do useful chemistry is the preferred approach.

ACKNOWLEDGEMENT

The authors would like to thank the US Department of Energy, Office of Solar Thermal, Biomass Power, and Hydrogen Technologies, for their financial support.

REFERENCES

- 1- R. Hill and F. Bendall, *Nature* (London), 1960, Vol. 186, 136.
- 2- C.A. Linkous, D.K. Slattery, A.J.A. Ouellette, G.T. McKaige, and B.C.N Austin, "Solar Photocatalytic H₂ from Water Using a Dual Bed Photosystem," *Hydrogen Energy Progress XI*, proceedings of the 11th World Hydrogen Energy Conference, Stuttgart, Germany, June 23-28, 1996, Schön and Wetzell GmbH, Frankfurt am Main, 1996, p. 2545.
- 3- R. Rocheleau, E. Miller, A. Misra, and S. Song, *Hydrogen Energy Progress XI*, p. 2755.
- 4- J.A. Turner, D. Arent, M. Peterson, and S. Kocha, *Hydrogen Energy Progress XI*, p. 2749.
- 5- O. Haselev and J.A. Turner, *Science*, April 7, 1998, Vol. 280, 425.

Table I. O₂ Evolution from TiO₂/IO₃⁻ Suspensions

250 mg photocatalyst
50 ml 1.0 N NaOH, 0.2 M KIO₃
1000 W Xe lamp irradiation
6 hour photolysis

Photocatalyst:	TiO ₂	Pt-TiO ₂	Ir-TiO ₂	Ir-TiO ₂ w/o IO ₃ ⁻
O ₂ evolved (ml):	0.58	1.3	2.5	< 0.02

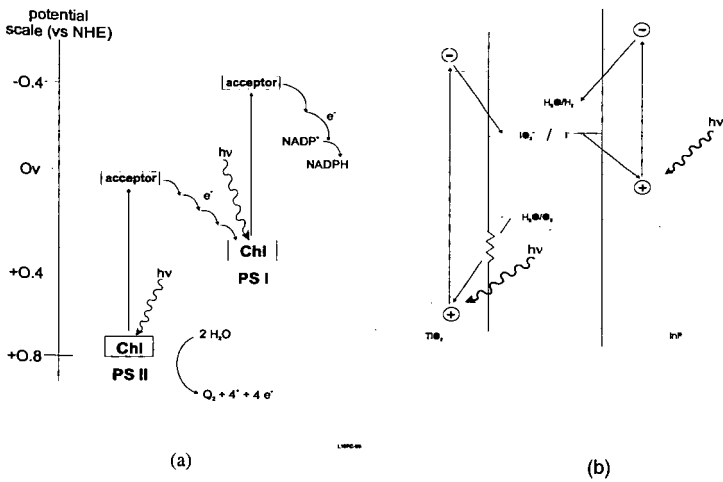


Figure 1. Energy level diagrams of: a) photosynthetic Z-scheme; and b) dual module water-splitting using semiconductor particulates.

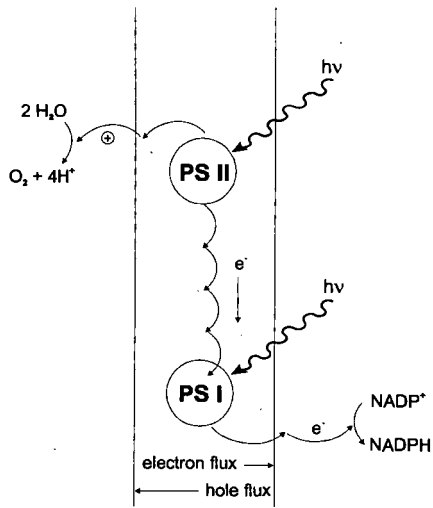
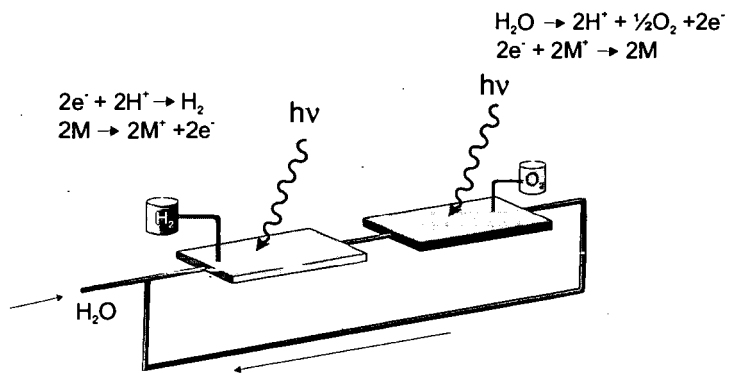


Figure 2. Schematic showing spatial arrangement of photosystems and charge flows in the thylakoid membrane of a chloroplast.



L106-98

Figure 3. Schematic of a dual bed photocatalytic water-splitting system.

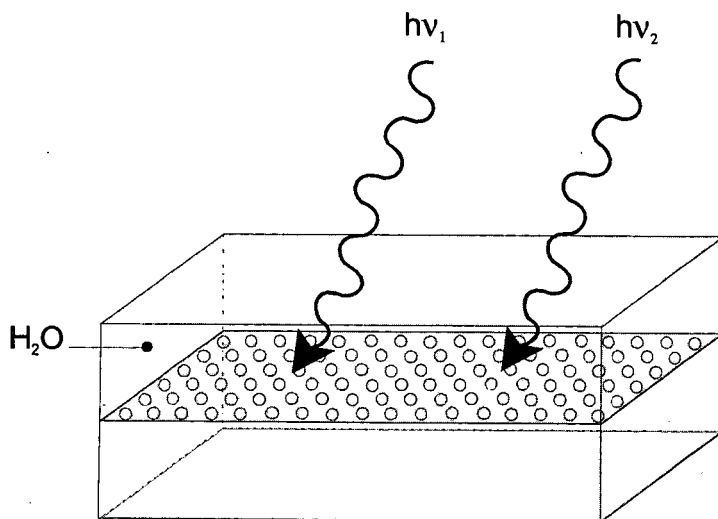


Figure 4. Schematic of a perforated, photocatalytic tandem membrane system.

A PRIVATE-FEDERAL COLLABORATIVE MODEL:
THE NATIONAL ALTERNATIVE FUELS LABORATORY PROGRAM

Ted Aulich, Tim Gerlach
University of North Dakota Energy & Environmental Research Center
Grand Forks, North Dakota 58202

KEYWORDS: ethanol, alternative fuels, aviation fuel

INTRODUCTION

The U.S. Department of Agriculture (USDA) -sponsored National Alternative Fuels Laboratory (NAFL) program at the University of North Dakota Energy & Environmental Research Center (EERC) was initiated to help build partnerships for demonstration and commercialization of alternative fuels. Approximately half of the NAFL annual budget is set aside for use in cost-share projects with nonfederal partners and advertised as the NAFL Request for Collaborative Proposals, which is published in ethanol industry newsletters and on the EERC Internet site. Successful proposals require 50% cost share and 90% of project labor performed at EERC. Descriptions of selected NAFL-initiated partnerships and projects are provided below.

AN ETHANOL-BASED ALTERNATIVE TO 100LL AVIATION FUEL

A team comprising EERC, South Dakota State University at Brookings (SDSU), Great Planes Fuel Development in Brookings, Lake Area Technical Institute at Watertown, South Dakota (LATI), the South Dakota Corn Marketing Board, and Texas Skyways, San Antonio, has developed and is pursuing commercialization of an economically competitive ethanol-based alternative to lead-containing aviation gasoline. Unlike essentially all commercial automobile fuel sold in the United States today, commercial 100-octane aviation fuel for piston engine aircraft (known as "avgas" or "100LL") still contains lead, which is a human health hazard. Replacing avgas with an ethanol-based aviation fuel will improve the environment (since the high octane rating of ethanol eliminates the need for lead) and reduce foreign oil dependency. Ethanol is also cheaper than avgas. Current ethanol and avgas prices are about \$1.50 and \$2.25 per gallon, respectively. An optimized blend of ethanol and a suitable petroleum-derived additive (to supply needed volatility and serve as a denaturant) can provide better engine performance and higher fuel efficiency than avgas by enabling the use of a higher engine compression ratio. An optimized ethanol blend will also enable better engine starting at lower temperatures than achievable with 98% (denatured) ethanol, because of an increase in Reid vapor pressure (Rvp) from about 2.3 pounds per square inch (psi) for 98% ethanol to about 7 psi for a blend of 80% to 85% ethanol with an appropriate additive.

Fuel formulations prepared using nondenatured ethanol and a high-octane petroleum blendstock from a major U.S. oil company were evaluated in the lab at EERC. Following optimization of a fuel comprising about 85% nondenatured ethanol and 15% petroleum blendstock-biodiesel mixture (biodiesel was added to provide lubrication), U.S. Bureau of Alcohol, Tobacco, and Firearms approval of the selected petroleum blendstock as an ethanol denaturant was requested and granted. GPFD successfully applied for Federal Aviation Administration (FAA) approval to flight-test two engine-airframe combinations with aviation-grade E85 (AGE85), and initiated on-ground engine testing and flight testing for FAA certification. As part of the certification process, EERC prepared a preliminary fuel specification for FAA review. Currently, GPFD is working with Texas Skyways to obtain FAA certification of three engine-airframe combinations for use with AGE85. In preliminary flight tests conducted with a Continental O-470-U/TS (that underwent minor carburetor modifications for use with AGE85 but no engine modifications), AGE85 and 100LL were shown to be essentially equal in performance, but the AGE85 provided significantly higher fuel energy utilization efficiency. Fuel utilization data acquired demonstrated that range is not simply a function of fuel energy content (about 88,200 and 120,000 Btu/gallon for AGE85 and 100LL, respectively), but also a function of how the energy is used. Because of its higher latent heat of vaporization than 100LL (and possibly, other factors), ethanol combustion produces less waste heat, which means that a greater portion of its energy goes toward moving a plane than compared to 100LL. This may be the

primary reason why the AGE85 range reduction is only about 10 to 15% versus 100LL, instead of the 27% that would be predicted based on the energy content difference between the two fuels and the assumption that the fuels will combust with equal thermodynamic efficiency. Fuel efficiency data for ethanol-based fuels versus petroleum fuels (with both aircraft and automobiles) need to be determined under lean-burn conditions that take advantage of ethanol's capability to provide engine-safe power and performance at higher air-to-fuel ratios than gasoline, especially under cruise conditions. Flight tests are ongoing, and oil company commitment is being sought to produce and distribute AGE85 or provide AGE85 petroleum blendstock for blending and distribution by another entity. Current effort is focused on companies with midwest oil production capability to enable use of regionally produced ethanol. Because of increasing U.S. EPA pressure that has resulted in the prohibition of avgas in pipelines and the need for shipment by truck, avgas producers are aware of the urgent need to develop unleaded avgas alternatives.

OFF-SITE REGENERATION OF ETHANOL DEHYDRATION MOLECULAR SIEVES

Molecular sieves (mol sieves) are used for dehydration at numerous ethanol production facilities and oil and gas refinery operations throughout the United States. In the ethanol industry, mol sieves adsorb water from 95% pure ethanol and yield 100% (200 proof) product, and sieve regeneration (dewatering) is performed on-site by applying a vacuum to the "bottles" in which the sieves are contained. In the event of a process upset or other unplanned occurrence, mol sieves can become contaminated and undergo a reduction in effectiveness, which may result in reduced product output. Remediation of reduced output requires either sieve replacement or off-site regeneration to remove the offending contamination. Off-site regeneration of mol sieves is common in the oil and gas industries and is normally achievable with thermal treatment under a specific atmosphere. Temperature and atmospheric requirements depend on type and extent of contamination.

Because of its demonstrated economic viability in the oil and gas industries, an EERC partnership with CRI International, a full-service catalyst management company, was initiated to pursue commercialization of off-site mol sieve regeneration for the ethanol industry. Normally, the price of off-site regeneration ranges from one half to two thirds the cost of new sieves. Factors affecting cost include treatment required (based on type of contamination, which can include carbohydrates and their polymerization products, sulfites, and lubricant entering the process stream due to a system upset), transportation, and amount of material requiring regeneration. Figure 1 compares the performance of contaminated mol sieves from a midwest ethanol plant to the performance of off-site regenerated sieves from the same plant. The figure demonstrates the technical feasibility of the process. Currently, EERC and CRI International are evaluating process economics with contaminated sieves from another producer.

FLEX-FUEL VEHICLE FUEL ECONOMY TESTING

Based on preliminary fuel economy data acquired during the above-described ethanol-based aviation fuel development effort, EERC initiated fuel economy testing with E85 automobiles. Initial results indicate highway and city driving mileage reductions of about 28%, which are consistent with industry-reported mileage and mileage calculated based on energy content per gallon versus gasoline and assuming gasoline thermodynamic efficiency. However, the E85 1997 flex-fuel Ford Taurus cars used for the tests are programmed to operate at stoichiometric fuel combustion conditions. While there are several reasons for avoiding "lean-of-stoichiometric" combustion of gasoline, including increased NO_x emissions and increased potential for valve damage, there are indications that leaner ethanol combustion may not produce the same negative effects (1-3). Current flex-fuel vehicle work is focused on adjusting fuel flow to achieve lean-of-stoichiometric combustion and monitoring emissions of NO_x , CO , CO_2 , O_2 , and total hydrocarbons in on-the-road tests with a vehicle-mounted infrared gas analyzer.

GASOLINE SURVEYING TO MONITOR COMMERCIAL FUEL COMPOSITION & PROPERTIES

To meet objectives of the 1990 Clean Air Act Amendments and help ensure against unsafe

levels of tropospheric carbon monoxide and ozone, many regions around the U.S. have implemented reformulated gasoline (RFG) or oxygenated gasoline (oxyfuel) programs. Programs that rely extensively on ethanol to meet fuel oxygen requirements are in a unique position to ensure and accelerate marketplace acceptance of ethanol as a high-octane blendstock for the U.S. gasoline pool. Success in these programs is crucial to the ethanol industry and requires that base gasolines used in ethanol blends meet health, environmental, and performance standards to ensure a positive relationship between ethanol and public health, air quality, and engine performance. Through the NAFL program, the EERC has formed partnerships with ethanol industry groups to perform gasoline surveys in which fuels are sampled (at the pump) and analyzed to provide data and insight on major supplier blending and marketing practices. Data from the surveys can be used to compare commercial fuel parameters to regulated parameters of the U.S. Environmental Protection Agency (EPA) RFG program, the California RFG program, other state gasoline programs, and the EPA Anti-Dumping Requirements for Conventional Gasoline. Table 1 lists EPA Phase 1 RFG typical properties, specifications for California Phase 2 RFG, and annual average parameters for "EPA Statutory Baseline" fuel.

To implement the anti-dumping requirements, EPA worked with gasoline refiners, blenders, and importers to develop individual "baseline fuel" specifications. Each refiner must meet individual baseline fuel requirements developed based on a set of fuel parameters, emissions, and volumes representing the quality and quantity of the refiner's 1990 gasoline. All individual baseline fuel specifications are confidential between EPA and refiners and are not available for public review. Anti-dumping compliance is based on annual average composition and characteristics for gasoline from each regulated refinery, refinery aggregate, importer, or blender. Each refiner reports annual gasoline data to EPA at the end of each production year, and EPA also periodically conducts audits of production, blending, storage, and loading facilities to help ensure that baseline fuel specifications are met. If a refiner does not have an established individual baseline fuel on file with EPA, this refiner is required to meet the specifications of the EPA Statutory Baseline. Demonstration of compliance using the statutory baseline is based on the annual fuel parameter values shown in Table 1. The statutory baseline fuel parameters were developed using 1990 fuel composition data compiled through a nationwide petroleum industry fuel survey. The data provided in the twice-annual industry gasoline surveys (which are guided by the American Petroleum Institute) are acquired by petroleum companies and supplied to the survey marketer compilation and reporting. All fuel composition data are reported without oil company identification, which prohibits use of the survey to associate a specific fuel with a specific refiner.

An EERC summer 1997 midwest region gasoline survey showed that 27 of 33 midgrade (89 octane) fuels sampled contained ethanol, including 15 of 21 fuels that were not required to contain oxygen, indicating the free-market use of ethanol to provide octane. The survey showed that although two of three major suppliers frequently chose to use ethanol as a viable blending component, one major supplier consistently avoided the use of ethanol except with fuels required to contain oxygen. Figure 2 compares EERC survey fuel data with BDM survey averages for the same region and EPA and California fuel specifications, and Figure 3 is a similar comparison using winter fuel data. The figures show that while both the EERC and BDM survey average fuel compositions meet EPA baseline specifications, one major supplier significantly exceeds (by almost double) the EPA statutory baseline value for olefins in both winter and summer. It is likely that this supplier has an individual baseline on file with EPA, and because this information is proprietary, it is impossible to determine compliance status with currently available information. Additionally, although EPA-specified sampling and analysis procedures were employed, compliance status determination would likely require a more extensive database than assembled for this survey. A key benefit of gasoline surveying is in helping to ensure that ethanol-blended gasolines are clean and perform well, which is crucial to ensuring ethanol's future as an automobile fuel.

ALTERNATIVE FUELS IMPLEMENTATION VIA RED RIVER VALLEY CLEAN CITIES

The Red River Valley Clean Cities (RRVCC) coalition was established to promote and implement regional alternative fuels use by building partnerships to erect alternative fuels

infrastructure, procure alternative fuel vehicles (AFVs), and demonstrate beneficial environmental, performance, and economic effects of alternative fuels. The NAFL-led coalition comprises government and industry stakeholders in Canada and the U.S. located in and between Grand Forks–East Grand Forks on the North Dakota–Minnesota border and Winnipeg, Manitoba, Canada. The route between Winnipeg and Grand Forks (Canada Highway 75 and U.S. I29) represents the northern end of the I29–I35 Midcontinent Trade Corridor. The coalition is fuel-neutral, as demonstrated by a stakeholder membership that includes regional ethanol and electricity interests and upper midwest propane and natural gas suppliers. Current RRVCC initiatives include working with the ethanol industry, grower organizations, state agencies, and gasoline retailers to establish commercial high-blend ethanol (E85) stations, working with the University of North Dakota to procure E85 and propane vehicles, establishing a group of natural gas interests, comprising natural gas and fueling equipment providers, state agencies and private fleets, and the U.S. Postal Service, which will construct compressed natural gas fueling sites in the region.

REFERENCES

1. Bechtold, R. L., J.B. Pullman, Society of Automotive Engineers Paper No. 800260, 1980.
2. Bechtold, R. L., *Alternative Fuels Guidebook*, Society of Automotive Engineers, 1997.
3. Thomas, K., *The Future of Avgas*, *TBO Advisor*, January–February 1998.

Table 1. Regulatory Fuel Specifications.

	EPA Phase 1 RFG Typical Properties	California Phase 2 RFG Specifications Average Limit	EPA Anti-Dumping Statutory Baseline Fuel Parameters Annual Average
Rvp, psi	7.2 – 15.0	7.0 ¹	8.7
T50, °F	202	200	Not reported
T90, °F	316	290	Not reported
Aromatics, vol%	23.4	22.0	28.6
Olefins, vol%	8.2	4.0	10.8
Benzene, vol%	1.0	0.8	1.6
Sulfur, ppm	302	30	338
Oxygen, wt%	2.0	1.8 – minimum ² 2.7 – maximum ²	Not required

¹ Absolute maximum limit – no average limit allowed.

² Absolute limits for winter gasoline – summer values are 0.0 minimum, 2.7 maximum.

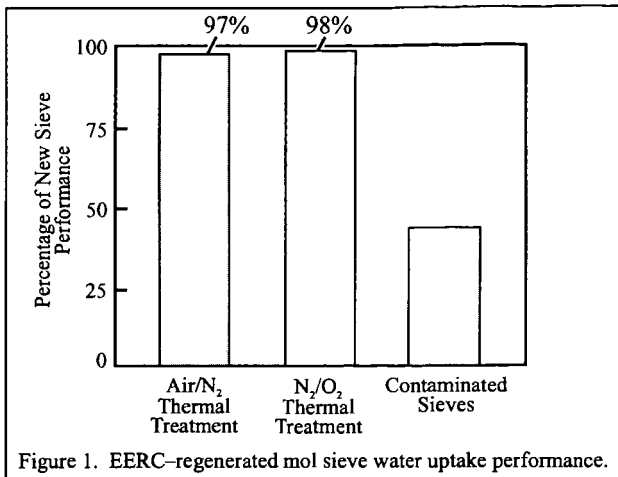


Figure 1. EERC-regenerated mol sieve water uptake performance.

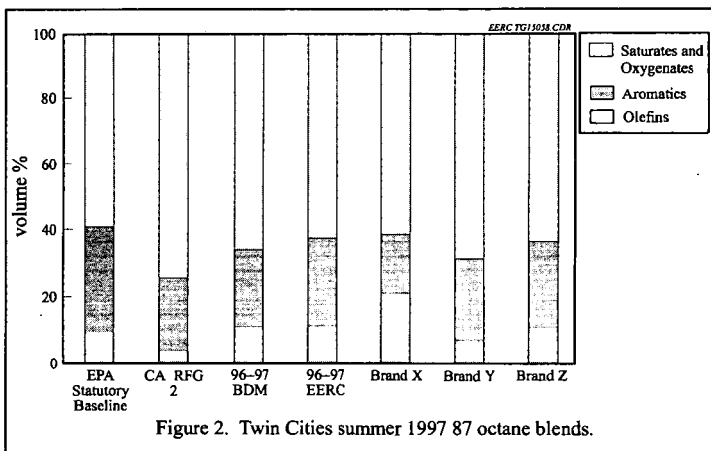


Figure 2. Twin Cities summer 1997 87 octane blends.

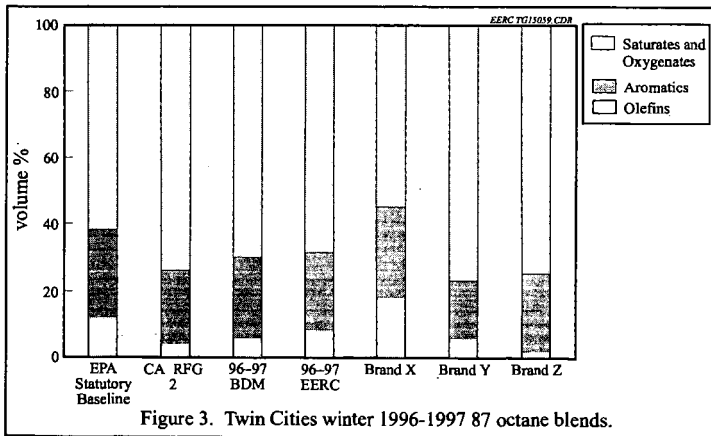


Figure 3. Twin Cities winter 1996-1997 87 octane blends.

HYDROCARBON FUELS FOR FUTURE AUTOMOTIVE ENGINES

Ramon L. Espino and John L. Robbins
Exxon Corporate Research Laboratories
Route 22 East
Annandale, NJ 08801

In response to a need for transportation vehicles with less environmental impact, automakers around the world have been exploring a variety of novel advanced vehicle engine technologies. Fuel cells, devices that electrochemically oxidize fuels, have emerged as the focus of long range vehicle engine research: at least thirteen major auto makers now are exploring their use in light duty vehicle applications.

The Polymer Electrolyte Membrane (PEM) fuel cell has been the focus of most vehicle fuel cell research. It produces power at near ambient temperature, and thus offers advantages vs. other fuel cells that require preheating to 200°C or above before they can generate electric power. Rapid startup, with minimum power input, is a critical requirement for any vehicular application of fuel cells.

Figure 1 describes the operational principles of a PEM fuel cell. Hydrogen fuel dissociates at the anode catalyst to hydrogen ions and electrons. Hydrogen ions migrate across the electrolyte to the cathode side. At the cathode, oxygen from the air combines with electrons from the anode and hydrogen ions traversing the membrane to form water. The flow of electrons from the anode to the cathode, and the production of water generates electric power. Advanced fuel cell stacks, such as those produced by Ballard Power Systems, have achieved power density levels of 1 kW/liter. These figures exceed targets set by the US PNGV program for fuel cells aimed at light duty vehicle applications.

Fuel cells offer potential for step-out changes in vehicle emissions and efficiency. The H₂/air fuel cell produces no CO, NO_x, or particulate matter emissions. However, H₂ production may lead to emissions of one or more of these air pollutants, depending on how it is produced. Peak steady-state efficiencies of H₂ PEM fuel cells approach 60% when operated at the low end of their maximum load, while compression-ignition or spark-ignition engines achieve peak efficiencies (up to 45%) near the higher end of their peak load. Net efficiency credits for fuel cell vehicle systems will again depend on how the H₂ fuel is produced and distributed, as well as the way fuel cells or internal combustion engines are incorporated into a vehicle power train, e.g. as a stand-alone power source, or as an electric generator in a hybrid vehicle.

Net Efficiency Estimates

Higher energy efficiency in transportation is a major factor driving efforts to develop fuel cell vehicles. Here we use a method to compare net efficiencies of fuel and fuel cell vehicle systems that considers energy losses in the fuel cycle (fuel production, refining, distribution) and in operation of the vehicle. We compare systems for vehicles that store H₂ produced at a retail station from natural gas, methanol produced from natural gas, and gasoline produced from petroleum.

The first option considers hydrogen production at a retail-refueling site by steam reforming of natural gas. We chose natural gas steam reforming because it is currently the lowest cost method to produce hydrogen. Currently 97% of the world's hydrogen is produced by this process, but it is possible that long term, technology advances will reduce cost of H₂ from renewable resources to economically competitive levels (1,2). Natural gas is widely distributed in many developed countries, so fuel availability is not an issue (where it is not available, one could instead steam reform or partially oxidize fuels like gasoline, diesel, alcohols, etc).

Steam reforming is an endothermic process that generates H₂ and CO₂ from methane and water: $\text{CH}_4 + 2 \text{H}_2\text{O} + \text{heat} = \text{CO}_2 + 4 \text{H}_2$. The heat requirement is substantial, over 253 kJ/mole methane, or about 31% of methane's lower heating value. After the reforming step, there is a purification train to remove CO₂ and CO, followed by two-stage compressors and high pressure storage tanks. Overall thermal efficiency (heating value of H₂/heating value of methane fuel) of the process is 70-80%, depending on the level of plant heat integration and the final H₂ storage pressure (2). Assuming 90% efficiency in delivering natural gas wellhead to retail station, we obtain a net 63-72% efficiency for H₂ production.

The second fuel option considered is methanol produced from natural gas. Nearly all methanol is now produced from natural gas, usually near large, remote gas fields where distance from population centers makes pipeline distribution/sale of the gas impractical. This low-cost gas is instead converted to methanol near the production site, which is then shipped to the market by liquid tankers.

Methanol is produced from natural gas in a multi-step process. Gas is first processed to remove impurities such as H₂S, and then converted to synthesis gas (a mixture of H₂, CO, and CO₂) by steam reforming (or partial oxidation) followed by water-gas shift reactions. This is fed to a methanol synthesis reactor where CO and CO₂ are catalytically hydrogenated to CH₃OH. The crude product is distilled and dehydrated to remove water, hydrocarbon, and alcohol impurities. The thermal efficiency of methanol production is typically 68-72% (3). Energy losses in transportation range from 1-2%, yielding a net fuel production efficiency of 67-71%.

The third option is a petroleum-based fuel (e.g. gasoline or diesel) stored and converted to an H₂-rich gas by partial oxidation on-board the vehicle. Gasoline delivered at the pump in a retail station typically carries 85-90% of the heating value available from petroleum produced at the wellhead.

Table 1 lists compares net efficiencies of the three fuel options, considering energy efficiency of fuel production, fuel processing on-board the vehicle, and the fuel cell. The previous paragraphs outline assumptions used in estimating fuel production efficiencies. On-board fuel processing and fuel cell efficiencies estimates reflect ranges cited by others (4,5). Net efficiencies of all the options are significant improvements over current gasoline-fueled IC engines. On highway drive cycles (which are closest to the steady-state fuel cell system efficiencies cited above), these engines are 20 % efficient in delivering power to the wheels (6), yielding a net efficiency of 17-18% when gasoline production/delivery is included.

The data used to construct Table 1 contain some uncertainties. Fuel production efficiency figures are fairly solid, relying on many years of commercial experience in production of gasoline, methanol, and hydrogen in large scale. Fuel cell and fuel processor efficiencies are less certain. These rely on models and limited hardware data measured under steady-state operating conditions. Still, the exercise is valuable in that it shows that the fuel cell options have potential to significantly improve efficiency vs. current generation ICE vehicles. Overlapping ranges of the gasoline and compressed H₂ fuel option efficiencies illustrates the need to determine efficiencies and emissions of these systems in vehicles under realistic drive cycles.

Fuels from Natural Gas

The equivalent of over 800 billion barrels of oil currently lies dormant in natural gas reserves largely inaccessible by pipeline. These previously untapped resources along with underutilized light hydrocarbons associated with crude oil production could become energy sources for gas-to-liquids conversion technologies emerging from research and development efforts.

Chemical conversion of natural gas is a relatively newer route for preparing liquid hydrocarbons for transport to markets. Although current conversion processes have lower thermal efficiencies than LNG processing, under some circumstances this debit can be largely offset by higher value liquids which can range from ultrahigh quality refinery and petrochemical feed stocks to finished products. Moreover, these streams can be shipped and stored in conventional facilities obviating the need for dedicated cryogenic transportation equipment and tankage.

Natural gas can be converted to zero sulfur, zero aromatic hydrocarbons and also to methanol and methanol derivatives like dimethyl ether. The table below lists the potential of the various products for natural gas as fuels for advanced automotive power plants.

	<u>Fuel Cell</u>	<u>Compressor Ignition Combustion</u>
Methanol	X	
Dimethylether	X	X
Fischer Tropsch Naphtha	X	
Fischer Tropsch Diesel		X

The process for producing methanol from natural gas was described earlier. Process schemes to convert natural gas to Fischer-Tropsch hydrocarbon products all start with the partial oxidation or

steam reforming of natural gas to a mixture of carbon monoxide and hydrogen. Various process schemes have been developed and demonstrated ranging from fluidized to packed bed reactors. All depend to varying degrees on the thermal combustion of the hydrocarbon and the reforming of the hydrocarbon with steam. The product is generally a synthesis gas with a ratio of hydrogen to carbon monoxide slightly above 2.0. This mixture is then converted at 25-40 atmospheres to a hydrocarbon mixture with a carbon distribution determined by a Schultz-Flory distribution. The product of the Fischer Tropsch reaction is in most cases further processed to adjust the product distribution according to market opportunities. The product options range from waxes, lubricant basestocks, specialty solvents, diesel fuel, naphthas and liquefied petroleum gas (7).

The transportation fuel market is by far the largest since worldwide consumption is on the order of 40 million barrels a day versus less than one million barrels for lubricant basestocks. The diesel product from Fischer Tropsch synthesis is particularly attractive since it has a very high cetane number, above 75, and essentially no sulfur or aromatics. The naphthas from Fischer Tropsch is not a very attractive gasoline component due to its low octane number (less than 50) however it is a very attractive fuel for the generation of hydrogen for fuel cell powered vehicles.

The Next Steps

At the present time there are many organizations, including Exxon, actively involved in evaluating the performance of a broad range of hydrocarbons and alcohols in fuel cell and internal combustion automotive power plants. The amount of data available is limited since research on these fuel/engine combinations are at the exploratory stage. In the next two years the results will begin to emerge and the assessment of their potential can begin under a sound footing of facts. The assessment process will not be easy since it will be necessary to balance complex factors like energy efficiency, emissions, vehicle and fuel cost and infrastructure costs. In the final analysis the public acceptance of the vehicle/fuel system will determine its market impact.

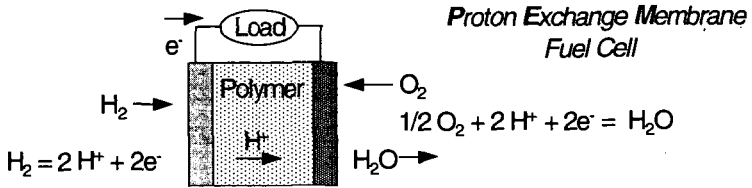
References

1. C. E. Borroni-Bird, **J. of Power Sources**, 6, 1966, 33-48.
2. K. DeJong and H. Van Wechem, **Intl. J. of H₂ Energy**, 20, 1995, 493-499.
3. Ullmann's Encyclopedia of Industrial Chemistry, 5th Edition (1990), Vol. A16, p.480.
4. A.D. Little Presentation to PNGV Peer Review Committee, October 17, 1996; also A.D. Little presentations in Proceedings of the 1995 Dept. of Energy Automotive Technology Development Contractors Coordination Meeting (Oct. 23, 1995).
5. S. Ahmed, R. Kumar, M. Krumpelt, R. Doshi, H. Geyer, and R. Ahluwalia, Dept. of Energy Fuel Cells for Transportation Exploratory R&D Review, Washington, DC, Sept. 1996.
6. PNGV Program Plan, revised edition published Nov. 29, 1995.
7. L. L. Ansell, R. F. Bauman, B. Eisenberg, and B. M. Everitt, Preprint: World Conference on Refining Technology and Reformulated Fuels, March 18-20, 1998, San Antonio, TX.

Table 1: Comparison of Net System Efficiencies

Fuel	Efficiencies			
	Fuel Production	Fuel Processor	Fuel Cell	Net Efficiency
Gasoline	0.85-0.90	0.75-0.83	0.45-0.50	0.29-0.37
Methanol	0.67-0.71	0.78-0.85	0.50-0.55	0.26-0.33
5000 psi H ₂	0.63-0.72	NA	0.55-0.60	0.35-0.43

Figure 1: Operational Principles of an H₂ PEM Fuel Cell



ROLE OF PETROLEUM PRODUCTS TO MEET CANADA'S FUTURE TRANSPORTATION NEEDS

Arun K. Palit
Sunoco Inc., Suncor Energy
Canadian Petroleum Products Institute
1000 - 275 Slater Street
Ottawa, Canada K1P 5H9

ABSTRACT

Petroleum products will continue to play an important role in Canada's transportation industry and in other sectors of the economy today and for the foreseeable future. In recent years, environmental, health and security of supply concerns have been raised about the role of petroleum products in the Canadian economy. These public concerns and actions taken by the petroleum industry are reviewed. This paper discusses the currently announced major capital spending plans underway by the Canadian oil sands crude producers that will significantly increase the flow of Canadian "synthetic" crude to the USA. Properties of oil products produced from these synthetic crudes are examined. In the future, market forces and quality requirements will determine how these synthetic crudes will be upgraded for their environmentally acceptable use as transportation fuels.

INTRODUCTION:

In recent years, concerns have been raised about the role of petroleum products in the Canadian economy. Environmental, health and security of supply concerns have led to suggestions that Canada should reduce its dependency on oil products. The purpose of this presentation is to demonstrate that, while some of the concerns are legitimate, petroleum products will continue to play an important role in Canada's transportation industry and other sectors of economy to-day and for the foreseeable future.

The paper begins by acknowledging Canadian Petroleum Products Institute's (CPPI) recognition of the environmental and social concerns that the Canadian public has about oil products. The first part of this paper labeled "Main Public Concerns and Beliefs" is our understanding of what the public is concerned about and what it believes. We then seek to put these concerns in perspective by quantifying the magnitude of the issues and referencing benchmarks. The paper demonstrates that the petroleum industry continues to take action on many of the public's concerns. It informs the reader as to the very strong economic and social benefits and the secure nature of the Canadian oil products business. The paper then discusses the major capital spending plan underway by the Canadian oil-sands crude producers which will significantly increase the flow of Canadian "synthetic" crude to the USA. We compare the favourable properties of oil products produced from synthetic crudes to the less favourable properties and conclude by noting that market forces and future quality requirements will determine how these synthetic crudes will be upgraded for their environmentally acceptable use.

MAIN PUBLIC CONCERNS AND BELIEFS

A survey of recent public opinion polls and Canadian media identify several main concerns the public has with respect to petroleum usage.

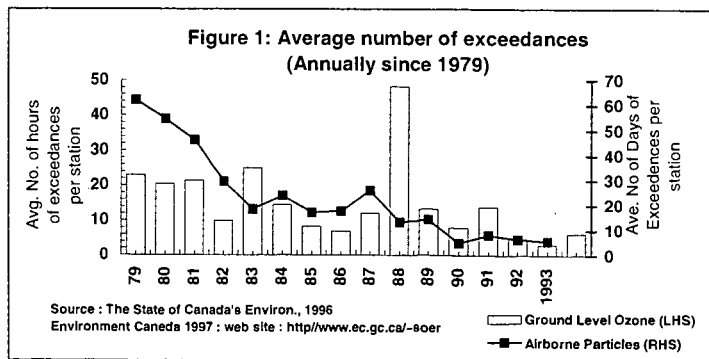
1. Pollution of air in our cities
2. Impact on personal health
3. High prices of oil products and consumer belief that prices are unfair
4. Oil spills and environmental damage
5. Global warming
6. Energy Security:
 - Do we have enough petroleum resources
 - What are the impacts from increasing demands
 - Are we using petroleum efficiently

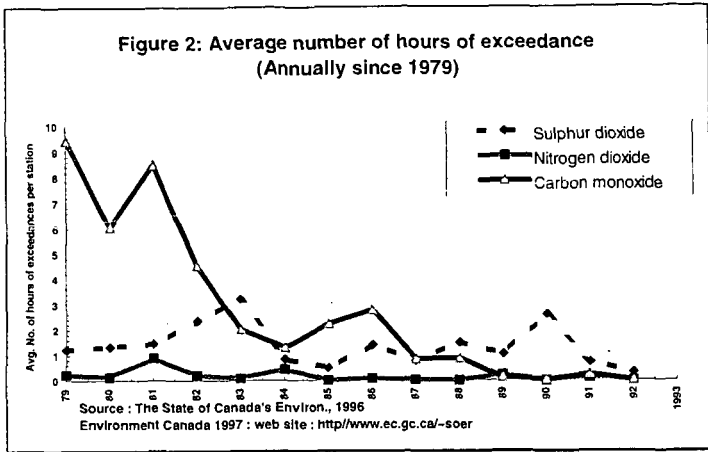
The public wants some actions now to address these concerns.

Clearly, oil products usage has an impact on urban air quality, and on air issues in general. Smog, a brown summer haze that intermittently forms over some of our cities, is comprised of ground level ozone (a combination of volatile organic compounds (VOC) and oxides of nitrogen (NOx) in the presence sun light) and fine particulates. VOCs are emissions of light volatile hydrocarbons. The transportation sector (that is the industry plus the end users) is responsible for the majority of the VOCs and part of the NOx. The government has declared that over half of the Canadian population is periodically subjected to unacceptable ozone levels. Smog causes respiratory impact on humans, particularly the young and elderly as well as damaging forests and crops. Transportation sector also contributes to sulphur oxides (Sox) emission which in combination with NOx forms acid rain, that is associated with injury to marine life and vegetation. Heavy fuel oil burned in refineries and commercial heaters and boilers also adds to Sox emission. People are concerned that the air quality is bad and is getting worse due to urban growth. Similarly, oil products use can be linked to other human health issues. Carbon Monoxide (CO), a product of incomplete combustion of carbon based fuels, is a hazardous pollutant and causes oxygen deficiency in human lungs. Major portion of CO emissions are related to the transportation sector. Gasoline contributes to most of man-made benzene emissions through evaporative and exhaust emissions from engines. Benzene is a cancer causing substance. Fine air borne particulates of microscopic size (less than 2.5 microns) from the transportation sector is a complex mixture soot, ash, metals, salts and acid. It has recently been associated with respiratory illness and premature deaths. People believe that oil products and their use are harmful to human health. Transportation cost, including petroleum products, is a major element of consumer spending, equaling food and greater than clothing. Gasoline price is an item of major debate. Most consumers do not understand why prices seem high, vary throughout Canada, are uniform all over a given market. People are concerned that there have been large international petroleum spills. Volume of transported oil is large, there have been some major international marine incidents and local spills continue to occur. People wonder whether the standards are too lax and will the industry ever improve its track record. Global warming is blamed for increased frequency of hurricanes, floods, fire, draught, loss of shoreline and such diseases as malaria. People believe that increasing emissions of greenhouse gases (GHG) are leading to global warming. In their mind they question the sustainability of fossil fuel burning, as over 75% of carbon dioxide, a leading greenhouse gas, comes from fossil fuel use. Finally, the public believes that we may be selfishly wasting petroleum, a precious non-renewable resource, thus depriving the future generations of its effective use. Overall, while oil products are central to modern life, public concerns about their use and effects are understandable and need to be addressed.

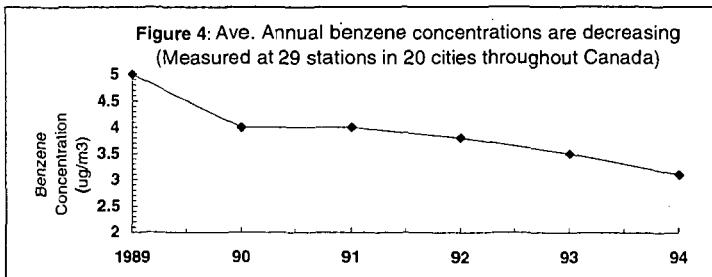
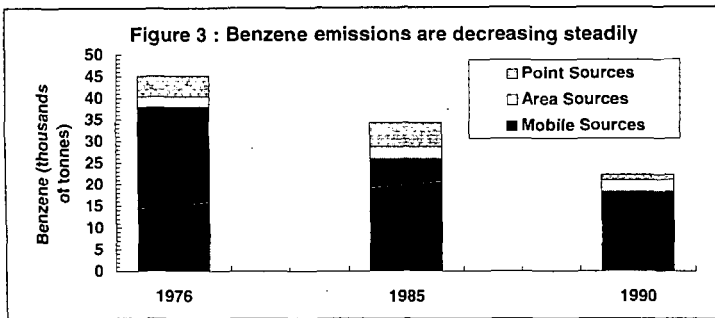
THE DIMENSIONS AND SCIENTIFIC ASPECTS OF THE PUBLIC CONCERNS

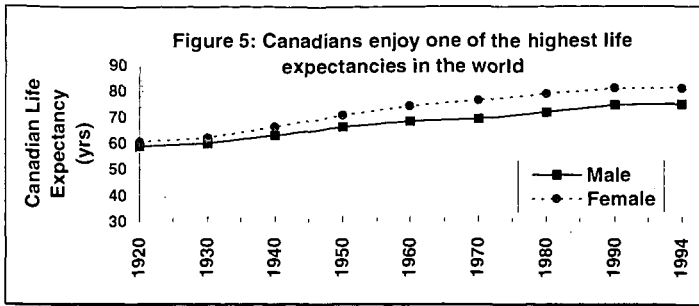
In fact, the Canadian air quality is very good and is getting better, but progress needs to continue. The figures below demonstrate that the average levels of pollutants measured in major cities throughout Canada are generally coming down (Figures 1, 2). Similarly, health issues related to oil product use will continue to diminish by sustained industry efforts to reduce toxic releases and reformulated oil products..





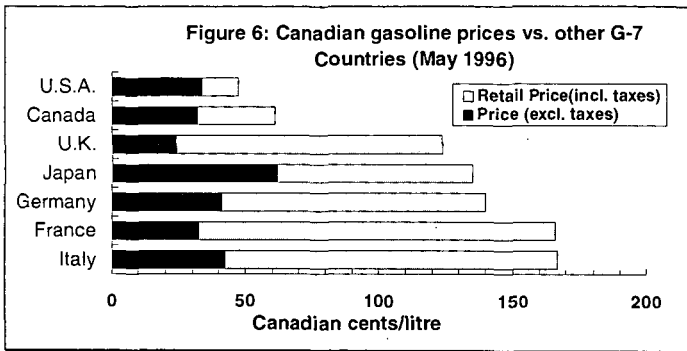
Canadians are fortunate to live in a beautiful land of great natural resources and to be among the healthiest people on earth (Figures 3,4,5). Gasoline is reasonably priced in Canada.



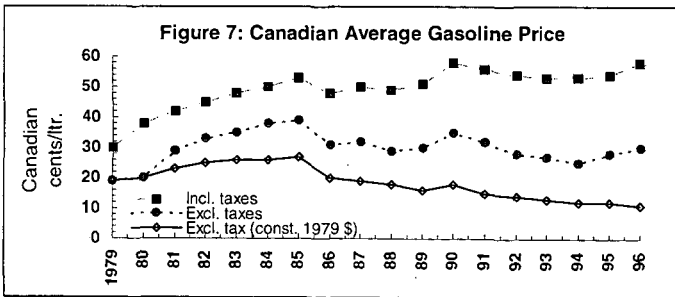


Source : Statistics Canada. Cat. 82-221-XDE

The Federal Competition Bureau has found through many investigations that our products are competitively priced. Canadian gasoline prices are lower than most G-7 countries. In fact, in real terms, gasoline prices have gone down (Figure 6, 7).



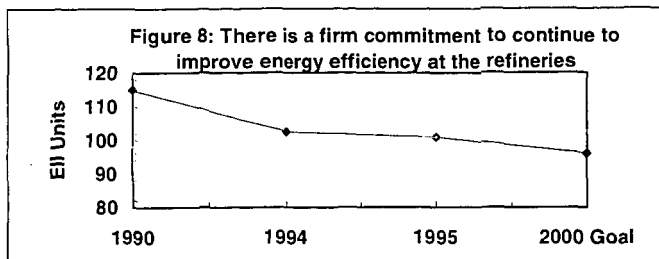
Source : Petroleum Communications Foundation, Gasoline Price Report, 05/28/96



Source : Sector Competitiveness Framework Study, 1994, Petroleum Communication Foundation, 05/28/96

To date, the size and the extent of Canadian spills cannot be compared with major ocean tanker disasters. The Canadian industry's goal is to achieve zero spills. Marine response continues to be a high priority for the industry. Three new response organizations became fully operational in 1995. Global climate change is an environmental issue with economic, social and trade dimensions. For sustainable development, these multi-dimensions need addressing in an integrated way considering Canada's unique national circumstances. Large, short term GHG reduction targets through limits on petroleum fuel use would significantly impair the Canadian economy. Climate change is a complex long term issue and the supporting science is still emerging. However, CPPI believes that reasonable steps can be taken meanwhile. Considering the impact that climate change actions would have on jobs, economic growth and deficit reduction, this long term issue needs flexible

long term goals as well as realistic short term targets. CPPI supports and is active on voluntary measures, improved energy efficiency (Figure 8) both in our operations and nationally through customer education.

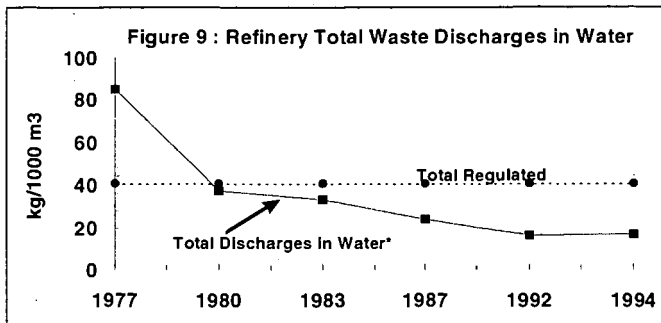


Source : CPPI 1995 Environmental and Safety Performance

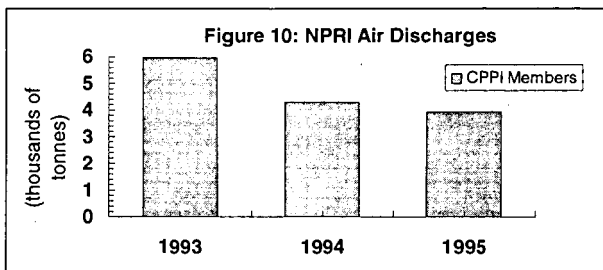
To achieve long term goals, CPPI supports R&D that allows emergence of new economically viable technology and reduces scientific and economic uncertainty as well as flexible policies which allow economic turnover of capital stocks towards least cost solution. Canada has abundant petroleum resources, proven hydrocarbon reserves which can be economically produced and the country is a net oil exporter. Canada has more oil in our oil sands than all the Mid-East combined. The industry is progressive, is a world leader in technological innovation and has increased investments and exploration activities which will extend the useful life of Canadian petroleum resources. In summary, the environmental issues and other public concerns surrounding oil products may not be as significant as one would initially suspect, but the industry need to continually improve its performance.

THE RECORD OF OIL PRODUCTS INDUSTRY IN RECOGNIZING AND RESPONDING TO ENVIRONMENTAL AND SOCIAL CONCERNS

Canadian oil products companies have continued to improve the environmental quality of products and operations to meet and better cleaner air goals. Some examples of the improvements are : gasoline reformulation to meet tough national standards to combat air pollution (1995), reduced gasoline volatility during the summer nationwide (1990), introduction of cleaner burning gasolines with deposit control additives (1985), gasoline vapour recovery implementation at terminals and other storage facilities (1991), national program for low sulphur diesel introduction (1994), fuel efficient lubricating oil introduction (1987) etc. Many changes are progressing in our manufacturing, oil product movement and retail operations. In refining facilities, fugitive emission control, enhanced sulphur recovery and flare minimization, toughest water effluent quality standards in the world and reduction of toxics are being achieved. In the area of oil and products movements we are trending towards double hull vessels to minimize spill impacts, pipeline leak detection systems, gasoline tank truck driver certification, and marine oil emergency plans are some areas to note. In retail operations we should list areas such as vapour recovery during gasoline delivery, replacement of underground tanks with new double walled fibreglass tanks, improved leak detection, ground water monitoring and contaminated soil remediation. We have significantly improved the environmental performance in areas such as refinery discharges to air and water. The bottom line is that the oil industry has recognized the importance of environmental issues and has taken real actions to improve performance of its products and operations (Figures 9,10).



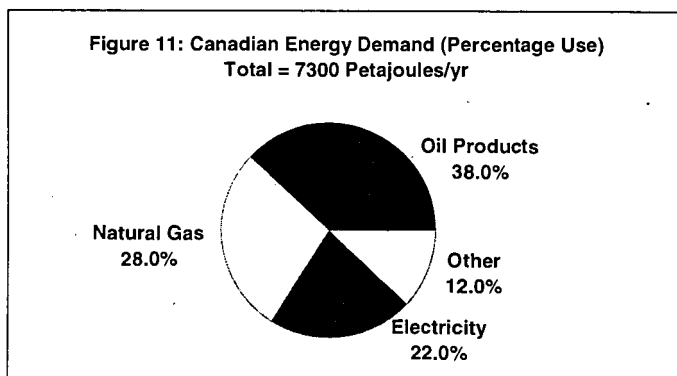
Source : CPPI, First Annual Performance Measures Report, April 24, 1996, P13



Source : CPPI Environmental and Safety Performance

THE IMPORTANCE OF THE PETROLEUM PRODUCTS INDUSTRY TO THE CANADIAN ECONOMY

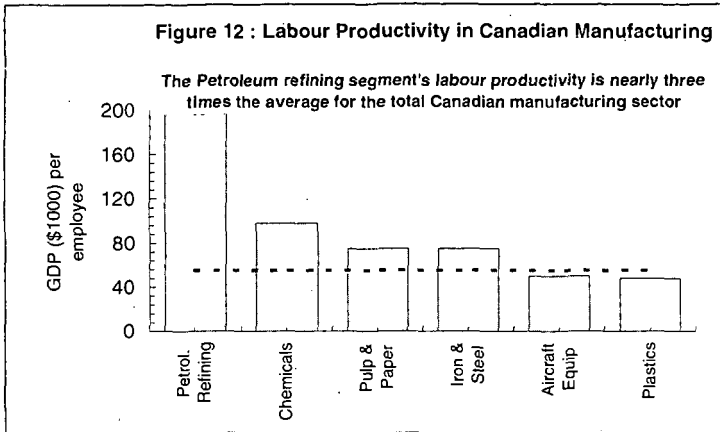
Oil products represent more than a third of Canada's current energy usage (Figure 11) and meet 98% of our transportation fuel needs. In fact, petroleum products are the competitive market place energy choices in most sectors of the Canadian economy. Given our vast size, climate and resource based economy, Canada is a high energy intense country.



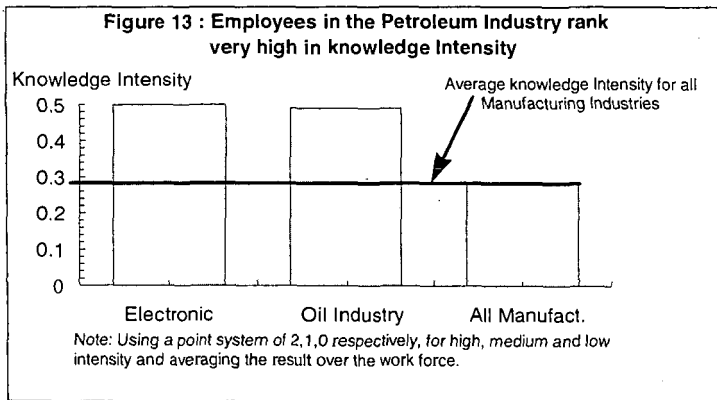
Source : Energy Efficiency trends in Canada : NRCan, April 1996, pp.85

However, Canada has the most diverse energy mix of the G7. The petroleum refining segment's labour productivity is nearly three times the average for the total Canadian manufacturing sector. In today's market, compared to other alternative fuels, oil products are the lowest priced transportation fuel on a pre tax basis. Taxes on the activities and products of the Canadian downstream industry are a major source of revenue to the

Canadian governments. Based on performance, reliability, safety and performance, Canadian consumers have made a substantial investment in vehicles and facilities designed to use oil products. The oil products industry is also a significant source of employment and highly skilled value adding jobs. Overall, the oil products industry is an important element of the Canadian economy, and is well positioned to meet Canada's energy needs (Figures 12, 13).



Source : Infometrics Limited, SCF Petroleum Products Part 1, 1996



Source : Sector Competitiveness Framework, Part I, 1996;
 Statistics Canada Census Data 1986-91

CANADIAN OIL SANDS SYNTHETIC CRUDE INDUSTRY

In 1996, Canada produced over 150 million barrels of oil from Alberta's oil sands which is equivalent to about 20% of Canada's crude oil production. Alberta has over 300 billion barrels of recoverable reserves in the oil sands deposits, greater than all the Mid East combined estimated reserves. Several companies have announced mega-plans for increased production of crude and bitumen blends from Canadian oil sands (Table 1). Projected investments of CS 25 billion by 2020 is expected to triple Canadian oil sands crude and bitumen production. A significant portion of the existing oil sands production and the expanded production will be supplied to the USA. Synthetic crude end products qualities are different from conventional crudes. The favourable properties of oil products produced from synthetic crudes are compared to the less desirable properties (Table 2). Market forces and future quality requirements will determine how these synthetic crudes will be refined to supply the fuels for the year 2000 and beyond.

TABLE 1 : MAJOR EXPANSION PLANS FOR OIL SANDS & HEAVY OIL

Company	Announced Capital (Billion \$C)	Comments
Suncor	2.2	Expands Capacity from 105,000 bbl/d to 210,000 bbl/d
Shell	1.0	Bitumen Production capability : \$375 MM for a Heavy Oil pipeline to its refinery in Edmonton & additional capital for Upgrader
Mobil	1.0	Bitumen production within next five years
Syncrude	3.0	Expands capacity from 208,000 bbl/d to 312,000 bbl/d
Koch	1.0	90,000 bbl/d of new bitumen facility by 2004
Amoco, Pan Canadian, CS Resources, Gulf, Imperial Oil, Elan etc.	2.5	Various announced projects in Alberta
IPL Energy	0.3	Pipeline to carry Suncor's products

TABLE 2 : SYNTHETIC CRUDE & PRODUCT QUALITIES DIFFER FROM CONVENTIONAL CRUDES

Desirable Features	Less Desirable Features
<u>Whole Crude</u>	
<ul style="list-style-type: none"> ■ Low Sulphur 0.1 - 0.3 % ■ Low Bottoms ■ Very Low Corrosive Contaminants ■ High Gas Oils 	<ul style="list-style-type: none"> ■ Diesel Cetane ~ 33 - 38 ■ Low Jet Smoke Point ■ High Diesel Aromatics ~ 45 % ■ High VGO Aromatics ~ 60 %
<u>Distillate Cut</u>	
<ul style="list-style-type: none"> ■ Low Sulphur ■ Low Pour Point < - 65 °F ■ Excellent Freeze Point & Cloud Point 	

ACKNOWLEDGEMENTS

The author wishes to acknowledge Ray Burton (Imperial Oil Ltd.), Gene Carignan (Petro-Canada), Gerry Ertel (Shell Canada Products Ltd.), Bruce Orr (Imperial Oil Ltd.) and the Canadian Petroleum Products Institute for their work on the original internal CPPI position paper which formed the basis of this article.

REQUIREMENTS FOR THE FUTURE AVIATION JET FUEL TO BE DEVELOPED BY MOLECULAR ENGINEERING OF LIQUID HYDROCARBON FRACTIONS

Jouni Enqvist, VTT Chemical Technology, P.O.Box 1402, 33101 Tampere, Finland and
Maarit Enqvist, J&M Group Ky, P.O.Box 61, 33960 Pirkkala, Finland

Abstract

Requirements for the molecular basis of the future aviation jet fuel will be discussed and the work going on in Finland for this goal will be reviewed. The most important environmental aspects are efficient combustion performance for suppressing formation of toxic compounds like nitrogen oxides and certain polycyclic aromatic hydrocarbons. The most harmful uncompleted combustion products are carbon containing nanoparticles that contain adsorbed nitrogen oxides and carcinogenic aromatic compounds. Therefore fuel combustion cleanliness is one of the most important goal in our investigations not only because of our health but also because of the cleanliness of critical fuel system components and the engine. These objectives together with the need of adding molecular specifications for the future fuel are discussed.

Introduction

The most important requirement for the future aviation jet fuel is to conserve the existing operational and handling safety of the present kerosene based fuels. Hydrogen and other gaseous or liquid low-boiling fuels require much more efforts to prevent fuel leakages and other safety arrangements in any accidental functional problems of the fuel system. Therefore, it is very likely that the jet fuel beyond the year 2000 will be a modified kerosene manufactured from crude oil, natural gas, coal or any carbon and hydrogen containing stock or waste material. This solution would be the most efficient for every day air traffic with jet engine air craft and also for the majority of the military air craft.

The necessary practical properties specified or otherwise important for commercial and military fuels like necessary chemical, physical and biological stability, clean combustion for the engine and environment, lubricity and corrosion prevention for the fuel system, conductivity to prevent electrical discharges, proper viscosity in different temperatures, proper temperature conductivity and cooling capacity for engine lubricant and other fuel cooled aircraft components and finally anti-icing property to prevent formation of ice crystals at low temperatures are presently obtained by formulating the kerosene fraction with several approved additives. In the future the above properties of the fuel will be most likely introduced to the kerosene in the fuel processing and therefore no or much less additives would be needed. This approach will simplify the fuel handling and logistics because specific fuel properties can be tailored in the refineries by molecular engineering of the kerosenes. There are several advantages of this approach because water separation will become unnecessary due to the controlled water solvating properties of the fuel and fuel compatibility with different types of engines, fuel system seals and any acceptable operating conditions.

The aim of this paper is to describe requirements for the future kerosene fuels on the basis the research work carried out several years in Finland and recently in a close cooperation with Finnish Air Force. The general approach has been to investigate and develop analytical methods for complete characterization of each of the hundreds of energy producing compounds of kerosenes as well as molecular structure and reaction mechanisms of natural and additive trace compounds that make kerosenes acceptable as the specified Jet A-1 or JP-8 fuels.

It is natural that new molecular specifications are needed in the future to achieve the perfect control of fuel performance in all conditions. Therefore, another goal of our research work is to develop chromatographic conditions for adequate separation of all jet fuel compounds that have significance on fuel behavior and specifications and, on the other hand, the development of retention index library for fuel compounds to make possible in the future an automated monitoring of molecular specifications of jet fuel compounds for principal energy producing molecules and for principal trace property molecules like stability, combustion, lubricity, anti-icing, conductivity etc. The complexity of kerosene fuels requires the use of hyphenated techniques like the two-stage retention index monitoring HRGC (RIM/RIM) method what we

have earlier used for monitoring benzene from gasoline. In development of RIM/RIM library mass spectrometric detection is necessary together with the high field NMR analysis of fuel fractions. The routine system would however be most likely based on HRGC/RIM/RIM with flame ionization detection (FID).¹⁻³

Experimental

Several Jet-A1 and JP-8 samples based on different kerosenes were analyzed using high resolution gas chromatography (HRGC), HRGC-mass spectrometry (MS) and high field nuclear magnetic resonance (NMR) spectrometry methods. Instruments used were Micromat HRGC 412 with two 15 m capillary columns (a cyanopropyl NB-1701 and a phenyl methyl silicone NB-30) and two flame ionization detectors (HNU Nordion) and Hewlett-Packard HP 5890 GC with HP 5970A Series Mass Selective Detector (MSD). Some samples were analyzed just as obtained from the refinery (Neste Oy), some of samples were of different age (Finnish Air Force) and one sample (Sabena Air Lines Depot) was allowed to stand up to two and half years before analysis. Some samples were also oxidized by bubbling air or oxygen through the fuel to follow the formation of oxidation products.⁴ NMR instrument used was Varian Unity 600 operating at 600 MHz for protons and at 150 MHz for carbon-13 measurements.

Results and Discussion

Jet fuel specifications were studied with the objective of elucidating chemical reaction mechanisms and physical interactions that determine the behavior of fuel as whole material and how individual major and trace compounds produce this bulk behavior for the fuel. Because some natural trace molecules and additives are extremely important in fuel performance careful library and patent search was carried out about these molecules and their functioning in combustion and fuel system was elucidated together with our own experimental work.

The most important result of this work is the critical evaluation of environmental aspects of jet fuel combustion. A conclusion was made on the basis of medical reasons. It is known that combustion exhaust of jet engine produces more or less small particles and gaseous contaminants from which nitrogen oxides and some polycyclic aromatic hydrocarbons are the most harmful. Amount and quality of these harmful exhausts depend on type and functioning of engine and amount of power taken from the engine at a moment of time and also on the chemical composition of the fuel.

While carbon dioxide has also been mentioned as a harmful exhaust it is not toxic and we consider it therefore as of the secondary importance. A sooting flame of jet engine produces visible particles of micron size or more but a non-sooting flame may also produce small nanometer scale particle that are not visible but may be even more harmful because of larger surface area which may be occupied by carcinogenic molecules. Therefore in the future the combustion should be perfect with any type of engines, with single or two-stage combustion zones, producing only carbon dioxide and water as the combustion products. This means that both the future engines and future fuels should be optimized and jointly developed. The fuel should be free of harmful trace elements and contain structural groups which enhance clean and efficient combustion without producing harmful deposits or other products.

Another important fuel property is its lubrication capability. Fuel is the only lubricant of fuel pumping system and the whole line of fuel system components up to the injector nozzle. It should therefore have an adequate corrosion inhibition and boundary lubrication behavior which works mainly through surface active alkyl phenols and carboxylic acids derivatives which are natural or additive trace molecules. We have studied commercial diesel fuels for boundary lubricants and use this data also for designing adequate lubricity for the future green jet fuel.⁵

Autooxidative, surface catalytic, pyrolytic and mechanochemical stability of fuel at high temperatures and the other necessary properties should on the basis of the above discussion be obtained by molecular tailoring of the fuel production process. With the present knowledge about catalysis these process modifications are realistic and cost effective so that production costs of the future green fuel will not be significantly higher compared to the present fuels.

To guide this work and also to make possible future fuel quality monitoring molecular specifications are needed and for this purpose we develop an automated sample preparation HRGC-RIM/RIM -system that can be used by oil companies, air line companies and military operators. Molecular procedure based on high field NMR and HRGC are being developed to

automatically determine combustion index, lubricity index, and fuel stability index from the analytical data. These figures are naturally calibrated with bulk property tests which data are used for refinement of fuel specification index calculations. This research and development work is going on in Finland and the first results will be a prototype green fuel according to the above guidelines and a prototype molecular level fuel analyzer.

References

1. Enqvist J., "Kinetic study of complicated reactions by glass capillary gas chromatography.", Symposium on Chromatography, Kemia Pääväät 77, Kemia-kemi 4 (1977) Nr 11.
2. Hesso, A., Siivinen, K., Enqvist, J. and Kuronen, R., "Interphasing of capillary columns to a mass spectrometer; influence of vacuum on the separation efficiency.", Symposium on Separation and Fractionation Methods in Chemistry, Kemia Pääväät 79, Kemia-Kemi 6 (1979) 12.
3. Enqvist, J. and Enqvist, M. "Comparison of two-stage retention index monitoring capillary gas chromatography and selected ion monitoring capillary gas chromatography - mass spectrometry as analytical tools", Journal of High Resolution Chromatography. Vol. 17 (1994) Nr: 3, pp. 141 - 144
4. Enqvist, J., Ranta, E. and Enqvist, M., "Characterization of Autooxidation Products of Aviation Jet Fuels by Gas Chromatography coupled with Mass Spectrometry. Preprints of the 215th ACS National Meeting, March 29 - April 2, 1998, Dallas, Texas.
5. Enqvist, J., Östman, P., Enqvist, M. and Wickström, J., "A High Resolution Gas Chromatography - Mass Spectrometric Selected Ion Monitoring Method for Determination of Boundary Lubricating Molecules in Cleanly Burning Diesel Fuels", ACS National Meeting at Boston, August 23-27, 1998. Symposium on Chemistry of Diesel Fuels, Division of Petroleum Chemistry.

A Perspective on Coal in the 21st Century

By

Craig Vogel
Manager, Technical Marketing
Cyprus Amax Coal Company

Abstract

Coal represents 95% of the United States fossil energy reserves and U.S. coal resources represent more energy than either world oil or natural gas reserves. Coal fired power plants currently produce 56% of U.S. electrical generation. Increasingly more stringent environmental standards for SO₂, NO_x, and mercury are putting pressure on future coal use. With current and evolving technologies, coal should be able to meet these new challenges and remain competitive with other generation options such as natural gas. There is, however, a major obstacle that severely threatens use of coal in the future. The issue of global climate change and corresponding requirements for CO₂ reductions present a major hurdle for the coal industry as we look towards the next century.

This paper presents a discussion of historical and projected electrical generation and fuel sources. It looks at technology options that will be cost effective and comply with increasingly more stringent environmental standards. Also, the issue of climate change and how coal could be affected by actions such as the Kyoto Protocol is presented.

Discussion

Coal currently is responsible for 56% of total electrical generation in the U.S.; natural gas, 13%; nuclear, 17%; hydro, 9%; renewables, 3%; oil, 2%. In EIA's 1998 forecast, coal is expected to grow at about 1% annually but will decrease its share of generation to 47% in 2015. Through retirements, nuclear's share decreases to 10%. Oil and hydro retain the same amount of generation but their contributions decrease to 1.5% and 7% respectively. Use of renewables increases slightly but its share remains around 3%.

While coal use increases, natural gas is forecast to be the big winner. The reason for this is partially due to the low capital costs of combined cycle gas plants and their attractive heat rates. The "wild card" is natural gas deliverability to utilities and delivered prices, which are assumed to increase only slightly from \$2.28/mmbtu in 1996 to \$2.74/mmbtu in 2015. Given natural gas' track record, these assumptions appear optimistic.

Comparing electricity prices for different regions we find that areas with the highest coal-fired generation have the lowest cost power. Interior regions relied on coal for 70% of generation in 1995 while coastal regions used 35% coal firing.

Lower cost coal fired generation has also resulted in increasing coal plant capacity factors.

The increasing concern over global climate change and carbon emissions reduction poses a significant threat for coal's future. Electric generation contributes about 36% of U.S. CO₂ emissions with transportation providing 33%. Both sectors are forecast to increase their emissions, however, due to the public's love affair with larger and less efficient vehicles, electrical generation may be called upon to bear a disproportionate amount of any required CO₂ reductions.

The Kyoto protocol requires the U.S. to reduce its carbon emissions to 7% below 1990 levels by 2008. This would require a 44% reduction from projected "business as usual" emissions in 2010.

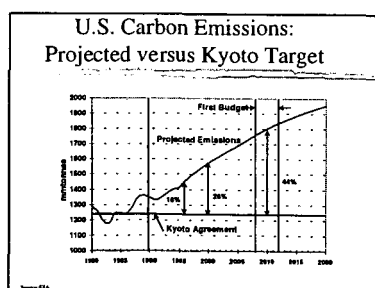
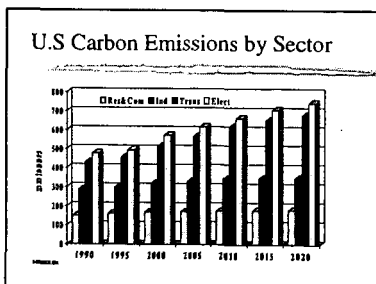
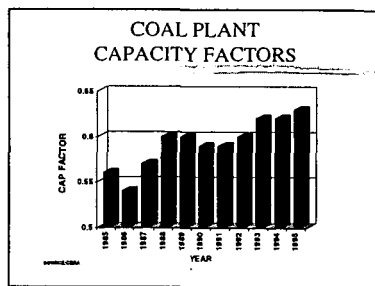
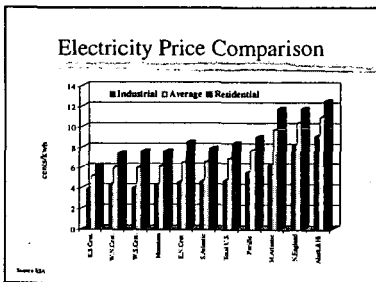
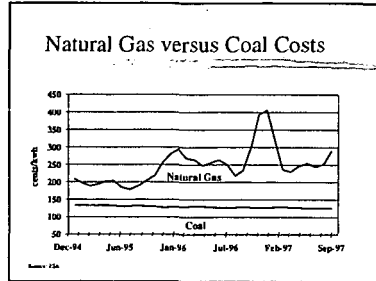
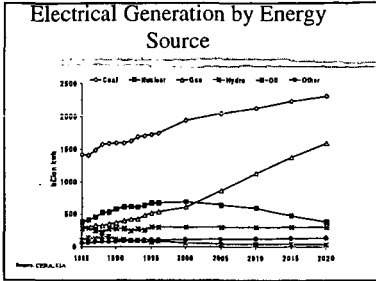
Historically, since 1970, the United States has had an average electrical growth rate of 3.14%. GDP has grown at a rate of 2.69% during this same period resulting in a ratio of electrical growth to GDP of about 1.2 to 1. U.S. total energy use grew at a rate of only 1.29%, about half that of electricity. This indicates that we are experiencing greater electrification. In 1995-96, the electrical growth to GDP ratio was 1.3 to 1. EIA's 1998 forecast assumes an increase in efficiency of more than 40% from today. This results in electrical growth to GDP ratio decreasing to 0.83 to 1 by 2000 and 0.73 to 1 by 2020.

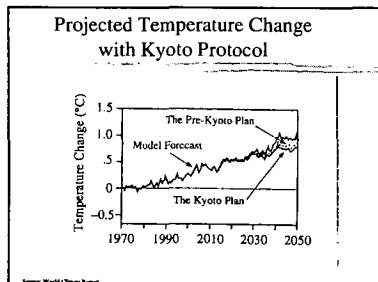
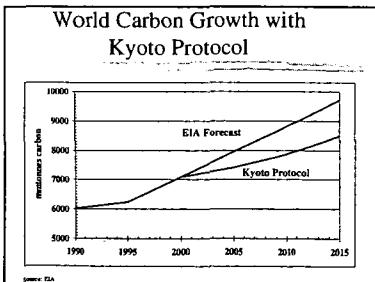
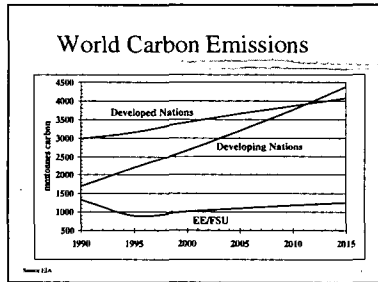
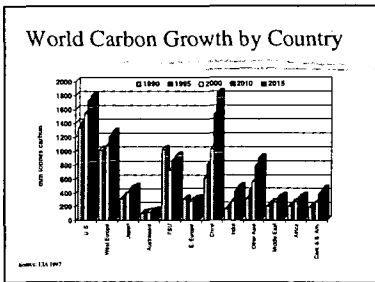
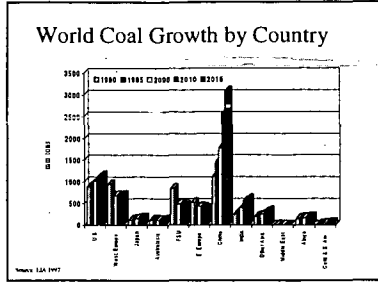
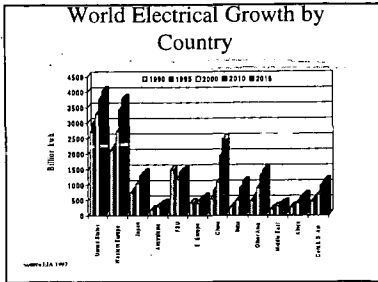
Since coal is carbon based, even with more efficient power plant designs such as the LEBS, with its 45% efficiency, coal emits twice as much CO₂ as a natural gas fired combined cycle gas turbine. Existing coal-fired plants can do little to improve efficiency to any great degree.

On a global basis, it is important that new technologies be continued to be developed and implemented for it is the developing nations that hold the key to future carbon emissions. While

the U.S. is clearly the largest emitter of carbon on both an absolute and per capita basis, projections show China to surpass the U.S. by 2015.

If the Kyoto Protocol were to be implemented, it would have little effect on global concentrations of carbon and projected global temperatures. It would have significant effects on the U.S. economy and would likely shift emissions from the U.S. to those countries not bound by the treaty. It would also prevent development of more efficient coal fired generation technologies that would help the third world nations as they grow their economies.





AUSTRALIAN FUELS, ENERGY, AND GREENHOUSE GAS EMISSIONS: IMPLICATIONS FOR THE 21ST CENTURY

B. C. Young, D. J. Allardice, and J. R. Hamilton
HRL Technology Pty Ltd, Mulgrave, Victoria, Australia 3170
ACS Paper, Boston, August 1998

INTRODUCTION

Australia with a population of only 18 million has abundant reserves of black and brown coal/lignite (hereafter referred to as brown coal), and substantial reserves of oil, natural gas, and uranium. Being a very large temperate-to-sub-tropical continent covering 7,682,300 km² (Australian Bureau of Statistics [ABS, 1997]), approximately equivalent in area to that of the continental U.S., Australia experiences abundant sunshine and significant windy regions. These natural characteristics along with the fossil fuels already mentioned, signifies the country as energy resource rich. As a consequence of its fossil fuel resources and its large reserves and diverse range of minerals, Australia has become both an export supplier of raw commodities, such as coal and iron ore, and of secondary processed materials, such as aluminium ingots and uranium yellowcake. These mining and mineral processing developments, along with the increased infrastructure and industrial, commercial, and domestic demands, and the large travel and transport distances, particularly over the last 25 years, have resulted in the country's greenhouse gas emissions being among the highest in the world on a per capita basis, (1.4 % of global greenhouse gas emissions [Skelton, 1997]).

This paper addresses fossil fuel resources and other energy sources in Australia, electricity generation and energy consumption, greenhouse gas emissions, and recent economic and structural changes in the electricity and gas industries. Issues to be briefly considered include new energy technologies, fuel alternatives, CO₂ reduction strategies, and future energy developments.

FOSSIL FUELS AND ENERGY SOURCES

By far the largest of Australia's fuel resources is coal, including bituminous, sub-bituminous, and brown coal, the resources of which are shown in Table 1. Australia is the world's largest exporter of black coal, exporting almost 146 million tonnes in 1997 (Australian Bureau of Agricultural and Resource Economics [ABARE, 1997]). It ranked as the fifth largest producer of hard coal in 1996 (World Coal Institute web page). In 1997 production was 6.7 % higher than that in 1996 at 207.5 million tonnes. The large black coal resources, mostly bituminous, are found in Queensland and New South Wales (NSW). Much smaller quantities of sub-bituminous coal exist in Western Australia, Queensland, and NSW. Brown coal is substantially located and mined in Victoria and lesser quantities in South Australia. This resource represents about 27 % of the Australia's total energy reserves.

Table 1 also shows the currently reported resources of gas, oil, and uranium. Australia is the second largest producer in the world of uranium (Uranium Institute, 1997) but it uses no uranium domestically for generating electricity. Self-sufficient in oil to the extent of 73 % at present, Australia is predicted to see a decline in self-sufficiency to about 61 % in the next five years, assuming no discovery of a major oil field [Private Communication, 1998]. Natural gas is produced in significant quantities on-shore, mainly in South Australia, Northern Territory, and Western Australia, as well as off-shore Victoria and Western Australia where the gas fields are much larger than on-shore. Significant quantities of liquefied natural gas are shipped in cryogenic form overseas but within Australia gas is the predominant fuel for domestic and industrial applications.

Australia's latitude enables it to receive monthly mean daily solar irradiation ranging from a minimum of 5.0 MJ/m² in Hobart and Launceston, Tasmania to a maximum of 31.0 MJ/m² at Geraldton, Western Australia, (Lee, Oppenheim and Williamson, 1995). Its solar potential is under utilised for energy generation but significant use is made of it for drying and heating purposes by the agricultural and chemical industries, e.g. for bagasse, salt, and by the domestic sector, e.g. for clothes drying, hot water systems. Australia is largely a dry continent, exhibiting substantial hot regions and variable but not extensive rainfall, from a minimum median annual rainfall of 100 mm at Lake Eyre in South Australia, to a maximum median annual rainfall of 4,048 mm at Tully in Queensland (ABS, 1997). These conditions along with extensive land clearing have led, in general, to sparse tree cover in areas beyond a relatively narrow strip around the eastern and southeastern seaboard and the island state of Tasmania.

Significant wind energy sources are located around the Australian mainland coast and southern islands, e.g. Tasmania, King Island, Lord Howe Island. Typically at selected points the wind speed will exceed 6 m/s at a height of 10 m, sufficient for a sustainable wind energy farm [Osborne, 1993].

Apart from solar and wind energy, other renewables available as energy sources in Australia are biomass and hydro. Particularly for Queensland, NSW, and Tasmania, there are significant quantities of bagasse from sugar cane production and other agricultural residues (e.g. cotton trash), forestry residues, saw mill waste, and municipal wastes (Spero, 1998). However, they are small in relation to the coal reserves and suffer from large volume to mass ratio, big distances between recovery points and end usage location, and consequently often greater cost and seasonal variability.

ELECTRICITY GENERATION AND ENERGY CONSUMPTION

Current electricity demand in Australia is around 160,000 GWh per year. Growth rate in electricity demand over the last decade has been 5 to 7 % per year [Schaap, 1998]. A lower growth rate is likely over the next decade, although the power demand in the manufacturing and commercial sectors is projected to be higher than that in the residential sector.

On a national basis the electricity generation supply mix is shown in Table 2. However, on a state by state basis there are significant variations, e.g. in Queensland and NSW 98 % and 93 % respectively of electricity generation is coal based; in Tasmania, virtually 100 % is based on hydro (Electricity Supply Association of Australia Limited, [ESAA, 1997]).

Brown coal, containing between 60 % and 70 % water, is Victoria's major fuel source for generating electricity, representing 97 % of the supply mix and producing 39,755 GWh in 1995/96 (ESAA, 1997). Victorian brown coal is also used to make briquettes in a cogeneration plant having a capacity of 1.2 million tonnes although recently operating at about half that throughput. The briquettes are used for steam raising, heating, and electricity generation by industry, hospitals, and residential homes (heating/cooking). A significant proportion of the production is exported to niche markets including Germany. The advantages of this solid fuel are low NO_x and SO₂ emissions on combustion, relatively low moisture (13-14 wt %) compared to the parent coal, very low mineral matter content (<2 wt %), ease of ignition and good combustion in a conveniently transportable solid form. Although the coal is reactive in the dried form, the briquettes can be safely stored and shipped in bulk to markets as far away as Europe.

Considering total energy consumption, it is noted that in 1995-96 the three dominant and virtually equal sectors are electricity generation, transport, and manufacturing at 26.9 %, 26.2 %, and 25.5 % share respectively. Far lower proportions of energy were consumed in the residential, mining and commercial sectors at 8.1 %, 5.1 % and 4.2 % respectively; the agriculture and other sectors were 1.5 % each. Over the next decade, the three major sectors are predicted to have similar shares of energy consumption but the mining sector will grow (to 6.5 %) and the residential decline (to 6.9 %) [Private Communication, 1998].

GREENHOUSE GAS EMISSIONS

Strategies for controlling and reducing greenhouse gas emissions are now receiving increased attention, especially in view of the recent Kyoto Greenhouse Summit in November 1997. In 1994, stationary energy (i.e., largely for power generation) produced 37 % of the total of CO₂-equivalent greenhouse gas emissions in Australia whereas the transport sector generated slightly less than a third of this amount (ESAA Greenhouse Challenge Workbook, August 1997). Given the commitments from Kyoto, and the Australian Federal Government Greenhouse Challenge Program, activities are in progress that are likely to change the type, mix, and use of fuels, as well as the implementation of new technology, as Australia enters the next century. The Australian Federal Government has also made a commitment to redefining strategies for land use clearing and forestry as well as defining objectives and offering incentives to enhance the use of renewables towards achieving a net reduction in Australia's release of CO₂, methane and other greenhouse gases. To stimulate the use of renewables, the Australian Government, for example, has set as a requirement an additional 2 % of electricity to be derived from renewable energy by 2010.

Already, efforts to increase efficiency of current plant equipment, and the installation of more efficient technology have begun as a means of reducing greenhouse gas emissions. For example, in Victoria, HRL Limited has anticipated the need for higher efficiency in future brown coal use (and low rank coal, in general) for electricity generation and has just completed a 3.5 year-development project, investigating the innovative technology of Integrated Drying Gasification

Combined Cycle (IDGCC) [Johnson et al, 1997]. The IDGCC concept essentially replaces a separate atmospheric pressure dryer before the gasifier and a high pressure gas cooler after the gasifier with a direct contact entrained flow dryer, which is a high-pressure pipe. Increased generation is achieved in the gas turbine cycle by the additional mass flow of the evaporated moisture passing through the turbine. The process is schematically shown in Figure 1. The project successfully demonstrated at a 10 MW scale a 20-30 % improvement in efficiency and a corresponding reduction in CO₂ emissions and cost over conventional thermal power generation using the same coal.

Other efforts to reduce greenhouse gas emissions have included the development and demonstration of photovoltaic receptor arrays and wind farms, albeit on a small scale at this stage. One Australian company, Pacific Solar, aims to construct its first facility for making 20 MW per year of photovoltaic modules in 1999 and be in operation by the last quarter of 2000. This first facility will produce, through a radically different manufacturing process, sufficient relatively low cost solar modules to meet the demands of 7000 homes per year, representing under 5 % on average of Australian homes built each year. The target installed cost is to be competitive with the current delivered price of conventional electricity in Australia (AUD 10-15 cents per kWh) [Lawley, 1998].

Wind farms are also on the agenda for achieving greenhouse gas reduction in Australia. States including Western Australia, N.S.W., Victoria and Tasmania have active programs, privately and publicly sponsored, to produce electricity from wind turbines. In Victoria, for example, a private company, Energy Equity Limited, has recently been granted approval to build Australia's largest renewable energy project excluding hydropower. Subject to resolving local objection, the company will install 35, 60-metre high wind turbines, about 400 metres apart, based on three sites near Portland, southwestern Victoria and generating 20 MW of power for domestic distribution (Watkins, 1998).

Electricity generation companies using coal as a fuel are taking steps to reduce CO₂ emissions apart from just increasing energy efficiency of existing plant. Plantations of fast growing trees have been established in the different regions adjacent to power stations and elsewhere. In Victoria, by the end of 1992, 1409 hectares of pine and eucalypt trees had been planted in proximity to the brown coal-fired electricity generation sites [State Electricity Commission of Victoria, 1992]. In addition, the various electricity generation companies and their consultants are watching developments in the sequestration of CO₂ such as via liquefaction and storage in deep caverns, and photosynthesis by specific algae. However, sequestration of CO₂ could cost AUD \$3-4 cents per kilowatt-hour, virtually doubling generation costs.

Adopting a "business as usual approach", the baseline Australian scenario for CO₂ emissions was projected to grow by 45 % between 1990 and 2010. In the Kyoto Protocol, Australia has been granted a national emissions budget of 108 % of the 1990 level. Given an estimated 20 % in population growth over next 20 years and an economic growth of 1.5 % per year, it has been concluded that absolute reductions would not have been possible and the special allowance was needed. Assuming CO₂ credits for reduction in land clearing and other changes in the forestry sector, it is possible that the energy sector emissions budget could approach 125 % of 1990 and still meet the Kyoto target for national greenhouse gas emissions for the period 2008-2012. Future developments in CO₂ emissions trading are also likely to offer the potential for offsetting expansion in the Australian energy sector (Key Economics, 1998).

ECONOMIC AND STRUCTURAL CHANGES IN ELECTRICITY AND GAS INDUSTRIES

The State of Victoria has led the way in the privatisation of the electricity industry in Australia. The four generating companies, privately owned by various consortia of international and national companies, are now operating in a deregulated market. Approximately AUD \$9,600 million has been paid for the 6000 MW of brown coal generating plants making premature closure an unrealistic option. The distribution companies are also under private control but not fully deregulated until 2001. Privatisation and deregulation of the gas industry is also progressing with sections of the former government-operated gas distribution entity being corporatised. Other Australian states are in various stages of privatisation of the electricity industry, with South Australia proceeding next.

The very substantial investments made in the Victorian electricity generating utilities are having major consequences. These include increased availability of generation plant (by 10-15 %), planned extension to operating life of the plant from 30 to 50 years typically, and new competitive constraints on the price of electricity "at the fence". The current effect of the latter is to drive the price dramatically downwards. In addition, a comprehensive review of personnel

levels, maintenance contracts, the implementation of new technology, environmental control and monitoring equipment, to name some issues, has led to radical changes concomitant with significant expenditure reductions. Economics is a major driver and long-term strategic planning needs are evaluated on a strict cost-benefit analysis. The new forces of economic and structural change will thus have a substantive and diverse impact on the development and practice of the electricity and gas industries as well as on the response of the consumers in the 21st Century. For future power requirements, gas is available particularly for peaking power, while advanced low rank coal technologies, having been demonstrated, will achieve substantial efficiency improvements in future brown coal plants.

CONCLUDING REMARKS

Coal is still Australia's dominant fuel resource for energy generation with reserves lasting about 550 years for brown coal and about 250 years for black coal, at present rates of usage, compared with reserves of oil and gas lasting approximately 40 and 60 years respectively. Coal fired power generation is forecast to be Australia's dominant stationary energy source well beyond the year 2000. Efforts are highly likely to be made to increase the use of alternative fuels, such as gas and biomass, and to implement new technologies along with alternative energy source options, such as photovoltaic arrays and wind power. However, their cost-effectiveness in relation to total plant investment will be closely scrutinised as the number of Australia's generation facilities are privatised. Also, fuel substitution on a large scale is a limited option due to cost, location, and availability factors but the creative use of biomass, say through reforestation, and a CO₂ emissions trading mechanism may provide alternative offsets to the greenhouse gas impact of energy expansion. Nonetheless, Australia in the 21st Century will probably see a greater mix of energy/fuel sources to meet the electrical, industrial, agricultural, and transport demands of the growing economy while concurrently endeavouring to limit the release of greenhouse gas emissions.

REFERENCES

- Australian Bureau of Agricultural and Resource Economics [ABARE, 1997]: Australian Commodities: Forecasts and Issues, 4 (4), 469-471, 1997.
- Australian Bureau of Statistics, [ABS, 1997]: Australian Year Book, 1997.
- Bureau of Resource Sciences (1997): "Australia's Identified Mineral Resources 1997"; "Oil and Gas Resources of Australia 1996"; Canberra, Australia.
- Electricity Supply Association of Australia Limited (ESAA, August 1997): Greenhouse Challenge Workbook.
- Electricity Supply Association of Australia Limited [ESAA 1997], Electricity Australia 1997, Fiftieth anniversary issue.
- Electricity Supply Association of Australia Limited [ESAA] web page.
- Johnson, T., Mouritz E., and Pleasance G.: "Development of the IDGCC Process for Cleaner and Cheaper Generation of Electricity from Low Rank Coal", Fifth Annual Technical Seminar "Clean Fossil Energy: APEC Choice for Today and Tomorrow" in the APEC Experts' Group on Clean Fossil Energy October 28-30, 1997, Reno, USA.
- Key Economics Pty Ltd: "Greenhouse Briefing: Australia After Kyoto", Report, March 1998, Kew, Victoria, Australia.
- Lawley, P.: "Photovoltaics: Future Directions", Proceedings of the 4th Renewable Energy Technologies & Remote Area Power Supplies Conference (ESAA), February 23-25, 1998, Hobart, Australia.
- Lee T., Oppenheim D., and Williamson, T. J., ERDC 249 Australian Solar Radiation Data Handbook - Main Report, Energy Research and Development Corporation [ERDC], April 1995.
- Osborne, J. (1993): Review of Renewable Energy Technologies for the Generation of Electricity in Victoria, June 1993.
- Private communication: ABARE Canberra, February 1998.

Schaap, H. A.: "Electricity and Greenhouse – The Challenge For Renewables", Proceedings of the 4th Renewable Energy Technologies & Remote Area Power Supplies Conference (ESAA), February 23-25, 1998, Hobart, Australia.

Skelton, R.: "The Heat's on the U.S.", The Age (Section: World), p. 21, Melbourne, 29 November 1997.

Spero, C.: "One Thousand MW of Biomass – Myth or Reality", (ESAA), Proceedings of the 4th Renewable Energy Technologies & Remote Area Power Supplies Conference (ESAA), February 23-25, 1998, Hobart, Australia.

State Electricity Commission of Victoria, [SECV 1992], "The SECV and the Greenhouse Effect", Discussion Paper Number 2, April 1992.

Uranium Institute [UI] web page.

Watkins, S.: "Residents' Fears Becalm' Wind Farm", The Sunday Age, Melbourne, 29 March 1998.

World Coal Institute, [WCI] web page.

Table 1: Estimated Resources of Australia's Principal Fuels as at 1996

Fuel	Quantity	Reference
Coal: Black Brown	Very large ⁺ > 200 Giga tonnes	BRS (1997) ⁺⁺ Mineral Resources BRS (1997) - Mineral Resources
Natural Gas	1857 Tera litres	BRS (1997) - Oil and Gas
Oil	111 Giga litres	BRS (1997) - Oil and Gas
Uranium (as U)	895 kilo tonnes	BRS (1997) - Mineral Resources

⁺ Demonstrated recoverable resources are 55 Giga tonnes

⁺⁺ Bureau of Resource Sciences

Table 2: Australian Electricity Generation Supply Mix in 1995/96

Electricity Generation: 165,062 GWh	
• Black coal	56.8 %
• Brown coal	25.9 %
• Hydro	9.5 %
• Gas	7.3 %
• Oil	0.5 %

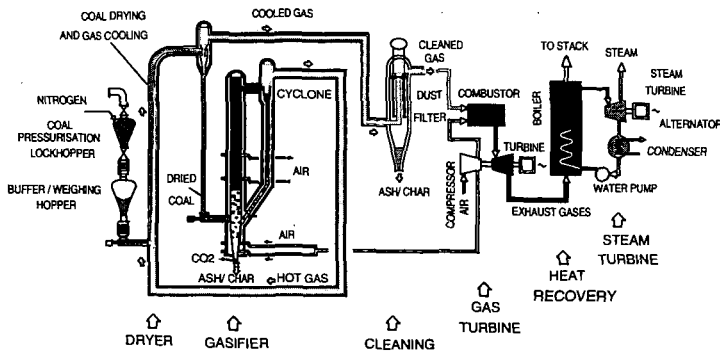


Figure 1: Schematic of the Integrated Drying Combined Cycle (IDGCC) Process

NATURAL GAS AND EFFICIENT TECHNOLOGIES A RESPONSE TO GLOBAL WARMING

Meyer Steinberg
Brookhaven National Laboratory
Upton, NY 11973

Key words - CO₂ mitigation, natural gas, efficient technologies

INTRODUCTION

Global Warming has become an environmental problem caused by the use of fossil energy. The emission of the radiative gas CO₂ from a particular country is intimately connected with the size of its population, its efficiency of utilization of fossil energy and the carbon content of the fuel. This paper deals with CO₂ mitigation technologies including the reuse of emitted CO₂ and indicates a direction for CO₂ emissions reduction for the U.S. economy.

The average CO₂ emissions for the three fossil fuels are as follows: Coal - 215 LbsCO₂/MMBTU (HHV = 11,000 BTU/Lb and C content of 76%); Oil - 160 Lbs CO₂/MMBTU (HHV = 6 MMBTU/Bbl) and Gas = 115 Lb CO₂/MMBTU (HHV = 1 M BTU/cu. ft.). Table 1 shows the U.S. fossil energy consumption and CO₂ emission, the total world consumption and emission and the principal energy supply service. In the U.S., most of the coal is used for generation of electrical power, in large central power stations. Oil is mainly used for production of transportation fuel (gasoline and diesel) with some limited electrical power production and gas is mainly used for industrial and domestic heating. However, there is also lately a growing consumption of natural gas for electrical power production.

Substituting Natural Gas for Coal for Electrical Power Production

If all the current electrical power production in the U.S. is generated by natural gas in combined cycle power plants, two benefits of CO₂ emission are achieved. First, the efficiency of electrical power production is increased from the current average coal-fired plant efficiency of 34% to over 55% for a modern natural gas fired turbine combined cycle plant and secondly the CO₂ emission per unit of energy from the fuel is reduced by 47% compared to the coal-fired plant. Applying this to the U.S. consumption, and assuming that natural gas usage remains the same a 22% reduction in the total CO₂ emission can be realized.

Substituting Natural Gas for Oil for Automotive Transportation

Compressed natural gas (CNG) vehicles are already on the market and if natural gas is substituted for oil in the transportation sector a 13% reduction in CO₂ emissions can be realized in the U.S. Thus, the substitution of natural gas for Coal and Oil in the electrical power and transportation sectors adds up to a 35% overall reduction in CO₂ emissions.

The Camol System for Preserving the Coal Industry for Electrical Power Production and Reducing Oil Consumption by Substituting Methanol in the Transportation Sector

The Camol System consists of generating hydrogen by the thermal decomposition of methane and reacting the hydrogen produced with CO₂ recovered from coal-fired central power stations to produce methanol as a liquid transportation fuel. Figure 1 illustrates the Carnol System which has the following advantages: 1. The Carnol System preserves the coal industry for electrical power production. 2. The Carnol System produces a liquid fuel for the transportation sector which fits in well with the current liquid fuel infrastructure. 3. The Carnol System reduces consumption of the dwindling domestic supplies of fuel oil in the U.S.

In the Camol System, the carbon from the coal is used twice, once for production of electricity and a second time for production of liquid fuel for fueling the transportation sector, in automobile vehicles. The reduction in CO₂ emissions results from two aspects. The elemental carbon produced from the thermal decomposition of the methane is not used as fuel. It is either sequestered or sold

*Based on the report by Meyer Steinberg, "Natural Gas and Efficient Technologies: A Response to Global Warming, BNL 65451, Brookhaven National Laboratory, Upton, NY 11973 (February 1998).

as a materials commodity. In this respect, thermal decomposition of methane (TDM) has an advantage over the conventional steam reforming of methane (SRM) for hydrogen production reduced. In the TDM process, carbon is produced as a solid which is much easier to sequester than CO₂ as a gas. Furthermore, the energy in the carbon sequestered is still available for possible future retrieval and use. The carbon can also be used as a materials commodity, for example, as a soil conditioner. Table 2 gives the estimate of CO₂ emissions using the Carnol System applied to the U.S. 1995 consumption and indicates a 45% overall CO₂ emissions reduction. The methanol in this case is used in conventional internal combustion engines (IC) which is 30% more efficient than gasoline driven IC engines. The natural gas requirement would have to increase to 62 Quad which is three times the current consumption of natural gas for heating purposes. The rise in natural gas requirement is because only about 58% of the natural gas energy is used for hydrogen for methanol. Methanol production and that carbon produced is sequestered unburned to the extent of 0.58 GT. This can be considerably reduced by going to fuel cell vehicles.

Carnol System with Methanol Fuel Cells for the Transportation Sector and Substituting Natural Gas with Combined Cycle Power for Coal Fired Central Station Power

In the not too distant future, fuel cells will be developed for automotive vehicles. This will improve the efficiency of automotive engines by at least 2.5 times compared to current gasoline driven internal combustion engines. Direct liquid methanol fuel cells are under development. If we use coal or oil for central power stations, there will be too much CO₂ generated for liquid fuel methanol by the Carnol Process for the transportation sector using fuel cells. Therefore, it is much more energy balanced if we use natural gas for power because it generates the least amount of CO₂ per unit of energy. In this scenario, the natural gas in a combined cycle plant displaces coal for power production and displaces oil for methanol by the Carnol Process for transportation. The results are shown in Table 3. Thus, by applying natural gas for electrical power production, liquid fuels production for fuel cell driven automotive engines and for heating purposes an overall CO₂ emissions reductions of over 60% can be achieved. This degree of CO₂ emission reduction could stabilize the CO₂ concentration and prevent the doubling of the CO₂ in the atmosphere expected by the middle of the next century if business is conducted as usual. The 0.32 GT of carbon required to be sequestered is about 3 times less than the amount of coal mined in the U.S. currently. If a market can be found for this elemental carbon, such as a soil conditioner, the cost of methanol production can be significantly decreased.

Natural Gas Supply and Utilization

The all natural gas energy system of Table 3 requires a three-fold annual consumption in natural gas. Recent reports indicate that the current estimated reserve of conventional natural gas is of the same order of magnitude as the current estimated oil reserves which might last only for another 80 years or so. However, unconventional resources, especially methane hydrates and coal bedded methane indicate an enormous resource which is estimated to be more than twice as large as all the fossil fuel resources currently estimated in the earth. If this is so, then we can begin to think of utilizing natural gas for reducing CO₂ emissions in all sectors of the economy. It appears that even today that deep mined coal in several parts of the world, especially in England, Germany, and the U.S., has become too expensive; and, as a result, many of these mines have been closed. Most economical coal used today comes from surface mined coal. Furthermore, the contaminants in coal, sulfur, nitrogen and ash in addition to the high CO₂ emission mitigate against its use. Rail transportation of coal also becomes a problem compared to pipeline delivery of natural gas. When natural gas becomes available, even at a somewhat higher cost, it can displace coal and even oil for power production and transportation. Long term supply of economical natural gas is the main concern for increased utilization of natural gas.

Economics of Natural Gas Displacing Coal and Oil

The current unit cost for fossil fuel in the U.S. is for coal \$1.00/MMBTU, oil \$3.00/MMBTU and for gas \$2.00/MMBTU. For the total consumption of 76 Quad in 1995, the primary fossil fuel energy bill was \$167 billion. Applying this to the all natural gas scenario of Table 3, we come up with a natural gas fuel bill for the required 49 quads of \$98 billion. So there is a resulting 41% savings in the current fossil fuel bill. The cost of natural gas could go up to \$3.50/MMBTU without the fuel bill exceeding the current energy bill. In order to achieve these results, capital investment in the replacement new technologies must be made. Only incremental replacement cost need be considered, since capital investment will be needed, in any case, to replace old equipment under

business as usual conditions. Table 4 indicates the incremental capital replacement cost to achieve the all natural gas economy based on the following data.

- a) Replacement of coal fired plants including scrubbers, etc., runs about \$2000/kw(€); for the more efficient natural gas combined cycle plants runs about \$1000/KW(€); thus, there is a \$1000/Kw(€) capital cost savings and when applied to an installed capacity of 400,000 MW(€), the savings amounts to \$400 billion.
- b) For replacing oil refineries with Carnol Methanol plants which require CO₂ removal and recovery from the natural gas power plants, it is estimated that the current unit cost is \$100,000 per daily ton of methanol. The total incremental cost to supply the total 14 quads of methanol for fuel cell vehicles is then \$220 Billion. No credit was taken for the replacement of oil refineries, over time, so that this incremental capital cost is probably high.
- c) New pipelines will have to be built to transport the natural gas and new methods of extracting natural gas eventually from deep sea wells containing methane hydrates. Assuming \$1 million per mile for these new gas supply facilities and a rough estimate of 200,000 miles needed gives a capital cost of roughly \$200 billion. It is also assumed that the liquid methanol pipeline and tanker distribution will be about equal to the current liquid gasoline distribution for the transportation sector.
- d) In terms of replacing the current existing more than 100 million gasoline driven IC engine vehicles with fuel cell vehicles, it eventually should not cost much more than the present average cost of \$15,000 to \$20,000 per vehicle. And, so the incremental cost should be negligible and may even show a savings because of the more efficient fuel cell vehicle than the IC engine vehicle.

Table 4 indicates that the incremental savings due to the new technologies in the one electrical power sector just about balances the incremental cost in the other three sectors. Thus, the new total incremental capital replacement cost is negligible compared to the capital cost requirement for continuing with the business as usual current power technology structures.

Conclusions

The ability of achieving a 60% reduction in the U.S. CO₂ emissions by natural gas fuel substitution with improved technologies is based on the following assumptions and developments:

1. that there are vast reserves of natural gas that can be recovered from both conventional and non-conventional natural gas resources especially from methane hydrates and coal bedded methane at costs which are not more than about double current gas productions cost.
2. that an efficient Carnol process for methanol production based on thermal decomposition of methane can be developed.
3. that an efficient direct methanol fuel cell vehicle can be developed.

The benefits in terms of mitigating global warming provides a strong incentive for working on and achieving the required development goals. The all natural gas economy with efficient technologies for CO₂ global warming mitigation avoids alternatives of (1) sequestering CO₂ in the ocean or underground, (2) switching to nuclear power, and (3) relying solely on solar and biomass energy.

Fig. 1

INTEGRATED SYSTEM FOR CO₂ EMISSION REDUCTION

CARNOL PROCESS

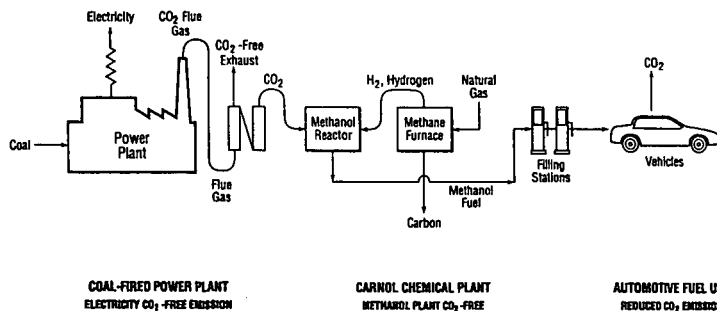


Table 1
Total Fossil Fuel Energy Consumption and CO₂ Emission for the U.S. in 1995^{a)}

Fuel Type	Quantity	Energy Consumption Quads 10 ¹⁵ Q BTU	Principal Energy Service	CO ₂ Emission	
				GT(CO ₂)	%
Coal	0.9x10 ⁹ tons	20	electricity	2.15	35%
Oil	5.8x10 ⁹ bbls	35	Auto transport	2.80	45%
Gas	21.0 TCF	21	heating	1.21	20%
U.S. Total		76		6.16 (1.68 GT(C))	
World Total		330		22.7 (6.2 GT(C))	

TCF = Trillion (10¹²) cubic feet
GT = Giga (10⁹) tons
Q = Quads (10¹⁵) BTU

Table 2
Carnol Methanol Substitution for Oil in the Conventional Auto Transportation Sector
Produced from Natural Gas and CO₂ from Coal-fired Power Plants

Fuel Type	Natural Gas Consumed Quads	Energy Consumed Quads	Energy Service	CO ₂ Emissions GT(CO ₂)
Coal ^{a)}	--	20	Electricity	0.22
Methanol ^{b)} substitutes for gasoline	41	24	Auto Transport	1.96
Gas	21	21	Heating	1.21
Total	62	65		3.39
Reduction from current CO ₂ emission				2.77
% CO ₂ Emission Reduction from 1995 level				45.0%
Elemental carbon sequestered				0.58 GT (C)

Table 3
Natural Gas substituted for Coal Fired Power Production, Carnol Process for Methanol Production,
Substituting for Oil in Fuel Cell Vehicles for the Transportation Sector

Fuel Type	Natural Gas Consumption Quads	Energy Consumption Quads	Energy Service	CO ₂ Emission GT (CO ₂)
Natural gas for coal ^{a)}	14	14	Electricity	0.08
Methanol for oil	24	14	Auto Transport Fuel Cells	1.12
Gas	21	21	Heating	1.21
Total	59	49		2.41
Reduction from Current CO ₂ Emissions				3.75
% CO ₂ Emission Reduction from 1995 level				61%
Elemental carbon sequestered				0.34 GT (C)

a) Natural gas for combined cycle power plant is 55% efficient and 90% of CO₂ emissions is recovered for Carnol plant.

Table 4
Capital Investment Required to Replace Present Power Structure

Present Power Structure (and capacity)	Replacement Structure (and capacity)	Incremental Unit Capital Cost	Incremental Replacement Capital Cost \$10 ⁹ (\$ Billions)
Coal fired electrical ^{a)} power 400,000 MWe	Natural gas fired combined cycle electrical power	- \$1000/kw (savings) ^{b)}	- \$400
Oil refineries ^{b)} 35 Quads	Carnol methanol plants 14 Quads	\$10 ⁹ /T/D Methanol ^{b)}	+ \$200
Wells and pipelines ^{c)}	additional pipeline and new methane hydrate wells	\$10 ⁹ /mile ^{c)} 200,000 miles of gas lines	+ \$200
Automotive IC vehicles 100 x 10 ⁶	Fuel cell vehicles	0 ^{d)}	- 0
Net total incremental replacement cost			- 0

THERMOCHEMICAL CONVERSION RESEARCH & DEVELOPMENT ACTIVITIES IN CANADA

E.N.Hogan
Bioenergy Development Program
CANMET Energy Technology Centre
Natural Resources Canada
Ottawa, Ontario. K1A 0E4 Canada

ABSTRACT

An overview of the R & D activities and strategies of the Canadian Biomass Thermochemical Conversion Program, part of the CANMET Energy Technology Centre(CETC) will be presented. The paper will focus on the pyrolysis technology area and examine both the current status of research activities in Canada and the future research directions.

The major objective of this program is the development of cost competitive technologies that convert biomass into gaseous and liquid fuels and chemicals to be used for process heat, electricity, alternate refinery feedstocks and value added products. The program can be divided into the following main project areas: i) assessment of the potential of thermochemical conversion systems to process new biomass and/or waste feedstocks; ii) process development and optimization of thermochemical conversion processes; iii) evaluation of the potential of producing value added chemicals from pyrolysis products and determination of end use industrial applications for these; v) assessment of the commercial utilization of pyrolysis oils for heat and/or electricity production in boilers, diesel engines and gas turbines; and, vi) continued development and optimization of the production of high cetane diesel fuel from plant and vegetable oils.

INTRODUCTION

The objective of the biomass thermochemical conversion program is to develop cost competitive technologies that can thermochemically transform biomass materials into liquid, solid and gaseous fuels which can be converted to process heat, electricity, refinery feedstocks and value added products. Research efforts are focussing on processing, upgrading and utilization issues that will result in an optimal system for energy production. Work will also increasingly focus on the production of value added chemicals from the products of thermochemical conversion and will address the fractionation, isolation, recovery and application issues related to this. This paper will focus on the technology development and commercialization activities associated with pyrolysis technologies.

MAJOR PYROLYSIS RESEARCH AREAS

1. Assessment of the potential of pyrolysis to process new biomass and waste feedstocks, particularly those causing environmental disposal problems.
2. Process development and optimization of thermochemical conversion processes, including oil quality improvement and health and safety related issues.
3. Evaluation of the potential of producing value added chemicals from pyrolysis products and determination of end use industrial applications for these.
4. Assessment of the commercial utilization of pyrolysis oils for heat and/or electricity production in boilers, diesel engines and gas turbines.
5. Continued development and optimization of the production of cetane enhancers from plant and vegetable oils, including process optimization and scale up, co-product upgrading, laboratory engine and emission testing and field trials.

STATUS OF PYROLYSIS DEVELOPMENT

1. Assessment of the Potential of Pyrolysis and other Thermochemical Conversion Systems

In order to assist the fast pyrolysis technology in penetrating new industrial markets, various biomass feedstocks, particularly wastes presenting disposal problems, need to be assessed for

their potential concerning oil yields, product characteristics, etc. Waste biomass from a number of forest products companies have been successfully pyrolyzed by various groups involved in fast pyrolysis. Research projects with Ensyn Technologies and Pyrovac Institut to assess whether bark residues could be pyrolyzed have been completed, and the results indicate that industrial softwood and hardwood bark can be processed without operational difficulties. As a result of these tests, a number of forest companies are exploring the application of fast pyrolysis technology in the treatment of their bark wastes. Ensyn recently announced that a RTP™ plant will be built in the Prince George area of British Columbia with Northwood Pulp Timber Ltd. to convert bark residues to both a liquid bio-oil fuel and a natural resin to be used as a replacement for phenol or phenol formaldehyde in wood composite adhesive formulations. Pyrovac Institut is installing a plant in the St. Jonquiere region of Quebec to convert bark residues from forest operations in the area to bio-oil.

A research project is starting up with Kemestrie and Tembec's Chemicals Division to investigate fractionation methods that will result in the removal and recovery of extractives from bark rich residues. The work will identify marketable co-products that can be isolated from the extractives and address the use of the remaining biomass for subsequent fermentation or pyrolysis processing.

In evaluating further feedstock availability, agricultural crops and residues continue to represent a considerable potential. Feedstocks such as grasses and animal wastes are being examined by Ensyn Technologies and Resource Transforms Intl. to determine if pyrolysis could be part of an integrated biomass refining concept to produce a number of value added products, including energy, thereby increasing the overall commercial viability of biomass systems. Another problem associated with agricultural residues is the materials handling costs associated with bringing the biomass into a processing facility and an overall program priority is to examine systems, ie, collection, compaction, that will reduce the input feedstock costs.

Industrial biomass wastes represent another large source of biomass feedstocks that could provide economic opportunity, especially if the material has limited reuse, recycling or disposal options. An example of this is creosote treated railway ties. They continue to be used by railroads, combustion and landfilling are no longer considered as viable disposal methods and there is no alternate recycling program available. Stockpiling of these ties are costly and could pose a number of environmental concerns. As a result of this need to dispose of this ties, work is underway to evaluate wood treated with creosote to determine if they can be converted by pyrolysis to useful products. Ensyn Technologies and Resource Transforms Intl.(RTI) have also successfully processed a number of cellulosic packaging waste streams - corrugated, bleached and waxed cardboard to determine they can be converted to bio-oil with good liquid yields.

2. Process Development and Optimization of Thermochemical Conversion Processes

As thermochemical processes progress to commercialization, new technical problems that were not apparent previously concerning various aspects of the processes need to be addressed. Improved efficiencies of process components such as filtration methods or char separation systems are being proposed based on experience derived experimental pyrolysis runs. Current research projects are examining the technical viability of these methods as means of improving the efficiencies of the fast pyrolysis systems.

RTI Ltd. has recently developed a new fluidized bed pyrolyzer based on some concepts arising from a recently completed contract with CETC. Some principal features of this design include: blown through mode of char removal; bed temperatures between 360-490°C; residence times that can be greater than 2 seconds; indirect heating; deep fluidized bed with a height to width ratio greater than one; a mass ratio of recirculated non-oxidizing gas to biomass that is less than 2; biomass particles that are less than 3mm; and char that is thermally gasified in situ.

In another project related to health and safety issues, RTI Ltd. has performed a preliminary study on measuring the biodegradability of bio-oil using respirometry methods. The project results indicate that bio-oils are biodegradable in aquatic and soil environments; the biodegradability of bio-oil is substantially higher as compared to diesel fuel; and the neutralization of the bio-oil enhances their biodegradation in water. Additional studies using this respirometric approach will be required in order to develop an acceptable standard methodology.

3. Production of Value Added Chemicals from Pyrolysis

The production of co-product, value added chemicals, will improve the overall economics of biomass pyrolysis processes. This integrated recovery of fuels and chemicals from pyrolysis oils

is in the preliminary stages of development but will provide considerable impetus to the commercial implementation of pyrolysis processes if the existing technical and market barriers can be addressed.

Pyrolysis oil products in the early stages of development include: i) the development by Resource Transforms Intl. of a slow release fertilizer using pyrolysis oil as the binder/carrier; ii) the evaluation by Pyrovac Institut and Ensyn Technologies of the potential of using pyrolysis oil to produce a 'green resin' to replace phenol formaldehyde resins currently used in the production of waferboard, and; iii) the production of calcium salts by Dynamotive Corp. which when injected into coal fired burners may provide an effective means of reducing SO_x and NO_x emissions.

Various techniques are also being examined for the fractionation, isolation and recovery of pyrolysis oil components including pyrolytic lignin, levoglucosan and aldehydes. Lignin for example could be depolymerized to oxyaromatic monomers that could be upgraded to a variety of end products, ie, oxycyclic compounds, hydroxylated aromatics and Kemestrie Inc. is performing a feasibility study to evaluate this approach.

Another research focus in this area has been to examine the upgrading of the char produced from fast pyrolysis. A series of devolatilization and activation test runs and pelletizing/briquetting evaluations have been performed by pyrolysis industry groups to determine the potential commercial production of activated charcoal from the pyrolytic char and initial results look promising. In another char utilization project, the University of Saskatchewan is examining the characterization and steam gasification of high ash content pyrolysis chars. Preliminary work has found that the conversion (only of the combustible material, not counting the ash) ranges from 59% wt. For a Danish wheat straw sample to 93% for rice straw. The conversion appears to be a function of the source of the char (the type of feed material) and its history (residence time in the reactor and temperature) rather than the ash content of the char.

4. Assessment of Commercial Utilization of Pyrolysis Oils for Electricity and Heat Production

Boilers

A significant barrier to the commercialization of pyrolysis technology relates to the market acceptance of a novel fuel having different characteristics from traditional fossil derived fuels. Bio-oil has been fired in combustion boilers in a number of tests in Canada, the US and Europe. These tests have demonstrated that only minor boiler retrofitting is required, and combustion is clean and self-sustaining with no adverse change in emission levels. As a result, the use of pyrolysis oils in large industrial units (those greater than 1MWe) can now be considered to be commercially viable. For example, at the Manitowoc Public Utilities, Wisconsin, USA, bio-oil was co-fired at a rate of about 11 million BTU/hr. in a coal-fired stoker boiler. This represented about 5% of the fuel input, or about 1Mwe of the 20 Mwe output of the was terminated when this bio-oil surplus supply was re-directed for internal boiler use at the Red Arrow Products facility where the bio-oil was produced. It should be noted that bio-oil has been commercially fired in a 20 MBTU/h West Waste Fuel Burner at the Red Arrow facility since 1989.

The remaining objective of this segment of the program is to work with burner manufacturers and end users to increase the applications of bio-oils in the area of small boiler and burners. As part of an international assessment of the feasibility of utilizing these oils as an energy source, the program will continue to provide technical support and oil samples to a number of industry and research groups, such as Neste Oy, Coen and VTT- Energy, who have projects underway in this area. Information from these groups on oil characteristics, combustion efficiencies, emissions, etc., will be made available to the pyrolysis community and accelerate the commercial acceptance of the technology.

Diesel Engines

The use of bio oils for power generation via diesel engines showed promise in preliminary tests performed in Finland. As a result, an industrial consortium from both Canada and Finland was formed to carry out a project to demonstrate the cost effective production of bio-oils from biomass feedstocks and to develop and warrantee a commercial diesel engine that would burn these bio oils in small to medium sized electrical generation systems. The consortium members from Finland included Wartsila Diesel, one of the world's largest suppliers of diesel engines for power applications; VAPO, a company involved in the sale of power and power generation equipment; and VTT-Energy, a government research agency involved in the development of bioenergy technologies. Ensyn Technologies and NRCan were the Canadian industrial member of this consortium. This project has been successfully completed and it is expected that diesel

engine manufacturers will be ready to provide performance warranties for bio-oil utilization in pyrolysis oil power production plants.

Gas Turbines

Orenda Aerospace has successfully completed a Phase I project to evaluate the concept of utilizing a biomass derived liquid fuel in a gas turbine, optimize the application of this concept and perform endurance testing of the gas turbine. Orenda was able to successfully operate the turbine over the full power range using 100% bio-oil. Performance tests were completed with detailed data acquisition at steady state operating points. Emission results were positive, with the bio-oil having lower levels of SO₂ and NO_x relative to diesel. As a result of the findings in this phase of the project, a Phase II project is planned to perform component and fuel system durability testing and a long term endurance test which will allow the turbine to be guaranteed for pyrolysis oil.

Microemulsions

Bio-oils have a number of technical problems including acidity, a calorific value half that of petroleum fuels, poor ignitability and high char and ash content. One of the ways to circumvent these problems would be to use the bio-oil as a diesel supplement by dispersing 10-30% of bio-oil in diesel. However, bio-oils are highly polar, retaining about 25% water and are immiscible with diesel. If a stable bio-oil in diesel microemulsion could be formed, it is likely that a conventional power generation systems could be run without major modifications. BDP has initiated a project in collaboration with the Processing and Environmental Catalysis Group, CETC which has shown that stable, combustible microemulsions can be produced from mixtures of bio-oil/diesel ranging from 5% - 40%. A 5 litre/hr. continuous unit has been built to demonstrate economic and technical viability at a larger scale and to produce larger samples for analysis and combustion tests. As a result of this work a follow project is being planned, which will include technical co-operation with VTT - Energy and the European Commission JOULE Programme under the Canada/EU Science & Technology Agreement. The objectives of this project are to optimize the microemulsion process and unit, including improved mixing and feeding systems, examining other surfactants, etc., testing pyrolysis oils derived from other biomass feedstocks, further combustion and emissions testing and the provision of samples to various groups for testing.

5. Development of Cetane Enhancer Technology

Arbokem Inc., in collaboration with BC Chemicals, was awarded the rights to this technology by the CANMET Energy Technology Centre(CETC) in 1991. As a result of successful pilot testing of the process and a positive independent study of the potential diesel market in North America, an industrial consortium was formed to commercialize the technology using tall oil derived from the pulping of softwoods as the input feedstock. The consortium successfully completed an research program to carry out scale up testing and production of a cetane fuel product (cetane numbers vary between 65 from tall oil feedstock to 90 for animal fats), laboratory vehicle emissions tests and field testing of the biodiesel fuel. The technology is now ready for commercialization and a number of implementation strategies are now being evaluated to determine which approach to take. In the interim, the IEA Alternative Motor Fuels has a project underway - "Annex XIII. Emissions Performance of Selected Biodiesel Fuels", and cetane fuel will be provided to these tests in order to further assess the emission characteristics of this fuel.

In the cetane enhancer process, conventional hydrotreating technology is used to convert tall oil and other biomass oils to a high cetane fuel through the addition of hydrogen. In addition to the middle distillate cetane enhancer fuel, heavy and light bio-naphtha fractions are produced as co-products. As part of a follow on project to improve the commercial opportunities of this process, a contract has recently been given to Kemestrie Inc to investigate the upgrading of these products. As part of their research on another project examining MSW gasification, Kemestrie developed a highly efficient catalyst that can generate hydrogen from the synthesis gas produced in biomass gasification processes. It was felt that this catalyst could produce similar results with the heavy bio-naphtha fraction from the cetane process. In recently completed tests, Kemestrie has shown that their catalyst can convert this fraction to hydrogen and that this hydrogen is of sufficient quality and quantity to more than provide all the infeed hydrogen required for the process(5 times the amount of hydrogen needed is produced), reducing the production costs of the cetane enhancer technology. It is estimated that the production of the hydrogen required from the heavy fraction could reduce treatment costs from approximately \$170/tonne to about \$150/tonne for a 25,000 tonne/year tall oil processing plant

Work is continuing to develop additional value added products from the light and remaining heavy bio-naphtha fractions.

International Activities

The Biomass Thermochemical Conversion R & D Program remains committed to maintaining good research links with the international biomass pyrolysis industry and research communities. In this regard it will continue to be active in Annexes of the International Energy Agency - Bioenergy Agreement and will join the Pyrolysis Network for Europe(PyNE) for its next triennium period.

TUNGSTATE-MODIFIED ZIRCONIA AS A HYDROISOMERIZATION CATALYST FOR HIGH MOLECULAR WEIGHT LINEAR PARAFFINS

Shuguang Zhang, Xin Xiao, John W. Tierney and Irving Wender*
Department of Chemical Engineering, 1249 Benedum Hall,
University of Pittsburgh, Pittsburgh, PA 15261

Keywords: tungstate-modified zirconia, hydroisomerization, linear alkanes

Introduction Isomerization of long-chain linear alkanes is desirable because isoparaffins, from C_{10} to C_{30} , are excellent solvents, have minimal odor, low reactivity and high stability. They are used in polyolefin manufacture, proprietary household products, food-related applications, pharmaceutical production and in many other ways. Oils rich in high molecular weight isoparaffins, rather than normal paraffins, are desired for use as motor oils, lubricants, diesel fuel and jet fuel due to their desirable low temperature properties.¹ Industry carries out oil dewaxing to lower the long-chain normal paraffin content in oils. Chevron has commercialized an all-catalytic wax isomerization process, called "isodewaxing", for the production of motor oils, lubricants and fuels.² This process converts linear alkanes to their isomers whose presence significantly improves the low temperature properties of the oils. Compared with widely used solvent dewaxing, catalytic dewaxing does not have environmental problems caused by fugitive emissions.³

In the Fischer-Tropsch (FT) synthesis, the yield of waxes can exceed 45 wt% of the total liquid products.⁴ Normal paraffins in the C_{20} - C_{30} range from this process require further processing to increase their commercial value. Isomers of these high molecular weight paraffins can be used as middle-distillate fuels and their low freezing points make them desirable for use as jet fuel.⁵ Upgrading waxes to lubricating oils is also possible.

Catalysts containing $AlCl_3$ or zeolites are traditionally used for isomerization. The former is corrosive and nonregenerable because of loss of chloride ions; the latter requires high operating temperatures (about 400°C) and favors cracking. SAPO-11 (a silicoaluminophosphate) is a relatively new molecular sieve; metal-promoted SAPO-11 is more selective than other zeolites for long-chain paraffin isomerization.^{6,7} However, it is generally used with high hydrogen to feed mole ratios (30/1) and high reaction temperatures.

Anion-modified metal oxides, such as sulfated zirconia (SO_4/ZrO_2) and tungstated zirconia (WO_3/ZrO_2), have been found to catalyze hydrocarbon conversions under mild conditions.⁸ These strong solid acids are environmentally benign and regenerable.⁹ Butane isomerization over sulfated zirconia has attracted considerable attention because isobutane is the precursor to methyl-t-butyl ether.¹⁰⁻¹³ Metal-promoted sulfated zirconia is effective for isomerization of short chain paraffins ($< C_7$) and for hydrocracking of long-chain paraffins including waxes and polyolefins.¹⁴⁻¹⁶ However, loss of activity due to coke formation and sulfur loss, especially under reducing conditions, are obstacles to certain practical uses of sulfated zirconia. Moreover, high isomerization selectivity is difficult to achieve over sulfated zirconia as the chain length increases, even at low conversions.¹⁵ Studies of tungstate-modified zirconia indicate that it is more stable than sulfated zirconia and is promising for hydroisomerization of high molecular weight linear paraffins.¹⁶⁻²⁰

It is known that there is an increasing ease of formation of carbenium ions on the interior carbons of linear molecules of long chains.²¹ Since isomerization of alkanes precedes cracking, catalysts with a certain optimal balance of metal and acid functions at suitable reaction conditions must be found to suppress cracking in order to achieve high isomerization selectivity for long-chain paraffins.^{7,22,23} Although these reactions proceed via carbenium ions, initiation of these species and subsequent reaction pathways on anion-modified zirconia catalysts are still unclear.^{24,25}

This study contributes to investigation of hydroisomerization of high molecular weight linear alkanes over metal-promoted tungstate-modified zirconia (metal/ WO_3/ZrO_2), using n-hexadecane as a model compound in a trickle bed reactor. Efforts are aimed at obtaining high hydroisomerization selectivity with high hydrocarbon conversion and at elucidating reaction pathways over this class of anion-modified metal oxide.

Experimental

Catalyst Preparation and Characterization The procedure for synthesis of metal/ WO_3/ZrO_2 consists of the following steps: (1) zirconium hydroxide precipitation by addition of ammonium

* Correspondence author

hydroxide to zirconium chloride; (2) anion-modification by addition of ammonium metatungstate solution; (3) impregnation of a metal (Pt, Pd, or Ni) salt; (4) calcination. Two preparation procedures (labeled I and II in Figure 1) were used. In I, there were two calcinations, one at 700°C for tungstate-modified zirconium hydroxide and the other at 500°C after metal salt impregnation; procedure II had only one calcination at 700°C after co-impregnation of zirconium hydroxide by the solution of tungsten and metal salts. The metal content and tungsten content in the catalysts were controlled by adjusting the concentration of salts. In this paper, the metal salt we used is $H_2PtCl_6 \cdot 6H_2O$. Figure 1 shows details of procedures I and II.

BET specific surface area (by nitrogen adsorption) and platinum distribution (by carbon monoxide adsorption) were measured using a Micromeritics ASAP 2010 instrument.

Reactor System and Operating Procedure Catalytic activity and selectivity tests were carried out in a continuous trickle bed stainless steel reactor with 0.305 inch i.d. Reaction temperature was controlled by a computer and system pressure by a back-pressure valve. *n*-C₁₆ (99 wt% from ICN Biomedical Inc.) was delivered from a feed tank into the reactor by a syringe pump at a constant rate of 6.6 ml/hr. Input rates of hydrogen and helium (make-up gas to keep gas flow rate constant when studying effects of pressure) were controlled by two mass flow meters, respectively. The catalyst was crushed to 40-60 mesh pellets and placed into the center of the reactor after mixing with an equal volume of quartz (50-70 mesh). Quartz was also used as packing at each end of the reactor. Variation in weight hour space velocity (WHSV) was obtained by changing the amount of catalyst. Before reaction, the catalyst was activated at 450°C with 20 ml/min of air for one hr. Liquid products were collected in an ice-water cooled vial for analysis using an HP-5980 GC.

Results and Discussion *n*-C₁₆ conversion is defined as the difference between *n*-C₁₆ weight percentage in the feed and that in the reaction products; *i*-C₁₆ selectivity is calculated by dividing *i*-C₁₆ percentage in the products with *n*-C₁₆ conversion; *i*-C₁₆ yield is the *i*-C₁₆ percentage. In order to obtain comparable *n*-C₁₆ conversion with different catalysts, we carried out the activity and selectivity tests at 300°C. Later, the possibility of operating reactions at lower temperatures, from 210 to 250°C, using our most active catalyst (6.5 wt% W) was investigated and the influence of reaction pressure was studied at 230°C.

Comparison of results from catalysts prepared by methods I and II These two Pt/WO₃/ZrO₂ catalysts, I and II, with the same composition (0.5 wt% platinum and 6.5 wt% tungsten) were tested under the same conditions but at varying WHSV: 300°C, 300 psig, H₂/*n*-C₁₆ (mole ratio)=2. Results are shown in Figure 2. *n*-C₁₆ conversion decreases and *i*-C₁₆ increases for both catalysts when WHSV increases, but the *n*-C₁₆ conversion with catalyst II declines more rapidly. At the same *n*-C₁₆ conversion, 90 wt%, for instance, the *i*-C₁₆ selectivity over catalyst I is about 20 wt% higher than that over catalyst II. A possible explanation is that the high temperature calcination (700°C) after platinum salt impregnation used in procedure II resulted in a low degree of platinum distribution and the metal function is weakened. These two catalysts have similar surface areas, about 67.5 m²/g, but carbon monoxide chemisorption experiments show platinum distribution of catalyst I is 0.63, which is much better than that of II (0.14). It is known that metals, such as platinum, palladium or nickel, can provide hydride ions²⁶ and enhance acidity by hydrogen spillover in the presence of hydrogen²⁷. Lack of available hydride ions may result in long residence times for reaction intermediates and increase the opportunity for β-scission which produces cracked products.

Effect of tungsten content on catalyst reactivity Five Pt/WO₃/ZrO₂ catalysts with different tungsten contents but the same amount of platinum content (0.5 wt%) were prepared by method I. Properties are shown in Table 1. These catalysts were tested at the same temperature, pressure and hydrogen to *n*-C₁₆ ratio (Figure 2). Catalysts with 6.5 and 8 wt% tungsten have high hydroisomerization activities at relatively high conversion. Data from BET nitrogen adsorption measurement indicates the surface area of Pt/WO₃/ZrO₂ increases with increasing tungsten content. It has been postulated that tungsten oxide is reduced in the presence of hydrogen; the reduced species may play an important part in the reaction mechanism.²⁸ Surface density and particle size of tungsten oxide as well as acidity will be studied by TEM, XPS and TPD.

Effect of reaction temperature and pressure Influence of reaction temperature and pressure on conversion and isomerization selectivity was investigated using a Pt(0.5 wt%)/WO₃/ZrO₂ (6.5 wt% W) catalyst prepared by procedure I. Data in Tables 2 and 3 indicates that *n*-C₁₆ conversion and *i*-C₁₆ selectivity are more sensitive to reaction temperature than to pressure. In the temperature range from 210 to 250°C, lowering the temperature resulted in low conversion but high selectivity. This catalyst is very active; 85.9 wt% *n*-C₁₆ conversion with 83.1 wt% *i*-C₁₆ selectivity was achieved at 230°C, WHSV = 1 hr⁻¹. Comparable *n*-C₁₆ conversion (82.8 wt%) was

also obtained at higher temperature and larger WHSV (300°C, WHSV=24 hr⁻¹, line C in Figure 3), but the i-C₁₆ selectivity was only 74.3 wt%. This suggests that large i-C₁₆ yields will be obtained at relatively low temperature and small WHSV, rather than high temperature and large WHSV. The increase of pressure resulted in low conversion with high selectivity, indicating a negative reaction order of hydrogen. A similar effect of hydrogen on conversion was observed by Iglesias *et al.* in heptane isomerization using Pt/WO₃/ZrO₂.²⁶

Comparison of Pt(0.5 wt%)/SO₄/ZrO₂ and Pt(0.5 wt%)/WO₃/ZrO₂ At relatively low temperature (150°C), platinum-promoted sulfated zirconia (calcined at 630°C for 3 hr in air) was tested for n-hexadecane hydroisomerization. Its preparation procedure is described elsewhere.¹⁴ Results with Pt(0.5 wt%)/SO₄/ZrO₂ are compared with those obtained using Pt(0.5 wt%)/WO₃/ZrO₂ (6.5 wt% W) in Table 4. Pt(0.5 wt%)/SO₄/ZrO₂ is active at 150°C, but it favors cracking. Pt(0.5 wt%)/WO₃/ZrO₂ requires higher temperature, but has high isomerization selectivity even at high hexadecane conversion.

Acknowledgment We acknowledge the financial support of this work by the U.S. Department of Energy (Grant No. DE-FC22-93PC93053).

REFERENCES

1. Encyclopedia of Chemical Processing and Design, 15, Mcketta, M., Dekker, M., Inc. (1982).
2. Miller, S. J., Studies in Surface Science and Catalysis, Vol. 84 (1994), pp. 2319-2326.
3. Kim, I., Chem. Eng., Dec. 1995, pp. 71.
4. Encyclopedia of Chemical Technology, Fourth Edition, Vol. 12 (1996).
5. Coppola, E. N., M. S. thesis, University of Utah (1987).
6. Miller, S. J., preprints of Div. Petrochem., Am. Chem. Soc., 38 (1993), pp. 788-793.
7. Taylor, R. J., Pretty, R., Appl. Catal. A 119 (1994), pp. 121-138.
8. Hino, M. and Arata, K., J. Am. Chem. Soc., 101 (1979), pp. 39-40.
9. Yori, J. C., Luy, J. C. and Parera, J. M., Appl. Catal. 46 (1989), pp. 102-112.
10. Corma, A., Juan-Rajadell, M. I., Lopez-Nieto, J. M., Martinez, A., Martinez, C., Appl. Catal. A 111 (1994), pp. 175-189.
11. Yori, J. C., Parera, J. M., Appl. Catal. A 129 (1995), pp. 83-91.
12. Arata, K., Appl. Catal. A 146 (1996), pp. 3-32.
13. Liu, H., Lei, G. D., Sachtler, W. M. H., Appl. Catal. A 146 (1996), pp. 165-180.
14. Wen, M. Y., Wender, I., Tierney, J. W., Energy & Fuels, 4 (1990), pp. 372-379.
15. Keogh, R. A., Sparks, D., Hu, J., Wender, I., Tierney, J. W., Wang, W., and Davis, B. H., Energy & Fuels, 8 (1994), pp. 755-762.
16. Venkatesh, K. R., Hu, J., Wang, W., Holder, G. D., Tierney, J. W., and Wender, I., Energy & Fuels, 10 (1996), pp. 1163-1170.
17. Chang, C.D., Santiesteban, J. G., Stern, D. L., U.S. Patent 5,345,026 (1994).
18. Soled, S. L., Gates, W. E., Iglesia, E., U.S. Patent 5,422,327 (1995).
19. Larsen, G., Lotero, E., Raghavan, S., Prira, R. D., Querini, C. A., Appl. Catal. A 139 (1996), pp. 201-211.
20. Iglesia, E., Barton, D. G., Soled, S. L., Miseo, S., Baumgartner, J. E., Gates, W. E., Fuentes, G. A., and Meitzner, G. D., Stud. Surf. Sci. and Catal., Vol. 101 (1996), pp. 533-542.
21. Corma, A. and Wojciechowski, B. W., Catal. Rev.-Sci. Eng., 27(1) (1985), pp. 83.
22. Weitkamp, J., Jacobs, P. A. and Martens, J. A., Appl. Catal. 8(1983), pp. 123-141.
23. Girgis, M. J. and Tsao, Y. P., Ind. Eng. Chem. Res., 35 (1996), pp. 386-396.
24. Farcasiu, D., Ghenciu, A., and Li, J. Q., J. Catal., 158 (1996), pp. 116-127.
25. Parera, J. M., Appl. Catal. A 167 (1998), pp. 75-84.
26. Iglesia, E., Soled, S. L., and Karmer, G. M., J. Catal., 144 (1993), pp. 238-253.
27. Shishido, T., Hattori, H., Appl. Catal. A 146 (1996), pp. 157-164.
28. Larsen, G., Lotero, E., and Parra, R., Stud. Surf. Sci. and Catal., Vol. 101 (1996), pp. 543-551.

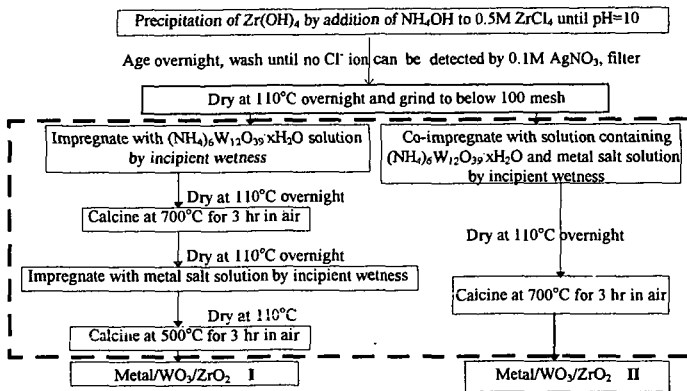


Figure 1 Two procedures for the preparation of Metal/ WO_3/ZrO_2 catalysts

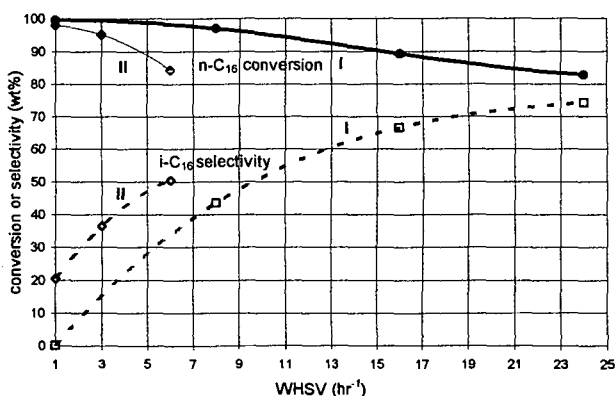


Figure 2 Comparison of conversion and selectivity for hydroisomerization of $n-C_{16}$ using $Pt(0.5wt\%)/WO_3/ZrO_2$ (6.5 wt% W) catalysts prepared by procedures I and II. [Reaction conditions: 300°C, 300 psig, $H_2/n-C_{16}$ (mole ratio)=2, 6th hr reaction results]

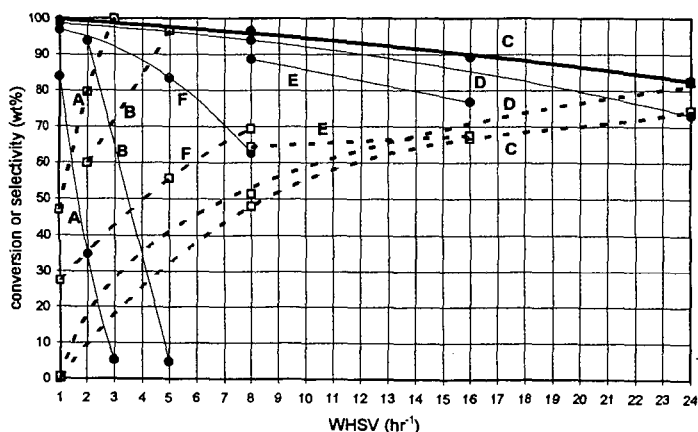


Figure 3 Effect of tungsten content in $Pt(0.5wt\%)/WO_3/ZrO_2$ on $n-C_{16}$ conversion (—) and $i-C_{16}$ selectivity (----) [catalysts prepared by procedure I; reaction conditions: 300°C, 300 psig, $H_2/n-C_{16}$ (mole ratio)=2, 6th hr results]

Table 1 Physical properties of Pt(0.5 wt%)/WO₃/ZrO₂ with different tungsten contents

catalyst	A	B	C	D	E	F
W wt%	3	4.5	6.5	8	10	15
surface area m ² /g	42.46	56.4	67.49	74.87	90.01	99.10
pore diameter Å	125.1	111.8	96.8	88.2	87.3	72.5
pore volume cm ³ /g	0.14	0.16	0.16	0.16	0.20	0.18

Table 2 Effect of reaction temperature on n-C₁₆ conversion and i-C₁₆ selectivity over Pt(0.5 wt%)/WO₃/ZrO₂ (6.5 wt% W) by procedure I

reaction temperature °C	210	220	230	250
n-C ₁₆ conversion, wt%	33.5	53.8	85.9	98.3
i-C ₁₆ selectivity, wt%	99.1	96.6	83.1	0
i-C ₁₆ yield, wt%	33.2	52.0	71.4	0
i-C ₁₆ distribution wt%				
multibranch i-C ₁₆	5.4	10.7	26.6	0
dimethyltetradecane	31.3	36.6	42.8	0
7- and 8-methylpentadecane	15.1	11.8	6.4	0
6-methylpentadecane	13.0	10.8	5.8	0
5-methylpentadecane	9.9	8.2	4.6	0
4-methylpentadecane	8.7	7.3	4.0	0
3-methylpentadecane	8.7	7.5	4.6	0
2-methylpentadecane	6.3	5.9	4.0	0
3-ethyltetradecane	1.5	1.2	0.8	0

Reaction conditions: 300 psig, H₂/n-C₁₆ (mole ratio)=2, WHSV= 1 hr⁻¹Table 3 Effect of reaction pressure on n-C₁₆ conversion and i-C₁₆ selectivity over Pt(0.5 wt%)/WO₃/ZrO₂ (6.5 wt% W) by procedure I

reaction pressure	300	400	500	600
n-C ₁₆ conversion, wt%	85.9	78.8	76.1	70.7
i-C ₁₆ selectivity, wt%	83.1	88.9	90.7	93
i-C ₁₆ yield, wt%	71.4	70.1	69.1	65.8
i-C ₁₆ distribution wt%				
multibranch i-C ₁₆	26.6	20.0	19.9	17.2
dimethyltetradecane	42.8	43.2	41.5	40.5
7- and 8-methylpentadecane	6.4	8.0	8.8	9.3
6-methylpentadecane	5.8	7.0	7.0	8.2
5-methylpentadecane	4.6	5.7	6.0	6.6
4-methylpentadecane	4.0	4.8	5.4	5.9
3-methylpentadecane	4.6	5.3	5.6	6.1
2-methylpentadecane	4.0	4.6	4.7	5.0
3-ethyltetradecane	0.8	1.0	1.0	1.1

Reaction conditions: 230°C, H₂/n-C₁₆ (mole ratio)=2, WHSV= 1 hr⁻¹Table 4 Comparison of Pt(0.5wt%)/SO₄/ZrO₂ (630°C) and Pt(0.5wt%)/WO₃/ZrO₂ [6.5wt% W (700, 500°C)]

Catalyst	Pt(0.5 wt%)/SO ₄ /ZrO ₂ (630°C)	Pt(0.5 wt%)/WO ₃ /ZrO ₂ 6.5 wt% W (700, 500°C)
Reaction conditions	150°C, 300 psig, WHSV=1hr ⁻¹	230°C, 300 psig, WHSV=1hr ⁻¹
n-C ₁₆ conversion, wt%	76.7	85.9
i-C ₁₆ selectivity, wt%	19.8	83.1
i-C ₁₆ yield, wt%	15.2	71.4
i-C ₁₆ distribution wt%		
multibranch i-C ₁₆	21.2	26.6
dimethyltetradecane	44.3	42.8
monomethylpentadecane	33.6	29.4
3-ethyltetradecane	0.6	0.8

THERMAL DECOMPOSITION CHARACTERISTIC OF VACUUM RESIDUE IN ATHABASCA TAR SAND BITUMEN

Masaaki Satou, Maki Mikuni and Hideshi Hattori
CARET, Hokkaido University, Sapporo 060-8628, Japan

Hiroshi Nagaishi and Tadashi Yoshida
Hokkaido National Industrial Research Institute, Sapporo 062-8517, Japan

Keywords: Tar sand bitumen, Thermal decomposition characteristic, Chemical structure

INTRODUCTION

To develop and establish the effective use of tar sand bitumen in the future, it is necessary to clarify the reaction characteristics related with the information of chemical structure. There were many studies on the chemical structure of tar sand bitumen¹⁻³⁾, and many kinetic reaction models were also proposed. However the study on the reaction characteristics concerned with the chemical structure is few^{4,5)}. The initial upgrading step in the conversion of bitumen to synthetic crude is the thermal decomposition of heavy macromolecule in bitumen, which would be the simplest reaction. This study aims at elucidating the thermal decomposition characteristic of vacuum residue in bitumen on the basis of conversion and chemical structure changes.

EXPERIMENTAL

Sample preparation

The used raw-bitumen is Athabasca tar sand bitumen (C: 82.6, H: 10.5, N: 0.5, O: 2.3, S (diff): 4.1 wt%). Two kinds of sample series were prepared by a vacuum distillation based on ASTM D1160. One is the light fraction (boiling point range, 723K under) and vacuum residue. The other is the blended sample of vacuum residue with light fraction by various weight fractions.

Thermal decomposition reaction

Thermal decomposition reaction was conducted in a 60 cm³ autoclave with an electromagnetic stirrer. The autoclave was heated at 90 K/min by an infrared image furnace and cooled at 100 K/min by blowing air. Connecting the reactor with a 500 cm³ buffer vessel kept the pressure almost constant through each reaction. Five grams of sample were loaded in the reactor. The reaction temperature and pressure were 693 K and 10 MPa in N₂, respectively.

Product characterization

After each reaction, a product was recovered with dichloromethane. Produced gas yield was obtained from the data of TCD gas chromatograms.

Boiling point distribution of the product was measured by a thermogravimetric analysis (SD-TGA), which was in good agreement with the standard distillation method (ASTM D2892^{6,7)}. The distribution was plotted as a function of boiling point index that is not true one but fairly corresponds to it.

Samples for the ¹H-, ¹³C-NMR measurements were dissolved in deuteriochloroform. Both spectra were obtained with a α -500 type Fourier transform spectrometer (JEOL Ltd.). ¹³C-NMR spectra were obtained by using a pulse width of 11.5 μ s, total of 1000 transients and gated decoupling to ensure quantitative results. Tris(acetylacetonate)chromium(III)(Cr(acac)₃) was used as the relaxation reagent⁸⁾. From conventional ¹H-NMR spectra, aromatic-H_{ar}, H α , H β and H γ illustrated hydrogen distribution.

Elemental analyses were carried out with a CHNO analyzer. Molecular weight measurements were made with a KNAUER vapor pressure osmometer.

RESULTS AND DISCUSSION

Thermal decomposition characteristics of vacuum residue

Figure 1 shows the variation of product yields with reaction time for the vacuum residue. Yields of heavy and light components in a sample were calculated from SD-TGA data and a cut point between both components was 723 K. Loss was a volatile matter that was lost in product recovery from a autoclave, and might be low molecular hydrocarbons such as hexane and heptane. With the progress of the reaction, gas, loss and light component gradually increased.

To discuss the degree of decomposition of macromolecule in vacuum residue, a conversion was defined as the weight ratio of decrease of heavy component to initial one. Figure 2 shows the change in conversion and average molecular weight with the reaction time. At 0 min of nominal reaction time, no remarkable change of molecular weight was observed, but it was reduced to almost half up to 10 min. This suggests the decomposition of macromolecule in the vacuum residue. The molecular weight was finally almost constant, namely, about 400. While the conversion gradually increased with the progress of the reaction.

Chemical structural change during thermal decomposition reaction

Figure 3 shows the weight change of various carbon types by unit gram of vacuum residue with the reaction time. Carbon weight by unit gram was calculated based on the carbon distribution obtained from ^{13}C -NMR, elemental analysis data and product yield. Carbons are assigned six types from the chemical shifts in ^{13}C -NMR spectra^{9,12}, named as methyl carbons, methylene carbons, α -methylene carbons, unsubstituted aromatic carbons, bridgehead aromatic carbons and substituted aromatic carbons.

In Fig. 3, a remarkable weight decrease of α -methylene carbons was recognized in the initial stage of reaction. Methylene carbons and unsubstituted aromatic carbons had gradually weight decreasing and increasing tendency with the progress of the reaction, respectively. While, the values of weight of the other carbons were almost constant.

Carbons assigned α -methylene carbons included α -methylene carbons on an aliphatic methylene bridge and a side chain except for ethyl group, and methine carbons in a naphthenic ring¹². Methylene carbons included methylene carbons in a naphthenic ring and β or further position on a side chain from an aromatic ring, α -methylene carbons on an ethyl group, and methine carbons on a side chain.

In the initial stage of reaction, the decomposition of an aliphatic bridge including in a macromolecule, resulting in the reduction of molecular weight to half in Fig. 2, could explain the remarkable weight decrease of α -methylene carbons. At the same time, the dehydrogenation of naphthenic ring and the cleavage of an aliphatic chain would bring about mainly the weight increase of unsubstituted aromatic carbons and decrease of methylene carbons. With the progress of the reaction, these reactions would be prior.

To confirm the above consideration, numbers of aromatic and naphthenic rings in an average molecule were estimated¹³ as shown in Fig. 4. The naphthenic ring number changed in unique manner with the reaction time. Considerable decrease of naphthenic ring number up to 10 min was corresponding with the reduction of molecular weight to half resulting from the decomposition of a macromolecule. Furthermore, the naphthenic ring number increased at 30 min by a ring formation on a still remaining aliphatic chain. On the contrary, the aromatic ring number decreased in the initial stage of reaction, but was not the reduction to half. This also suggests the dehydrogenation of naphthenic ring. Subsequently aromatic ring number gradually increased after 30 min.

The conversion at 0 min of reaction time was not so high in spite of the reduction of molecular weight to half. The values of molecular weight and estimated total carbon number in an average molecule were about 540 and 38, respectively. According to our boiling point calculation¹⁴, the boiling point of this average molecule should be at least 790 K. At 60 min of reaction time, the boiling point of product would be 720 K as the total carbon number fell to about 30. Consequently, the conversion was still low in the initial stage of the reaction, and gradually increased with the progress of reaction.

Influence of light component on conversion of heavy one in a bitumen

To clarify the decomposition characteristics of heavy component in the presence of light one in bitumen, vacuum residues blended with light fraction in different ratios were prepared. If the thermal decomposition of heavy and light components occur independently each other, the conversion should not change regardless of light fraction content. In Fig. 5, the change in conversion at 60 min of reaction time with weight content of light fraction is shown. The conversion decreased with the increase of the weight content of light fraction. This suggests that the light component affects the conversion of heavy component to light one. In this section, interactions between the heavy and light components in a thermal decomposition would be clarified on the basis of chemical structure changes in a product.

Figures 6 and 7 show differences in the weight of aromatic and aliphatic carbon types by unit gram before and after reaction versus the weight ratio of light component to heavy one in a blended sample, respectively. The plots are scattered to some extent in both figures. A dashed line and open symbols were calculated on the assumption that the thermal decomposition of heavy and light components occurs independently each other, and a solid line is smoothing experimental values indicated by solid symbols. As a vacuum residue contains about 30 wt% of light component by SD-TGA, the minimum weight ratios in both figures are not zero but about 0.5. The differences in weight of aromatic and aliphatic carbons before and after reaction of 60 min became plus and minus values, respectively. If examined in detail, weight increase of unsubstituted aromatic carbons was remarkably kept down with the increase of light component content, and weight decrease of α -methylene carbons was also controlled by light component. The weight differences of other carbons were almost equal between calculated and observed ones in the presence of light component. These controls of weight change would be explained by some interpretations on the interaction between heavy and light components in the thermal decomposition. The condensed naphthenic ring formation and the polymerization of light component with heavy one would contribute the weight increase of α -methylene carbons. The control of dehydrogenation on a naphthenic ring would bring about the weight decrease of unsubstituted aromatic carbons.

Summarizing above discussion, the thermal decomposition characteristic of a blended sample was related with the chemical structure changes, though a detailed reaction scheme could not be illustrated at the present time.

CONCLUSIONS

A thermal decomposition characteristic of vacuum residue in bitumen is discussed from conversion and chemical structure changes.

In the initial stage of reaction, cleavage of aliphatic bridge occurs, resulting in the decrease in average molecular weight. With the progress of the reaction, the dehydrogenation at naphthenic rings and release of low molecular weight hydrocarbon from side chain take place, therefore a remarkable change of average molecular weight was not observed, but the conversion is gradually increasing.

In the thermal decomposition of residue with the light fraction, the conversion decreased with the increase in weight ratio of light fraction in blended samples. Polymerization of the light component with the heavy one would be suggested.

ACKNOWLEDGMENTS

The authors gratefully acknowledge Prof. M.R.Gray and Syncrude Canada Ltd. for supply of the tar sand bitumen sample.

REFERENCES

- 1) T.Suzuki, M.Itoh, Y.Takegami and Y.Watanabe, *Fuel*, 61, 402(1982)
- 2) F.Khorasheh, M.R.Gray and I.G.D.Lana, *Fuel*, 66, 505(1987)
- 3) M.R.Gray, J.H.K.Choi, N.O.Egiebor, R.P.Kirchen and E.C.Sanford, *Fuel Sci. Tech. Int'l.*, 7, 599(1989)
- 4) M.R.Gray, *Ind. Eng. Chem. Res.*, 29, 505(1990)
- 5) M.R.Gray, P.Jokuty, H.Yeniova, L.Nazarewycz, S.E.Wanke, U.Achia, A.Krzywicki, E.C.Sanford and O.K.Y.Sy, *Can. J. Chem. Eng.*, 69, 833(1991)
- 6) Y.Hasegawa, T.Yoshida, H.Narita and Y.Maekawa, *J. Fuel Soc. Japan*, 66, 855(1987)
- 7) H.Nagaishi, M.Sasaki, T.Kotanigawa and Y.Maekawa, *J. Japan Inst. Energy*, 72, 964(1993)
- 8) T.Yoshida, Y.Maekawa, H.Uchino and S.Yokoyama, *Bull. Chem. Soc. Jpn.*, 52, 3676(1979)
- 9) T.Yohida, Y.Narita, R.Yoshida, S.Ueda, N.Kanda and Y.Maekawa, *Fuel*, 61, 824(1982)
- 10) J-M. Derreppe, C.Moreaux, P.Landais and M.Monthieux, *Fuel*, 66, 594(1987)
- 11) L.Michon, D.Martin, J-P.Planche and B.Hanquet, *Fuel*, 76, 9(1997)
- 12) K.Hayamizu and O.Yamamoto, "¹³C NMR Spectra of Polycyclic Aromatic Compounds", Japan Industrial Technology Association, Tokyo, 1982
- 13) K.H.Altgelt and M.M.Boduszynski, "Composition and Analysis of Heavy Petroleum Fractions", Marcel Dekker, New York, 1994, pp. 335
- 14) M.Satou, S.Yokoyama and Y.Sanada, *Fuel*, 71, 565(1992)

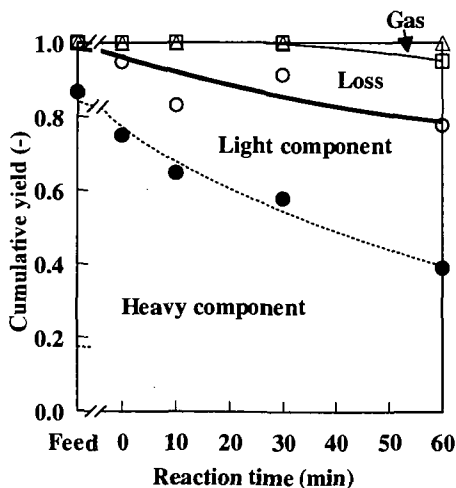


Fig. 1 Change in cumulative yield of product with reaction time

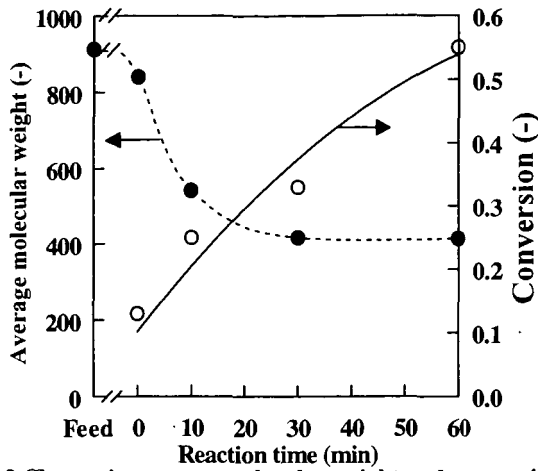


Fig. 2 Change in average molecular weight and conversion with reaction time

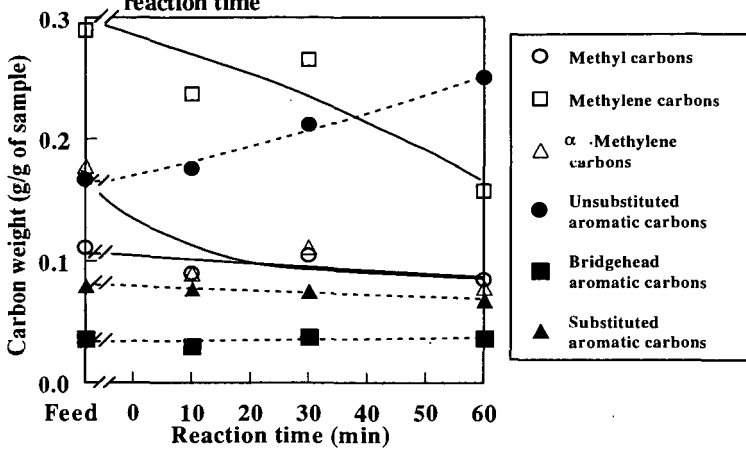


Fig. 3 Change in carbon weight by unit weight of sample with reaction time

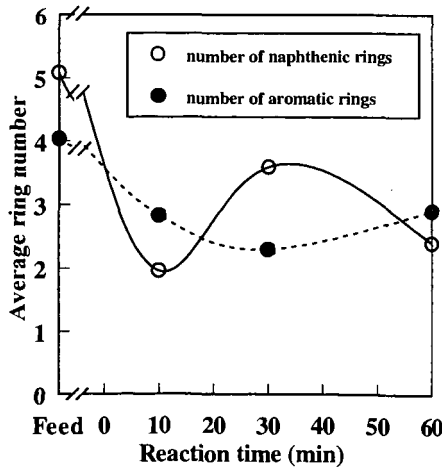


Fig. 4 Change in aromatic and naphthenic ring with reaction time

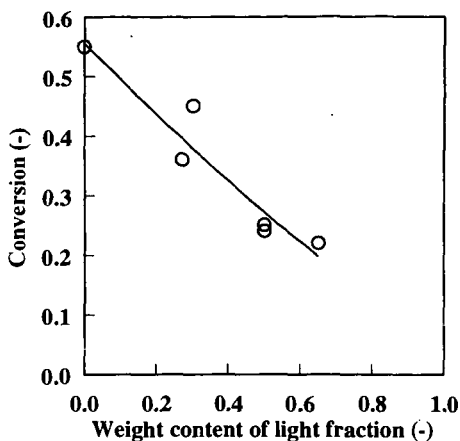


Fig. 5 Change in conversion for blended sample with weight content of light fraction

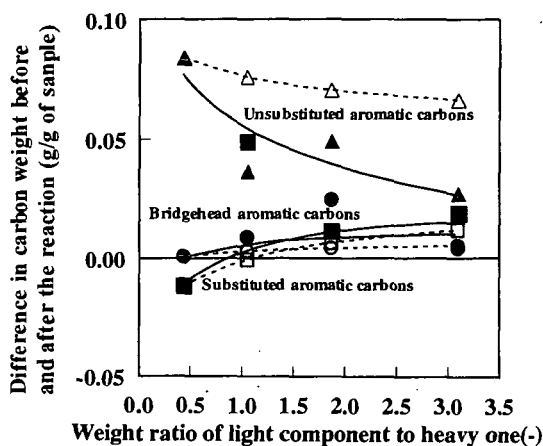


Fig. 6 Change in weight difference of aromatic carbons with weight ratio of light component to heavy one

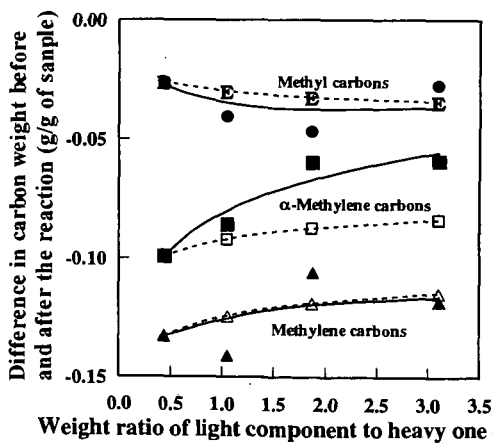


Fig. 7 Change in weight difference of aliphatic carbons with weight ratio of light component to heavy one

ADDITIVE FOR VISBREAKING: AVB-95

J.A. Carrillo Guarin and F. Pantoja
ECOPETROL-ICP
Piedecuesta, Santander
A.A. 4185 Bucaramanga, Colombia

Key Words: visbreaking, additives

SUMMARY

The primary goal for visbreaking is reducing the viscosity of heavy feedstocks by means of a mild thermal breakdown so it may be possible to produce fuel oils, as well as to prepare the load for subsequent catalytic breakdown. The major operating costs of this process are strongly dependent on two factors: diluent consumption needed in the fuel oil formulation, and plant's coking rate resulting from the severity of the treatment. Some additives available on the market are specifically designed to exert a counteraction against the coking tendency of the heavy feedstocks inside the furnace tubes; and they, to a greater or lesser degree, accomplish this task. These commercial additives performance was evaluated and compared to that of an additive package, based on several mechanisms of action, recently developed by Instituto Colombiano del Petróleo (ICP). As a result of the pilot plant experiments and field trials, it was found that the new additive considerably reduces the quantity of diluent necessary for fuel oil preparation; and moreover, the run time is increased with less plant maintenance requirements.

INTRODUCTION

The visbreaking process is a mild thermal cracking process wherein vacuum residues and asphalt are processed in order to prepare the feedstock for FCC and to reduce the viscosity of these loads to produce fuel oil (1-3).

Among the reactions taking place in the visbreaking process we have:

- Side-chains from resins and aromatics are broken leading to further decrease in the average molecular weight, and consequently reducing their peptizing capability.
- Free radicals are reacted to form asphaltenes.
- The asphaltenes are subjected to dealkylation and dehydrogenation reactions whose products are more difficult to peptize, causing the colloidal system destabilization and asphalt precipitation.
- The saturated components (paraffins) are split into shorter, non-polar compounds which facilitate asphaltene precipitation.

These undesired reactions are responsible for the main drawbacks and limitations in the run time and severity applied in visbreaking operations. This is why we rely on additives (4-7) to avoid the aforementioned problems.

MATERIALS AND METHODS

Three commercial additives already tried at an industrial scale were chosen for evaluation on a visbreaking pilot unit built by the ICP (Figure 1). Besides, the heavy residues used in the experiments came from Ecopetrol's refinery in Barrancabermeja, and had the physicochemical characteristics sketched in Table 1. The operating conditions set up were 870°F (465°C), and 25 minutes residence time.

The working mechanism for these latter additives is based on the formation of a protective film over the tubes metallic walls at the prevailing operating conditions, but they do not act upon the system stability. At the beginning of the run the surface temperature is around 870°F (465°C) and becomes slowly increased with time as the coke layer starts to deposit, forming an insulating barrier. The evaluation at pilot scale showed that, coincidentally, the additive having the best performance was the one being used at the Ecopetrol's plants at that time. It was also observed that said commercial additives were not effective as operating temperatures were over 884°F (473°C), maybe due to product decomposition.

This clear disadvantage of available commercial additives led us to think about developing new additives working under mechanisms, different from that of film-forming, such as: hydrogen transfer, metal passivators, and free radicals scavengers. As a result

we obtained a package of additives having a higher protective efficiency against coking than commercial products, as it is seen in Figure 3.

RESULTS

With the available additive used by the Cartagena Refinery, acceptable gas, nafta and gas-oil performance was obtained, which was increased by the application of the AVB-95 additive. These differences are shown in table 2.

Benefits from the application of AVB-95

Although performance of the commercial additive being used in the Cartagena refinery was considered satisfactory from the standpoints of gas, naphta, and gas-oil yields; a remarkable increase in these variables output was seen once the AVB-95 was applied. The additional benefits are clearly depicted in Figure 4.

1. Profit due to VBN (viscosity blending number) increase

Depending on the severity and the additive dosage, an increase in VBN from 1.0 to 2.5 points is easily reached. It should be carefully considered that a single point increase in VBN for a plant that processes vacuum residues means total savings of about KUS \$800 per year.

2. Savings with maintenance

Due to a more porous and softer coke formation caused by the additive action, maintenance work on the furnace and the fractional towers is made easier, and cost noticeably reduced. These savings equal to KUS\$220 per year.

In the Cartagena refinery the average coke film thickness within the furnace tubes was reduced in almost 1.5 cm. The coke deposition rate in the fractional towers was also lowered and its smooth consistency allowed an easier removal.

3. Increase in the service factor

For run #37 at the Cartagena refinery, an increase in the service factor of 76% was registered due to a greater operating time equivalent time to 9 days a year. The benefit was then around KUS \$583 per year.

4. Versatility in operation

Through the use of this additive it may be possible to obtain a reaction product having a lower asphaltene content and greater distillate production, which at the same time permits operating at the same severity levels for longer run times. These latter condition bear an increase in conversion without risking the stability of the fuel oil or coking the furnace.

5. Product performance

The Cartagena refinery plant used a commercial additive and for this reason the action of additive AVB-95 is not compared with an actual target, but additional benefits are readily achieved over the commercial additive (See Table 2).

Through the addition of the new additive we were able to increase the conversion by 1.52%, specially in nafta production, by 0.71%, but also in gas-oil, by 0.81%.

The analysis of saturate, aromatic, resin and asphaltene content (SARA) of the visbreaking tars shows a broad change in the distribution of each family as a result of the free radicals capping action and the increase of hydrogen concentration in the system foreseen by the anti-coking agent AVB-95.

The average changes in composition for the visbroken resids are:

Saturates: increased by 1.21%

Aromatics: increased by 10.0%

Resins: decreased by 8.9%

Asphaltenes: decreased by 3.0%

This new chemical distribution improves the VBN in the visbreaking tar, allowing the operating plant a severity similar to previous runs, increasing run time due to a lower quantity of asphaltenes in the system, hence producing less coke. As a secondary

effect there is an increase in the conversion of nafta and gas-oils, operating at the same severity.

CONCLUSIONS

With the use of AVB-95 there are the followings benefits:

- Increase in the Δ VBN of the tars.
- Less coke production in the fumace and run time increases.
- Easy removal of the coke.
- More conversion.

REFERENCES

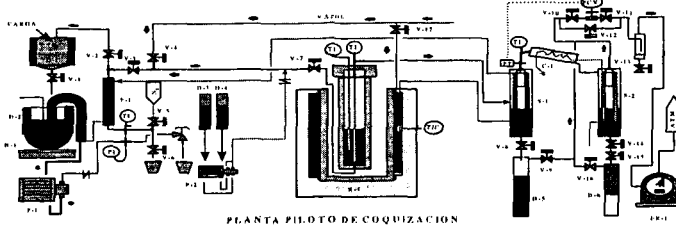
1. José A. Celestinos Y., René Hernández Pérez. Processes compared for upping Maya distillate yield. Technology, Oil & Gas Journal, April 26, 1982, 111-115.
2. A. Del Bianco, N. Panariti, M. Anelli, P.L. Beltrame and P. Carniti. Thermal cracking of petroleum residues. Fuel, 1993, Vol 72, January, 75-80.
3. Indra D. Singh, Vilmal Kothiyal, Mahendra P. Kapoor, Veda Ramaswamy and Mahesh K. S. Aloopwan. Structural changes during visbreaking of light Arabian mix short residue: comparison of feed and product asphaltenes. Fuel 1993, Vol 72, Number 6, 751-754.
4. Michel Thomas, Bernard Fixari, Pierre Le Perchec, Yves Princic and Louis Lena. Visbreaking of Safaniya vacuum residue in the presence of additives. Fuel, 1989, vol 68, March, 318-322.
5. A. Del Bianco, N. Panariti, B. Prandini, P.L. Beltrame and P. Carniti. Thermal cracking of petroleum residues. Hydrogen-donor solvent addition. Fuel, 1993, Vol 72, January, 81-86.
6. P. Le Perchec, M. Thomas and B. Fixari. Fraction characterization of safaniya vacuum residue from visbeaking in the presence of sulfides and H-donor additives. Symposium on correlations between resid characterization and processability. American chemical society. Dallas meeting, April 1989, 422-427.
7. A.S. Bakshi, Y. H. Lutz. Adding hydrogen donor to visbreaking improves distillate yields. Oil and Gas Journal, July 13, 1987, 84-87.

Table 1. Characterization of visbreaking loads

Property	Vacuum residue	Demex residue
Density, 15,6 °C	0.989	1.08
Sulfur, %w	2.26	2.32
Conradson Carbon, %w	18.98	31.5
Penetration, 25 °C, 1/10 mm	2.8	0
Softening point, °C	57	91
Ni, ppm	119	195.1
V, ppm	343	403.7
	2.3	-2.1

Table 2. Performance with additives

Additive	Commercial	AVB-95
Load, BPD	20.000	17.000
Fraction	Output, % wt	Output, % wt
Gases	3.90	3.68
Naphta	5.45	6.16
Gasoil	34.36	35.17
Residues	59.00	57.60
Conversion	39.80	41.32



B-1: celda de carga, D-1: embudo de carga, D-2: tambor de carga, D-3: tambor de aditivos, D-4: tambor de aditivos, D-5: tambor de lodos, D-6: tambor de naftas, S-1: Separador de naftas y gases, S-2: separador de gases, E-1 y E-2: Interchambios, C-1: condensador, FR-1: medidor de gases, P-1: bomba de carga, P-2: bomba de aditivos, H-1: horno de vaporización.

Figure 2. Evaluation of commercial additives

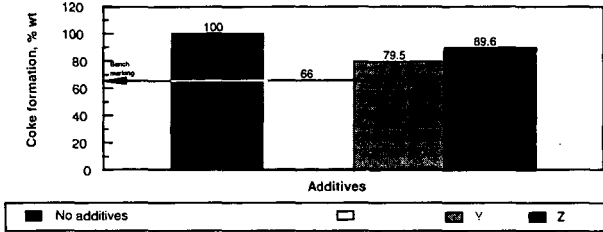


Figure 3. Evaluation of additives developed by the ICP

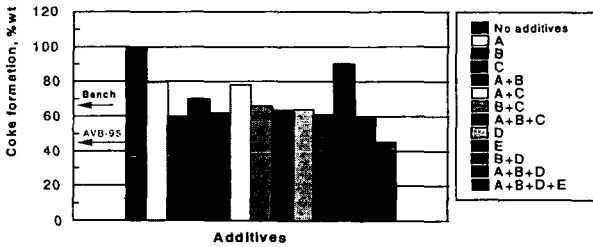
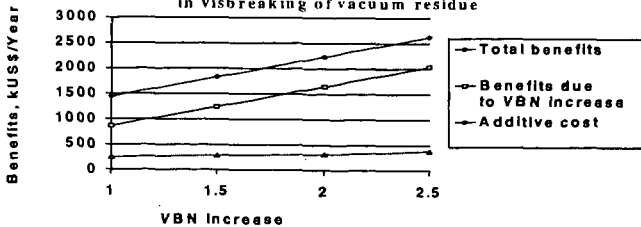


Figure 4. Benefits from the use of the AVB-95 additive in visbreaking of vacuum residue



COMPARISON OF OIL-SANDS-DERIVED AND CONVENTIONAL-CRUDE-OIL-DERIVED DIESEL FUELS AT DIFFERENT ENGINE OPERATING CONDITIONS

Xiaobin Li and Ömer L. Gülder
Combustion Research Group
Institute for Chemical Process and Environmental Technology
National Research Council Canada
Building M-9, Montreal Road, NRC
Ottawa, Ontario, Canada K1A 0R6

KEYWORDS: Diesel Fuels, Exhaust Emissions, Oil Sands

INTRODUCTION

In Canada, 21% of annual petroleum crude processed is oil-sands-derived crude oil. This figure is expected to increase as the conventional crude oil resources are depleted. In the diesel boiling range, the oil-sands-derived crude oil is low in sulfur but higher in aromatics (although low in multi-ring aromatics) compared to conventional crude oil. The oil-sands-derived crude also contains more cycloparaffins. Diesel fuels produced from oil-sands-derived crude tend to have relatively poor cetane quality but good low temperature properties. The specific emission behavior of oil-sands-derived diesel fuels is not well documented.

The general approach in fuel property studies is to blend fuels such that a single fuel property can be varied in a large range while maintaining the other fuel properties within a narrow span. This task is always challenging and sometimes impossible. Consequently, most of the studies to investigate the influence of fuel properties on diesel emissions are biased by the specific fuel matrix design and by the inter-correlation between the fuel properties. One way of alleviating this problem is a careful fuel matrix design consisting of a large number of fuels.

One of the disadvantages of running the U.S. EPA heavy-duty transient emission tests is that it is not possible to differentiate the contributions of different operating conditions to exhaust emissions. Some of the engine operating conditions are more sensitive to fuel properties than some others. In this study, the AVL 8-mode steady state simulation of the EPA transient test procedure was used. The composite emissions obtained from steady-state tests simulate the EPA transient results. The emission test results are therefore comparable to the results obtained with EPA transient test. At the same time, the engine test results from different engine modes offer detailed information so that the influence of each fuel property on oxides of nitrogen (NO_x) and particulate matter (PM) formation at different engine operating conditions can be investigated.

The focus of this study was to investigate the emission behavior of oil-sands-derived diesel fuels and compare it with diesel fuels derived from conventional crude oil. The effects of total aromatic content and fuel density were also investigated. We used two fuel matrices consisting a total of 19 diesel fuels.

EXPERIMENTAL

The engine used in this study is a single-cylinder research version (Ricardo Proteus) of a Volvo TD123 heavy-duty truck engine. The engine is a direct injection type and has a displacement volume of 2 liters. The research engine incorporates many features of contemporary medium- to heavy-duty diesel engines. It is tuned to meet the U.S. EPA 1994 emission standards. Detailed information on the test engine can be found in [1, 2]. The test procedure used in this study is the AVL eight-mode steady-state simulation of the U.S. EPA transient test procedure [3]. The engine speed and load at each of the eight modes are listed in Table I. To check the repeatability of the emission measurements, a low sulfur fuel obtained locally (Table III, fuel Ref2) was run in the engine periodically. The results showed that the standard deviations of NO_x and PM emission measurements were 0.9% and 4.3% of their means, respectively. No engine performance shift was

observed and the experimental data obtained with all test fuels were not adjusted for engine shift or experimental system error.

Among the 19 test fuels, 12 were blended using refinery streams. Six of these 12 fuels were originated from oil sands and the other six were derived from conventional crudes. A total of 22 components obtained from seven refineries were used in this fuel matrix. The parameters controlled in this fuel matrix were:

- total aromatics (10, 20 and 30% by mass)
- ♦ sulfur content (<500 ppm by weight)
- ♦ cetane number (42 to 46)
- ♦ viscosity, cloud point and distillation properties (within the typical range of current commercial diesel fuels in Canada).

The major properties of these test fuels are listed in Table II.

Seven other fuels obtained from various sources were run in the engine so that the regression models generated using the 12 blended fuels can be examined. The major properties of these fuels are listed in Table III.

RESULTS AND DISCUSSION

Composite Emissions

Using correction factors generated in the earlier stages of this research program[5], the composite NO_x and PM emission results were corrected to 150 ppm sulfur content and 44 cetane number. The effect of a small change in injection timing caused by the differences in fuel properties was also corrected. The NO_x and PM emission results are shown in Figure 1 and Figure 2 versus total aromatic content and fuel density.

The oil-sands-derived fuels yield NO_x emissions similar to the conventional-crude-oil-derived fuel blends. A good correlation between the composite NO_x emissions and fuel aromatic content and density was observed. The higher the total aromatic content and the density, the higher the composite NO_x emissions. NO_x emissions do not correlate with T90 or viscosity.

Comparing the two fuel groups, oil-sands-derived fuels generated higher composite PM emissions at the same aromatic level. This difference can be attributed mostly to the density difference between the two fuel groups in the test fuel matrix – the oil-sands-derived fuels having higher densities than the conventional-crude-oil-derived fuels at the same aromatic level. A modest correlation between composite PM emissions and fuel density was observed. A higher density leads to higher PM emissions. A slight increasing trend was also observed in PM emissions when total aromatic content was increased. There was no correlation between PM emissions and T90 or viscosity.

Regression analyses were performed to examine the correlation between the engine exhaust emissions and various fuel properties. The fuel properties considered in the regression analyses are: density, viscosity, T90, T50, T10, total aromatic content, and poly-aromatic content (di+-aromatics). The regression analysis results are shown in Table IV. Fuel density and total aromatic content were found to be the significant variables for NO_x emissions. These two properties account for 92.8% of the total changes in NO_x emissions ($R^2 = 0.928$). Both factors are highly significant, although total aromatic content is more so:

Density is the sole significant variable for PM emissions, accounting for 53.2% of the changes. The total aromatic content was not a significant variable. Considering the low R^2 value, the model can not be viewed as conclusive.

The proposed models were used to predict the NO_x and PM emissions of the 7 test fuels that had not been included in generating the correlations. The NO_x emission model was able to predict the NO_x emission results of six test fuels. The only exception was fuel Ref3 that has properties far away from those represented by the 12 test fuels. This indicates that total aromatic content and density are likely to be two important factors

affecting NO_x emissions. The PM model predictions for 6 of the 7 fuels were reasonable. The exception was fuel F. The model prediction was substantially lower than the actual measured PM emission result. Since fuel F had a substantially higher tri-+aromatic content, the result seems to suggest that multi-ring aromatics might be a factor influencing PM emissions.

Exhaust Emissions at Different Engine Operating Conditions

The eight-mode steady-state test procedure enables us to examine the impact of fuel properties at different engine operating conditions. The effects of cetane number and cetane improvers were significant at low load conditions such as modes 1, 2 and 5. An increase in cetane number from 44 to 64 reduced NO_x emissions by as much as 25% [2][4]. At the same time, PM emissions at low load conditions tended to increase when cetane number was increased. The effects of cetane number on NO_x and PM emissions were not significant at medium to high load conditions. Therefore, the cetane number corrections were performed on NO_x and PM emissions at modes 1, 2 and 5 only using the individual correction formula obtained from engine tests for each corresponding mode.

The sulfur correction formulas were found to be different for different modes. In general, the effect of sulfur appeared to be the largest at the low idle condition, mode 1. Individual correction formulas were used for corresponding modes.

The effects of injection timing on NO_x emissions could be described using second order polynomials for all the modes [5]. This effect was greater at low speed and low load conditions (such as modes 1 and 2). The effects of injection timing on PM emissions were best described using linear relationships. The engine injection timing affected PM emissions more at high load conditions (such as modes 4 and 8).

The corrected brake specific NO_x and PM emissions at each mode were calculated. The results at low idle and the heavy load conditions are plotted in Figure 1 and Figure 2 in comparison with the composite emissions. For NO_x emissions, the oil-sands-derived fuels behaved the same as the conventional-crude-oil-derived fuels at all eight modes. At medium to high load conditions (modes 3,4,6,7 and 8), the NO_x emissions increased with total aromatic content and fuel density. At light load conditions (modes 1,2 and 5), NO_x emissions were not affected by fuel properties.

The PM emissions at individual modes had relatively larger scattering than the composite PM emissions. Consequently, the oil-sands-derived fuels did not show clear difference from conventional-crude-oil-derived fuels in terms of PM emissions at individual modes. The total aromatic content and fuel density impacted on PM emissions differently at different modes. The effects of fuel properties on PM emissions appeared greater at low load conditions (modes 1 and 5); an increase in PM emissions was observed when total aromatic content and fuel density were increased. However, at heavy load conditions (such as modes 4 and 8), the effects of fuel properties on PM emissions were not significant.

The fuel density generally affects the fuelling rate when conducting transient tests. If all the test fuels are run using the same power curve that is generated from a reference fuel, the fuel with a higher density will run at a higher fuelling rate on mass basis. This fuelling discrepancy can bias emission comparison between fuels. In this study, steady-state tests were conducted, and the power outputs of all the fuels were kept the same. This minimized the fuelling discrepancy between the test fuels. The specific fuel consumption changed less than 1% and was not a function of density.

The effect of fuel density on NO_x emissions is likely to be a physical one. A higher fuel density leads to a higher injection rate on a mass basis and therefore shorter injection duration. This effect becomes more significant at heavy load condition due to longer injection duration. Between the heaviest and the lightest fuels, a 4% difference was observed in the mean cylinder pressure that was averaged from the start of mixing controlled burning to the end of fuel injection. This indicates that a higher injection rate

caused more fuel to be injected into the high temperature region, leading to higher NO_x emissions.

The effect of total aromatic content on NO_x emissions could be a chemical one. At high load conditions, major portion of the fuel was burned at fuel-rich locations where the chemical composition of the fuel is likely to have an impact on the local gas temperature. The fuel with a higher total aromatic content can be expected to generate a higher temperature in these fuel-rich regions because the adiabatic temperatures of the hydrocarbons with ring structures tend to be higher.

CONCLUSIONS

In this work, we compared the emission behaviors of fuels derived from oil sands and from conventional crude oil at different engine operating conditions. We also investigated the effects of total aromatic content and density of diesel fuels on NO_x and PM emissions. Our results lead to the following conclusions:

- Oil-sands-derived diesel fuels behave similarly as conventional-crude-oil derived diesel fuels in terms of NO_x emissions at all engine operating conditions.
- Oil-sands-derived diesel fuels exhibit higher composite PM emissions than their conventional-crude-oil-derived counterparts at the same total aromatic content. This can be attributed to the higher densities of the oil-sands-derived fuels. However, this trend was not clear at each individual engine operating mode.
- Different fuel properties influence NO_x and PM emissions at different engine operating conditions. Fuel density and total aromatic content influence NO_x emissions at medium to heavy load conditions, whereas the effects of fuel density and total aromatic content on PM emissions appear to be greater at low load conditions. It is therefore important to investigate the interaction between fuel properties and engine operating conditions.

ACKNOWLEDGEMENTS

We thank Mr. W. L. Chippior for his assistance in obtaining engine experimental data. Funding of the study has been provided by National Research Council Canada, Program for Energy Research and Development, Shell Canada Ltd., Syncrude Canada Ltd. and Imperial Oil Ltd. The majority of the test fuels were blended by Shell. The fuel properties were analyzed by NRC, Syncrude, Shell and National Centre for Upgrading Technology. We acknowledge Ken Mitchell, Jean Cooley, Keith Richardson, Maya Veljkovic and Craig Fairbridge for their valuable comments.

REFERENCES

- [1] Li, X., Chippior, W. L. and Gülder, Ö. L., "Effects of Fuel Properties on Exhaust Emissions of a Single Cylinder DI Diesel Engine", 1996 SAE Transactions, Paper No. 962116, 1996.
- [2] Li, X., Chippior, W. L. and Gülder, Ö. L., "Effects of Cetane Enhancing Additives and Ignition Quality on Diesel Engine Emissions", 1997 SAE Transactions, Paper No. 972968, 1997.
- [3] Cartellieri, W. P. and Herzog, P. L., "Swirl Supported or Quiescent Combustion for 1990's Heavy-Duty DI Diesel Engines - An Analysis", SAE Paper No. 880342, 1988.
- [4] Li, X. and Gülder, Ö. L., "Effects of Fuel Cetane Number, Density and Aromatic Content on Diesel Engine NO_x Emissions at Different Operating Conditions", Fourth International Symposium on Diagnostics and Modeling of Combustion in Internal Combustion Engines, July 20-23, Kyoto, Japan, 1998.
- [5] Li, X., Chippior, W. L. and Gülder, Ö. L., "Canadian Diesel Fuel Composition and Emissions - I", NRC Report No. 37645, 1997.

TABLE I AVL 8-MODE STEADY-STATE SIMULATION OF EPA TRANSIENT TEST PROCEDURE

Mode	Speed (rpm)	Load (%)	Weighting Factor
1	600	0	35.01
2	743	25	6.34
3	873	63	2.91
4	1016	84	3.34
5	1900	18	8.40
6	1835	40	10.45
7	1835	69	10.21
8	1757	95	7.34

TABLE II PROPERTIES OF BLENDED TEST FUELS

FUEL ID	Oil-sands-derived						Conventional-crude-oil-derived					
	S10A	S10B	S20A	S20B	S30A	S30B	C10A	C10B	C20A	C20B	C30A	C30B
Density	827.2	834.2	833.6	838.4	840.8	838.4	804.9	817.1	821.4	823.1	835.4	828.1
Viscosity	1.65	2.14	1.7	1.92	1.81	1.73	1.62	2.01	1.97	1.66	2.18	1.70
Cloud Point C	-44	-27	-26	-25	-28	-33	<-70	-27	3	-39	-10	-37
IBP, C	155.0	158.5	156.5	156.5	170.5	170.5	189.5	201.5	187.0	173.5	178.5	175.5
T10, C	175.5	183.0	181.0	179.0	185.0	186.5	200.0	207.5	191.0	194.0	198.5	198.5
T50, C	217.5	244.0	224.0	232.0	222.5	224.5	212.5	221.5	223.0	219.5	244.0	231.0
T90, C	286.0	317.0	284.5	323.5	324.0	301.5	242.0	285.5	335.0	272.0	317.0	268.0
EP, C	313.5	344.5	310.5	348.5	347.5	334.5	284.5	320.5	379.0	315.0	352.0	301.0
Cetane Index	41.0	46.8	40.9	41.8	37.9	39.5	47.4	46.1	45.0	43.2	46.5	45.1
Cetane No.	41.0	43.4	40.2	42.9	42.3	42.0	40.4	41.6	46.5	41.9	43.9	44.2
Sulphur, ppm	13.2	2.4	28.8	31.1	84.7	3.0	8.1	131	31.4	134.0	270.0	202.0
Hy. Cont. m%	13.75	13.73	13.49	13.42	13.08	13.16	14.18	14.13	13.72	13.68	13.28	13.40
Nitrogen, ppm	27.9	0.3	56.4	1.5	24.8	2.5	1.0	17.5	4.7	19.7	41.2	21.8
Total arom. %	12.4	12.9	20.2	23.5	30.0	31.4	10.8	11.0	20.7	20.2	30.0	29.8
1-Ring	10.9	9.5	17.9	2.02	25.2	27.4	9.6	7.8	16.0	16.8	22.1	25.1
2-Ring	1.5	2.9	2.2	2.7	4.3	3.6	1.1	2.9	4.3	3.2	7.1	4.4
3+-Ring	0.0	0.5	0.1	0.5	0.6	0.3	0.1	0.3	0.3	0.3	0.8	0.3

TABLE III PROPERTIES OF OTHER FUELS

FUEL ID	Ref1	Ref2	Ref3	A	C	E	F
Source	Conven.	Conven.	Conven.	Both	Both	Both	Both
Density	836.2	835.0	842.0	829.7	841.0	836.8	857.3
Viscosity	2.135	2.207	4.03	1.752	1.723	1.439	2.464
Cloud Point C	-22	-19	-6				
IBP, C	178.5	172.9	175.5	166	170	170	170
T10, C	205.6	198.9	244.8	183	185	183	189
T50, C	245.5	255.9	297.8	220	224	209	245
T90, C	306.1	311.4	333.8	284	284	251	344
EP, C	343.3	336.7	352.6	317	313	282	378
Cetane Index	46.6	49.7	55.5	40.7	38.0	34.2	39.5
Cetane No.	43.9	46.2	55.4	45.8	43.5	40.3	43.1
Sulphur, ppm	287.0	351.0	9.2	466	460	374	299
Hy. Cont. m%	13.38	13.37	13.95	13.78	13.28	13.29	13.19
Nitrogen, ppm	54.1	42.9	2.5				
Total arom. %	27.3	27.5	4.8	10.8	24.5	25.2	23.5
1-Ring	21.8	19.9	4.0	6.5	17.8	20.4	11.4
2-Ring	4.9	6.7	0.7	3.6	6.2	4.7	8.6
3+-Ring	0.5	1.0	0.1	0.7	0.5	0.1	3.6

TABLE IV REGRESSION ANALYSIS OF CORRECTED COMPOSITE EMISSIONS

Emission	Variables	Std. Error	Std. Coefficient	F-Value	Probability	R ²
NO _x	Density	0.0012	0.4559	14.31	0.0043	0.928
	Total Arom.	0.0016	0.5964	24.48	0.0008	
PM	Density	0.0004	0.7293	11.36	0.0071	0.532

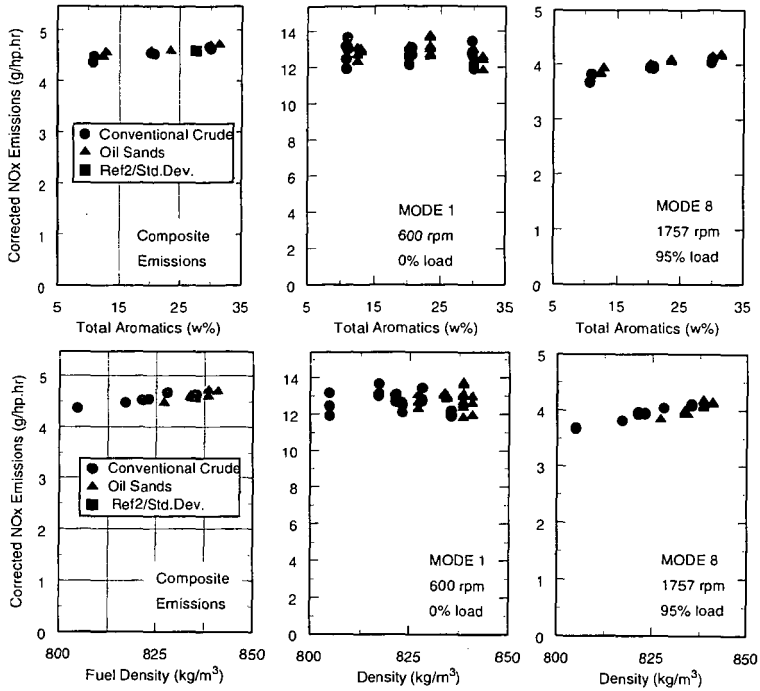


Figure 1 Corrected NO_x Emissions versus Total Aromatic Content and Fuel Density

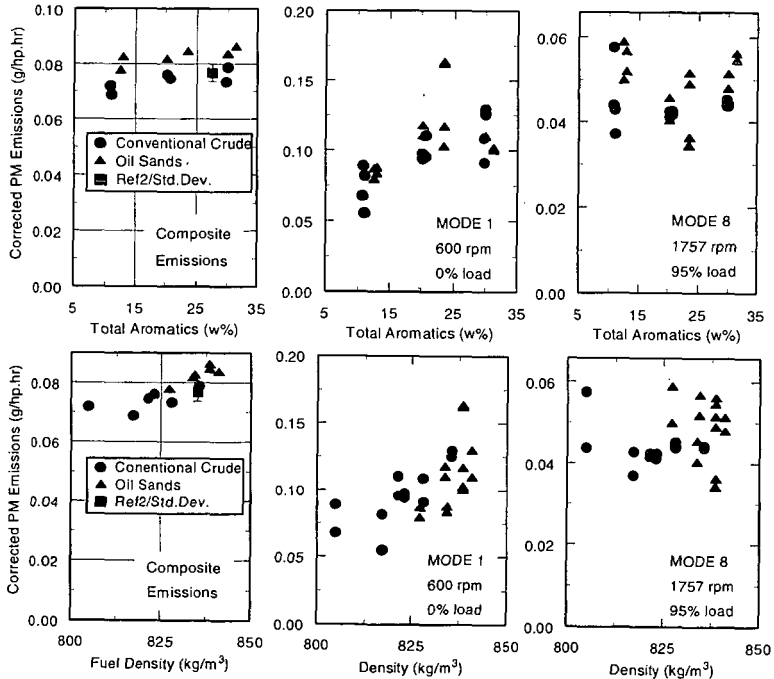


Figure 2 Corrected PM Emissions versus Total Aromatic Content and Fuel Density

THE SHENHUA DIRECT LIQUEFACTION PLANT

Alfred G. Comolli, Theo L.K. Lee, Gabriel A. Popper, Robert H. Stalzer,
And Peizheng Zhou (Project Manager)
Hydrocarbon Technologies, Inc. (HTI)
1501 New York Avenue
Lawrenceville, NJ 08648

INTRODUCTION

On September 22, 1997, Hydrocarbon Technologies Inc. (HTI) signed an agreement with Shenhua Clean Coal Technology Development Company, Ltd. (SCCT) and China Coal Research Institute (CCRI) on the feasibility study for a Direct Coal Liquefaction plant in China, one major project in China's ninth five-year plan. China is the world's largest hard coal producer and possesses huge reserves in trillions of tons of all types of coal and, although China also ranks as about the eighth largest worldwide producer of oil, it is now a net importer. This is due to its expanding economy and 1 billion plus population. Consequently, the cost-effective use of coal for transportation fuels in an environmentally-friendly manner is justified for China.

The project is to build a mine-mouth liquefaction plant using coals produced in the Shenhua coalfield in Northern Shaanxi Province and Inner Mongolia near Baotou City. Shenhua coalfield, previously known as Shenmu coalfield, is the largest developing coalfield in China and the eighth largest deposit of coal in the world, with coal mines owned and operated by Shenhua Group Corporation, Ltd., the parent company of SCCT. China's State Planning Commission has selected Shenhua coal as a candidate for liquefaction on the basis of its abundant reserves, good quality, reasonable cost, and a strategic location. See *Figure 1*, Map of China.

According to the Agreement, the study includes two phases of work. Phase I is a preliminary feasibility study that involves a bench-scale continuous flow unit (CFU) test at HTI and a preliminary economic evaluation based on the test results and local economic data for the plant. Phase II will be a Process Development Unit (PDU)-scale testing and a more in-depth techno-economic analysis. Following Phase II, the detailed engineering design, procurement, and construction would commence on the \$1.5 billion China grassroots plant complex.

PROCESS

The HTI COAL™ Process consists primarily of two backmixed reactor stages utilizing a proprietary dispersed superfine, iron catalyst (GelCat™) and fixed bed in-line hydrotreating. Operations are in the resid extinction mode, whereby unconverted residuum is recycled or used for hydrogen production, and a 750°F minus refined product is produced. A low/high reactor temperature staging that promotes hydrogenation and improves solvent quality is practiced. The process operates under a pressure of 17 MPa.

A slurry of pulverized coal in recycled, heavy coal-derived oil is premixed and pumped through a preheater along with hydrogen and catalyst into the first stage reactor. The effluent from the first stage undergoes separation to remove gases and light ends with the heavier liquid stream flowing to the higher temperature second stage. Effluent from the second stage, joined with overhead from the interstage separator, flows to the fixed bed in-line hydrotreater for enhanced upgrading to very clean fuels. The effluent from the hydrotreater is the major liquefaction product, mostly diesel, naphtha, and a jet fuel fraction. Bottoms product from the second-stage separator is flashed, and the overheads are pumped to the in-line hydrotreater for upgrading. The atmospheric bottoms stream containing solids is used as recycle with a portion going to a vacuum still and to solvent solids separation, with the resulting bottoms going to partial oxidation and the overheads to recycle. A condensed flow diagram is shown in *Figure 2*.

PROGRAM

The overall program consists of two stages. Stage 1 comprises the agreement to conduct a feasibility study and technical assessment of the HTI technology applied to Shenhua coal. Stage 2 is the financing, design, and construction phase of the project. Further detail is provided in *Figure 3*, Pioneer Plant Project Task and Schedule.

Phase I of Stage 1 has been successfully completed and reported to China. Results as discussed further were very encouraging; higher than predicted yields of clean distillate fuels were produced projecting improved economics.

Planning for Phase II is now underway with coal being readied for shipment to HTI from the new mine-mouth plant site. A 5 ton/day 30-day Process Development Unit run is scheduled for July of this year to provide scale-up data and products for evaluation and to prove the concept.

Ford Motor Company has included data from HTI's Direct Liquefaction into a Fuel Life Cycle Analysis for China, and an engineering relationship is being established with ABB Lummus Global, Inc. of New Jersey. The US Department of Energy is providing support and guidance for the project work at HTI. China is providing technical assistance, coal preparation, and the end use evaluation. China has also indicated a willingness to the containment and control of CO₂ and other emissions. A project schedule is shown in *Figure 3*.

DEVELOPMENTS

Samples of two major Shenhua Coal seams were selected and shipped to HTI for Continuous Flow Unit (50 Kg/day) CFU testing using HTI's COAL™ Process. See *Figure 2*. Data from this run was then used to conduct a pre-feasibility study using Chinese economic data. The coal analysis, as shown in *Table 1*, classifies the coal as a low ash, high volatile bituminous coal.

A CFU run of 26 days was conducted to maximize distillate yield, quality, and selectivity. Test conditions for the two coal samples were selected based on batch experimental results previously obtained by CCRI and HTI. Variables studied were catalyst concentration, space velocity, and reaction temperatures.

Coal conversions for the entire run varied from 90 to 93 percent on moisture, ash free basis (maf) with an average of 91 percent for both coals. The C₄-524°C distillate and 524°C resid yields were higher than projected by batch experiments. Distillate yields varied between 52 to 68 percent maf, and 824°C⁺ residuum yields varied between 7 to 22 percent maf. The Shenhua #2 seam coal gave lower distillate yields at 54 to 63W percent maf. Distillate selectivity, naphtha (IBP-177°C), middle distillate (177 to 343°C), and heavy distillate (343-524°C) varied with higher catalyst loading and recycle ratio. At the highest yield condition, there was 15 percent naphtha, 55 percent middle distillate, and 30 percent heavy distillate. *Figure 4* illustrates the varying selectivity at each run condition. For China, the mid-distillate for diesel fuel is preferred.

Hydrogen efficiency, distillate/hydrogen ratio, varied between 7.3 to 8.8 while consumption averaged 6.5 wt% maf. C₁-C₃ gas selectivity, gas/distillate ratio, varied between 0.18 to 0.22 with the lowest occurring at the highest distillate rates.

The total distillate product was subjected to a true boiling point distillation, and the fractions were characterized. The sulfur content of the medium naphtha (82-204°C) was 11 ppm, and the light naphtha (IBP-82°C) had a content less than 1.0 ppm. Since gasoline is made from these two coals, the sulfur levels far below specs for the US and China for the year 2000 (309 ppm and 1500 ppm, respectively). Also, the aromatic content at 3.11 percent and the olefin content at 1.4 percent are well under target for the US where aromatic is 22.0 percent and olefin is 4.0 percent, respectively. The light distillate cut (204-228°C) had a sulfur content of 475 ppm versus the China limit of 2000 ppm, while the freeze points are much lower than required.

Based on the overall distillate fraction properties, the gasoline (IBP-204°C) and diesel fuel (204-343°C) fractions most likely do not need to be further hydrotreated. Also, they can be a component in the refinery gasoline and diesel pools where the gasoline octane number and the diesel fuel cetane number can be met by blending with other refinery product streams.

The preliminary feasibility study envisions construction of a 12,000 metric ton per day coal liquefaction complex, complete and stand-alone with facilities for coal preparation, coal mixing, and liquefaction, hydrogen manufacture, and product upgrading to finished product gasoline and diesel fuels. Also included are by-product recovery, effluent handling and treatment, and utility generation except for power.

A coal liquefaction flow and block diagram are shown in *Figure 5* and *Figure 6*. As depicted in *Figure 6*, coal is received at the site from the coal mine, and is crushed, dried, and ground to size in the coal preparation plant. A portion of the coal is used in manufacturing hydrogen by partial oxidation, while the majority of coal is fed to the liquefaction plant. In the liquefaction facility, coal is reacted with hydrogen in the presence of a catalyst, to produce liquids, gases, and unconverted coal plus residual oil. Liquid products from coal liquefaction consist of a C₃ to 204°C naphtha fraction, a light distillate boiling in the 204 to 343°C range, and a heavy distillate boiling in the 343 to 524°C range. Naphtha is hydrotreated and then catalytically reformed to a

finished gasoline product. Light distillate is sent directly to diesel fuel product, and heavy distillate is mildly hydrotreated and sent to a fluid catalytic cracker (FCC) for conversion into gasoline and diesel fuel products.

Unconverted coal and residual oil, boiling above 524°C, are sent to the partial oxidation (POX) plant, along with some of the coal previously mentioned. The bulk of the hydrogen requirement of the complex is produced in this unit.

Gaseous and aqueous products from liquefaction and from product upgrading are handled separately and conventionally.

The 12,000 metric ton/day Pioneer Plant is based on three train two-reactor systems using 33.3 percent equity with long term (10 years) debt at 10.53 percent interest, 20-year plant life, and China raw material and product prices and tax structures. The model calculates the financial net present value (FNPV), defined as the sum of the annual cash flows discounted yearly at 12 percent, compounded over the life of the project. Factors were applied to US Gulf Coast Construction prices for labor and construction costs in China, and a 15 percent contingency was added for the total constructed units including fee. Salvage value was taken as zero.

The total plant cost was estimated to be 12,576 MM RMB, or US \$1.52 billion, with annual revenues and operating costs of 6,599 MM RMB (US \$796 million) per year and 5,297 MM RMB (US \$639 million), respectively. The net cash flow before taxes was estimated to be 1,302 MM RMB (US \$157 million) per year.

Rates of return and FNPV, before and after China taxes, are:

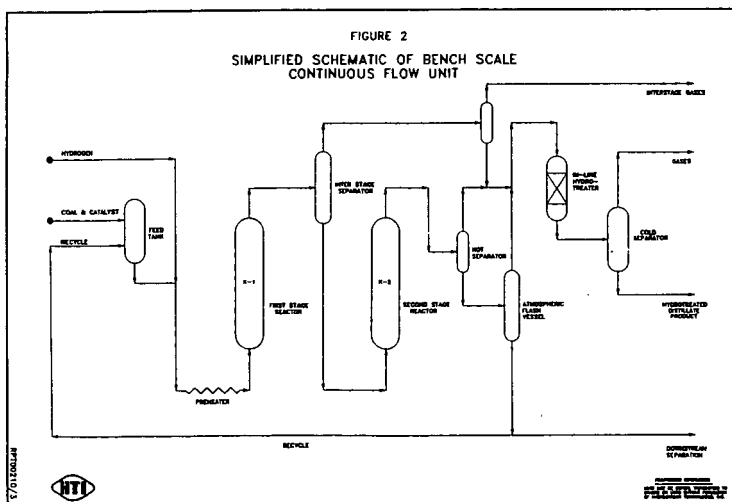
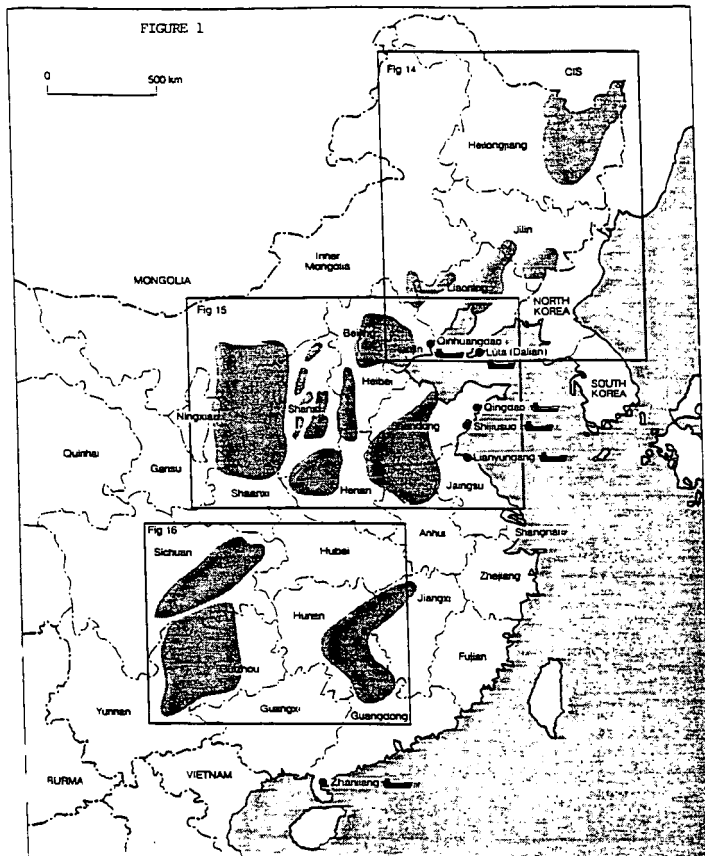
	<i>Before Tax</i>	<i>After Tax</i>
Rate of Return, %	23.3	18.5
FNPV @ 12%, MM RMB	4,524	2,282

CONCLUSIONS

Specific conclusions of the study are:

- With HTI's advanced liquefaction technology, GelCat™ catalyst, and at proven reactor operating conditions, both Shenhua #2 and Shenhua #3 coals can be processed in excess of 92 percent coal conversion to produce C₄-524°C distillate yields in the range of 63 – 68 W% maf coal. This could be processed with liquid product qualities comparable to those obtained with US coals.
- The products from coal liquefaction should meet or exceed SINOPEC Standards for gasoline and diesel fuel products, using commercially-proven refinery techniques for product upgrading.
- A site has been chosen for a commercial coal liquefaction venture near Baotou City, Inner Mongolia, close to the coal mine and conveniently located for access to railway and highway transportation of the raw materials and products.
- Using liquefaction yields demonstrated with Shenhua #3 coal, a conceptual process design for a commercial standalone grassroots facility has been completed for a coal feed rate of 12,000 MT/D. The facility would produce 3,073 MT/D of gasoline and 18 MT/D ammonia and 53 MT/D sulfur.
- The economics of a commercial coal liquefaction plant are promising, showing an 18.5 percent discounted-cash-flow rate of return, with 33.3 percent equity financing and a 10-year debt carrying an interest rate of 10.5 percent.
- Economics are improved by decreasing the investment cost and the coal price, extending the operating life, by being exempt of state and local taxes, and by increasing the selling price of the gasoline and diesel fuel products.
- Use of natural gas to make hydrogen is less preferable than use of coal, at the prices expected in China.
- Proper management of air, water, and solid waste qualities will permit existing and anticipated environmental standards to be met and exceeded.

Acknowledgments: CCRI, China Coal Research Institute, Shenhua Coal Company, United States Department of Energy, and Hydrocarbon Technologies, Inc. (HTI)



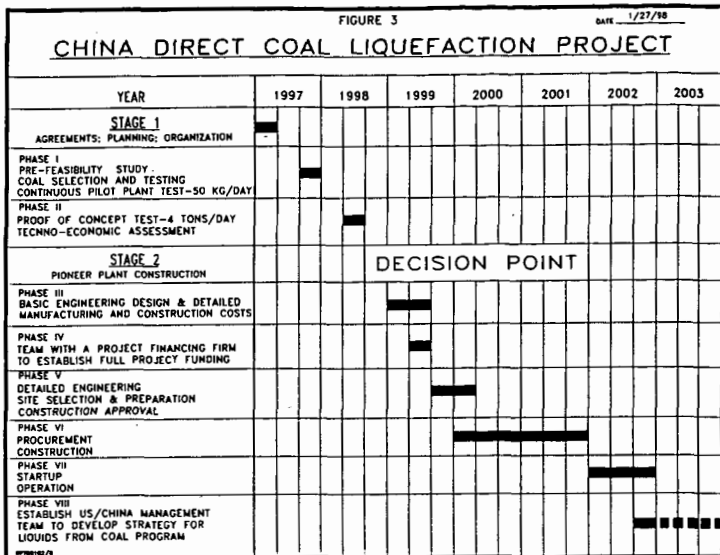
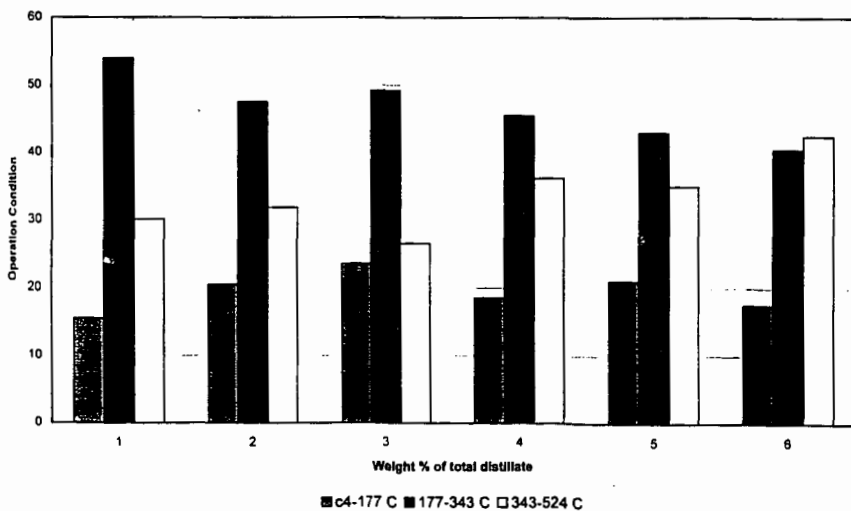


TABLE 1
ANALYSIS OF SHENHUA COALS

Seam Number	Proximate Analysis			Ultimate Analysis						
	Fixed Carbon	Volatile Matter	Ash	Carbon	Hydrogen	Nitrogen	Sulfur	Oxygen	Ash	H/C Atomic Ratio
2	57.95	35.84	6.21	75.87	4.24	0.98	0.42	12.28	6.21	0.67
3	61.79	36.47	4.25	79.47	4.13	1.05	0.42	10.68	4.25	0.62

Figure 4: Distillate Selectivity



ESTER FUELS VIA NON-AQUEOUS
ENZYME-CATALYZED REACTIONS OF FATTY ACIDS

E.S. Olson, H. K. Singh, and M. Yagelowich
Universal Fuel Development Associates, Inc.
223 Circle Hills Drive, Grand Forks, ND 58201

ABSTRACT

The use of nonaqueous enzyme slurries for the production of fatty ester fuels from coal-derived alcohols and fatty acids was investigated. Phenolic tars from coal gasification wastes were fractionated and treated with ethylene oxide to convert them to an alcohol, and the intermediate alcohols were esterified with the fatty acids in a nonaqueous lipase system. Lipases in a variety of organic solvents were investigated for acylation of coal-derived alcohols. The two step process transformed the black poorly soluble phenolics to clean paraffin-soluble esters. Diesel testing demonstrated that the phenoxyethyl esters could be substituted for diesel fuels.

INTRODUCTION

The production of diesel fuels from vegetable oils by conversion of the triglyceride to a less viscous ester has been extensively investigated. Most of the focus has been on methyl and ethyl esters, because of the ease of preparation and the low cost of methanol. Coal-derived alcohols may represent another inexpensive alcohol source for forming the ester diesel fuel. Phenolic materials are produced in large amounts during coal conversion processing to coke, liquids, or synthesis gas. Coal gasification produces a crude phenol/cresol stream from extraction of the condensate water. At the Great Plains Gasification plant operated by Dakota Gasification Company, the Phenosolvan extraction process recovers about 97 million pounds per year of the crude phenolics (1). The phenolics can be esterified with acid chlorides and anhydrides, but not with the less expensive esters or acids.

Alcohols can be produced from coal liquefaction and gasification byproduct phenolics by reaction of the phenolic hydroxyl groups with epoxides to give phenoxyalkanols. The hydroxyethylated and hydroxypropylated phenolics undergo esterification reactions at the alcohol group with esters and acids that do not occur readily with the original phenolic group.

Non-aqueous enzyme systems can greatly facilitate many organic reactions, especially those that result in formation of esters and amides. We previously reported the application of non-aqueous enzyme slurries to the production of fatty ester fuels from coal-derived alcohols (2,3). Most of our earlier work utilized triglyceride substrates as the acyl source for transesterification or interesterification reactions of these alcohols. But some inexpensive fatty acids are available from sources such as tall soaps and wastes from vegetable oil processing.

In order to develop an economical process for production of alternative ester fuels, a study of lipase-catalyzed reactions of fatty acids was carried out in nonaqueous solvents. The goal of this work was to exploit the advantage that enzymes in nonaqueous solvents can offer by driving the equilibrium toward the ester products. This paper will discuss the conversion of phenolic materials from coal gasification byproduct streams to a diesel fuel by using enzyme-catalyzed esterification reactions.

EXPERIMENTAL

Hydroxyethylated phenolics

The hydroxyethylation of the Great Plains crude phenols with ethylene oxide or other reagents was previously discussed (2,3). The composition of the hydroxyethylated intermediate was determined to be as follows: 2-phenoxyethanol, 45%; 2-(2'-methylphenoxy)ethanol, 10%; 2-(3- and 4-methylphenoxy)ethanol, 23%; other alkylphenoxyethanols 22%.

Acylation of hydroxyethylated phenolics

Hydroxyethylated Great Plain phenols (0.300 g) were reacted with 0.600 g of oleic acid in a slurry containing 100 mg Amano PS-30 lipase in 15 ml of solvent at 65°C. The reaction was allowed to proceed for 20 hrs. The product mixture was centrifuged to separate the enzyme, and the reaction mixture was analyzed by GC.

RESULTS AND DISCUSSION

The crude phenolic stream from the Great Plains Gasification Plant was reacted with ethylene oxide to give a hydroxyethylated intermediate (2). The lipase-catalyzed esterification reaction of the hydroxyethylated phenolics with equimolar amounts of oleic acid (free acid form) was found to give a high yield of the oleate ester in hexane solvent. With the Amano PS-30 lipase, a conversion of 83% to oleate ester was achieved for both the phenoxyethanol and the methylphenoxyethanol components of the intermediate. The corresponding transesterification conversions obtained using triglyceride substrates (tripalmitin, canola oil) were 90-95% (3), but these transesterification reactions used an excess of the triglyceride to drive the reaction. The reaction of oleic acid was repeated on a large batch to verify the high yield of ester product. The same yield of ester was obtained.

The reaction of 2-phenoxyethanol (the major component of the hydroxyethylated phenolic mixture) with oleic acid was further investigated with Amano PS lipase and with porcine pancreatic lipase in various solvents to determine the role of the organic solvent in the reaction. Yields of the phenoxyethyl ester product from oleic acid utilizing Amano PS lipase as a slurry phase in various organic solvents are reported in Table 1. The high yield of ester in the nonpolar hydrocarbon solvents may be attributed to formation of reverse micelles of unreacted fatty acid that can trap the water byproduct so that the reverse reaction (hydrolysis) does not occur at a fast rate. The reverse micelles do not form in the polar solvents, and the water is miscible and able to participate in the hydrolysis (reverse) reaction. Thus, the esterification reaction can be effectively driven to high conversion only in a nonpolar solvent. An excess of the fatty acid could probably give even higher yields by driving the equilibrium to the right, but this was not investigated, since an excess of fatty acid is not desirable in the fuel product. An extra step might then be required for removal of unreacted fatty acid.

The high conversion found for toluene as the solvent contrast significantly with the results obtained earlier for the transesterification with triglyceride. In these earlier studies with canola oil, use of toluene as the solvent resulted in poor conversions to the ester. The low transesterification reactivity in toluene has not been adequately explained. Hexane is a good solvent for both esterification and transesterification, however.

An additional tactic for shifting the equilibrium and thereby increasing the conversion to ester is the removal of product water from the reaction by the addition of molecular sieves. Several attempts were made to increase the ester yields for the reaction of phenoxyethanol and hydroxyethylated Great Plains phenols by adding molecular sieves to the bacterial lipase slurry. These experiments gave low yields of ester, unfortunately. The molecular sieve may have efficiently absorbed the water byproduct and then effectively catalyzed the hydrolysis reaction, overcoming the enzyme-catalyzed esterification. Also the molecular sieve may have removed the essential water associated with the enzyme protein, resulting in conformation changes that deactivated the enzyme.

The lipase-catalyzed reaction of the potassium salt (soap) of oleic acid was also investigated, since soaps are the form of tall acid byproduct obtained directly from the Kraft process. The reaction was carried out in chloroform. It was hoped that the metal ion would be carried along in the micellar form. The reaction gave no ester product, however. Possibly the carboxylate form of the acid was not acceptable at the lipase active site.

The direct esterification reaction of oleic acid with 2-phenoxyethanol was also investigated with porcine pancreatic lipase but poor yields (1-6%) of ester were obtained with this enzyme even in the nonpolar solvents. In contrast, good yields were obtained in earlier studies of transesterification with this lipase. The reason for the inactivity of the pancreatic enzyme in esterification reactions has not been determined. The esterification results with the Amano AK lipase obtained from a different *Pseudomonas* strain paralleled the lower rates found for this enzyme in other catalytic reactions.

Another set of experiments was carried out to determine the extent to which the lipases are deactivated by the gasification byproduct derivatives. The samples contain small amounts of soluble black materials that are not easily removed by distillation, adsorption, or solvent extraction. These are possibly condensation products of dihydroxybenzenes and indoles or other nitrogen heterocyclics. Accumulation of these impurities at the enzyme sites might be responsible for considerable shortening the lifetime of an enzyme catalyst bed. Earlier

experience with coals, humates, and low-severity liquefaction products from several coals showed that the lipases are substantially inhibited by many coal-derived materials (1).

The series of reactions carried out with recovered enzymes demonstrated that significant deactivation of the enzyme occurred. In a series of four reactions, the activity decreased by 20% in each successive reaction. The enzymes recovered from the fourth reaction were washed with acetone to determine whether substances that deactivated the enzyme could be removed by a more polar solvent or were instead bound reversibly. Reaction of the acetone-washed enzymes in the same system as above resulted in no ester formation initially. However, it was known from previous work that acetone removes essential water from the bacterial lipases, converting them to an inactive form. Thus, a small amount of water was added back to the enzymes which were then used for oleic acid esterification. The ester yield from the rehydrated or regenerated lipase was 25%, demonstrating partial restoration of the activity.

In previous studies with triglycerides, enzyme deactivation of the lipase was observed, but only to 3 to 10% of the original activity. Thus, there may be some kind of synergistic inhibitory effect involving the free fatty acid forms and the inhibitors present in the hydroxyethylated GP phenol intermediate.

Ester fuel prepared by acylation of hydroxyethylated GP phenols with canola oil exhibited a viscosity of 32.8 centipoise. This is substantially higher than that of sunflower methyl ester or #2 diesel oil. A 1:1 mixture of the ester product with #2 diesel gave acceptable viscosity (12.2 centipoise). Diesel tests with the mixture showed ignition delays (1.97 ms) that were slightly longer than the #2 diesel (1.84), but pressure curves were virtually identical.

CONCLUSIONS

Lipase-catalyzed reactions of inexpensive fatty acids with coal-derived alcohols in hydrocarbon solvents gave high yields of ester products. The high conversion of the acid form is very interesting, since it means that the very poorest grades of vegetable oils and the byproducts from their refining can be used in the preparation of esters. These oils contain high concentrations of the fatty acids. Raw tall oil from the Kraft pulping process also contains high concentrations of fatty acids. Much of the tall soap has no market and is mostly burned on site for heating the black liquor for recovering sulfide. Tall fatty acids are mainly oleic and linoleic acid.

The enzyme-deactivation results demonstrate that the impure hydroxyethylated phenolic streams cannot be effectively utilized without purification to remove the inhibitory compounds prior to the enzymatic reactions. Thus, the use of cleaner alcohols (from fermentation or Fischer-Tropsch) offer a better possibility for lipase-catalyzed fatty acid esterification. Alternatively, acid-catalyzed reactions in nonpolar solvents might give high enough yields of paraffin-soluble esters for use in diesel engines.

ACKNOWLEDGEMENTS

The support of the U.S. Department of Energy SBIR Contract # DE-AC02-88ER80614 is gratefully acknowledged.

REFERENCES

1. Sinor, J.E. *Production of Jet Fuels from Coal Derived Liquids Vol. 1*. 1987. Air Force Wright Aeronautical Lab Technical Report AFWAL-TR-87-2042, Vol. I. J.E. Sinor Consultants Inc.
2. Olson, E.S.; Singh, H.K.; Yagelowich, M.L.; Diehl, J.W.; Heintz, M.J.; Sharma, R.K.; Stanley, D.C. *Fuel*, **1993**, *73*, 1687.
3. Olson, E.S.; Singh, H.K.; Yagelowich, M.L. *Proceedings: First Biomass Conference of the Americas*, Vol. II, August 30, 1993, Burlington, VT, 837.
4. Kirchner, G.; Schollar, M.P.; Klibanov, A.M. *J. Amer. Chem. Soc.* **1985**, *107*, 7072.

Table 1. Yields of 2-phenoxyethyl oleate from Amano PS 30 lipase-catalyzed reaction of oleic acid with 2-phenoxyethanol (55°C for 24 hrs).

Test	Solvent	% Yield
1	Hexane	86
2	Toluene	86
3	Acetone	24
4	THF	0

TOXICOLOGY OF SYNTHETIC FUELS - A MINI REVIEW

Raymond Poon and Ih Chu
Bureau of Chemical Hazards,
Health Canada, Ottawa, Canada

Recent analytical and toxicological studies on synthetic fuels have confirmed previous observations that higher boiling fractions and blends are more toxic. It has also been reported that toxic effects of synfuels are related to the polycyclic aromatic hydrocarbon (PAH) content, including nitrogen containing and polar PAHs. Although carcinogenicity and mutagenicity are the main health concern of higher boiling synthetic fuels, the systemic toxicity (effects on liver, blood, bone marrow, thymus and thyroid) should not be overlooked. The marked thymic atrophy and perturbation of immune cells of PAH treated animals suggest that these fractions are immuno-suppressive. The lower-boiling fractions possess relatively weak carcinogenicity, mutagenicity and systemic toxicity, but their dermal irritant effects are still of concern in occupational settings. In the fractions and blends studied, the benzo(a)pyrene level is an indicator of their PAH content and hence toxicity. However, it is also clear that different composition of PAH mixtures in the high boiling fractions produce interactive effects that results in complex toxic and biochemical manifestations. The purpose of this article is to review recent mammalian toxicity data of various synfuels, and to shed some light on their potential human health hazards.

CARCINOGENICITY AND MUTAGENICITY

Early epidemiological studies showed that workers involving in the production of coal gas had a significantly higher rate of bladder and lung cancer (Doll et al., 1972), and those in the production of shale oils had a higher incidence of skin and scrotum cancer (Costello, 1979; Purde and Etlin, 1980). Reviews conducted by the International Agency for Research on Cancer concluded that shale oils were human carcinogen (IARC 1985), and exposure to "older" coal-gasification processes was carcinogenic to humans (IARC 1984). Workers in coal liquefaction plants were also reported to have a higher incidence of skin cancer (Shepard, 1981). A large body of evidence indicated that coal-derived synthetic fuels (Reilly and Renne, 1988; McKee et al., 1995; for review see Chu et al., 1994) and shale oils (Holland et al., 1981) were carcinogenic in animal studies and mutagenic in bacterial bioassays. In general, the middle and high boiling streams were more tumorigenic. More recent studies on coal coprocessing products and bitumen derived products also indicated that the middle and high-boiling fractions were more mutagenic (Table 1) (Otson and Peake, 1993).

SUBCHRONIC TOXICITY

Although carcinogenicity and mutagenicity are the main health concern of high-boiling synthetic fuels, their subchronic toxicity data are also required for health risk assessment. Table 2 summarizes the data from animal studies that provide no-observed-adverse-effect levels (NOAELs) for the fuels tested. It can be seen that the major target organs are liver, blood, bone marrow, thymus and thyroid. The effects on hematological disorders, and on the liver, consisting principally of hepatomegaly and microsomal enzyme induction were reported (Chu et al., 1988, 1992, 1994; Poon et al., 1994, 1996). The higher boiling fractions were more toxic and had NOAELs of less than 8 mg/kg/day. In contrast, petroleum derived unleaded gasoline and Fuel Oil no. 1 were less toxic, with NOAELs of greater than 250 mg/kg/day (Table 2).

EFFECTS ON THE SKIN

While the lowest boiling distillates showed the weakest tumor induction and systemic effects, they were shown to be a strong skin irritant. For example, shale-oil derived distillates, jet fuels (Holland et al., 1981; ATSDR, 1995), and the light gas oil fraction of bitumen upgrading products (Poon et al., 1994) produced severe skin lesions in rats. Feuston (1994) suggested that the skin irritation was associated with 2-ring aromatics, which were found to be most abundant in the low-boiling fractions. Chemical-induced skin phototoxicity appears to be a major concern for high-boiling distillates and bottom fractions. McKee and Maibach (1985) reported that EDS liquids with boiling points above 200°C produced skin phototoxic effects in guinea pigs. In a survey of workers at a pilot coal liquefaction plant, Driscoll et al., (1995) noted that self-reported photosensitivity reactions were strongly associated with dermal exposure to the solvents containing bottom fractions of coal liquids. Paint that contained bitumen was considered to be the cause of an outbreak of skin phototoxicity and ocular symptoms in workers in a dockyard (Davies, 1996). Coal tar and its products have been known to cause photosensitive skin reactions (Gould et al., 1995). PAHs in coal tar and bitumens, such as acridine, pyrene, and phenanthrene were reported to be potent phototoxins (Gendimenico and Kochevar, 1984; Davies, 1996). These compounds are also present in the high-boiling fractions

(Table 1).

EFFECTS ON IMMUNE FUNCTIONS

Studies with laboratory animals showed that high-boiling coal liquefaction products (Springer et al., 1986), high-boiling coal co-processing products, and medium- and high-boiling bitumen upgrading products (Chu et al., 1992; Poon et al., 1994) produced thymic atrophy. Because the thymus is an essential organ for the normal development of immunological functions in early life, these observations suggest that treatment with higher-boiling fuels may compromise the immune system. In contrast to a paucity of immunotoxicity data on synthetic fuels, these effects of PAHs were well documented (reviewed in Ward et al., 1985; Davila et al., 1997). In addition to benzo(a)pyrene, other PAHs such as phenanthrene and fluoranthene, which are widely present in synthetic fuels, were also found to have immunosuppressive effects (Davila et al., 1996; Yamaguchi et al., 1996; Tsien et al., 1997). Recent surveys of coke-oven workers exposed to PAHs revealed significant changes in their immune functions (Szczeklik et al., 1994; Winker et al., 1996).

COMPLEX MIXTURES

It is generally accepted that the toxicities of higher boiling synthetic fuels are predominantly related to their high PAH level, and the benzo[a]pyrene content is often used as an indicator of the total PAHs in synfuels (Table 3). However, it would be an oversimplification to solely rely on the benzo[a]pyrene level as the predictor of toxicity because different fuels have different PAH compositions, and various chemicals in the mixtures may exert individual and interactive effects. For example, individual PAHs were reported to exert an interactive effect on the mutagenicity of the other hydrocarbon components coexisted in the mixtures (Hermann, 1981). Neutral PAHs were associated with skin carcinogenicity while nitroaromatic and other polar aromatic compounds appeared to be potent mutagen (Otson and Peake, 1993; McKee et al., 1995). Hydrotreatment is known to substantially reduce the carcinogenicity, mutagenicity and acute toxicity of various synthetic fuels (Holland et al., 1981; McKee and Lewis 1987). However, detail studies on the effect of hydrotreatment on the PAH composition are still lacking.

SUMMARY

Prolonged exposure to synthetic fuels produces a broad range of systemic effects which include carcinogenicity, growth suppression, biochemical changes, anemia and other hematological disorders. Bone marrow, liver, kidney, thymus and skin are target organs affected by treatment. The effects are more severe with heavy distillates, and distillates containing N-PAHs are more biologically active. Although there is limited information on the occupational effects of synthetic fuels, experience in the health effects of workers in petroleum industry and coke-oven operations can serve as a guide in the implementation of industrial hygiene programs for synthetic fuel operations. These include engineering controls, personal monitoring, hygiene practices and medical surveillance.

REFERENCES

- ATSDR. Agency for Toxic Substances and Disease Registry. Toxicological Profile for "Jet Fuels (JP4 and JP7)". 1995, U.S. Department of Health and Human Services. Atlanta, Georgia.
- Beck, L.S., Hepler, D.I., and Hansen, K.L., 1983, The acute toxicology of selected petroleum hydrocarbons. In: MacFarland H.N., Holdsworth, L.E., MacGregor J.A., et al., eds. Proceedings on the 1st Symposium on the toxicology of petroleum hydrocarbons. Washington, DC: American Petroleum Institute. May 1982. 1-12.
- Chu, I., Villeneuve, D.C., Cote, M., Secours, V., Otson, R., and Valli, V.E., J. Toxicol. Environ. Health. 25:509-525, 1988.
- Chu, I., Suzuki, C.A.M., Villeneuve, D.C., and Valli, V.E., Fundam. Appl. Toxicol. 19:246-257, 1992.
- Chu, I., Villeneuve, D.C., and Rousseaux, C.G., J. Appl. Toxicol. 14: 241-256, 1994.
- Costello, J., Environ. Health Perspect. 30:205-208, 1979.
- Cruzan, G., Low, L.K., Cox, G.E., Meeks, J.R., Mackerer, C.R., Craig, P.H., Singer, E.J., and Mehlman, M.A., Toxicol. Ind. Health. 2:429-444, 1986.

- Davies, M.G., Cont. *Dermatitis*. 35:188-189, 1996.
- Davila, D.R., Romero, D.L., and Burchiel, S.W., *Toxicol. Appl. Pharmacol.* 139: 333-341, 1996.
- Davila, D.R., Mounho, B.J., And Burchiel, S.W., *Toxicol Ecotoxicol. News/Review*. 4:5-9, 1997.
- Doll, R., Vessey, M.P., Beasley, R.W.R., Buckley, A.R., Fear, E.C., Fisher, R.E.W., Gammon, E.J., Gunn, W., Hughes, G.O., Lee, K., and Norman-Smith, B., *Br. J. Med.* 29:394-406, 1972.
- Driscoll, T., Mandryk, J., Corvalan, C., Nurminen, M., Hull, B., Rogers, A., Yeung, P., Hollo, C., Ruck, E., and Leigh, J. *Occup. Med.* 45:239-246, 1995.
- Feuston, M.H., Low, L.K., Hamilton, C.E., and Mackerer, C.R., *Fund. Appl. Toxicol.* 22:622-630, 1994.
- Gendimenico, G.J., and Kochevar, I.E., *Toxicol. Appl. Pharmacol.* 76: 374-382, 1984.
- Gould, J.W., Mercurio, M.G., and Elmets, C.A., *J. Am Acad. Dermatol.* 33:551-573, 1995.
- Griest, W.H., Guerin, M.R., Yeatts, L.B., and Clark, B.R. 1981. Sample management and chemical characterization of the PARAHO/SOHIO/U.S. Navy crude and refined shale oil suite. In: Griest W.H., Guerin, M.R., and Coffin, D.L. eds. *Health Effects Investigation of Oil Shale Development*. Ann Arbor Science, Ann Arbor, Michigan. 1981. P. 27-44.
- Hermann, M., *Mut. Res.* 90:399-409, 1981.
- Holland, J.M., Gibson, L.C., Whittaker, M.J., and Stephens, T.J. 1981. Chronic dermal toxicity of Paraho shale oil and distillates. In: Griest, W.H., Guerin, M.R., Coffin, D.L. (Eds): *Health Effects Investigation of Oil Shale Development*. Ann Arbor Science, Ann Arbor, Michigan, pp 97-116.
- IARC 1984. International Agency for Research on Cancer Monograph no. 34. Polynuclear Aromatic Compounds, Part 3, Industrial exposures. World Health Organization. Lyon, France.
- IARC 1985. International Agency for Research on Cancer Monograph no. 35. Polynuclear Aromatic Compounds, Part 4, Bitumens, Coal-tars and Derived Products, Shale-oils and Soots. World Health Organization. Lyon, France.
- McKee R.H., and Maibach, H.I., *Cont. Dermatitis*. 13:72-79, 1985.
- McKee, R.H., and Lewis, S.C., *Can. J. Physiol. Pharmacol.* 65:1793-1797, 1987.
- McKee, R.H., Traul, K.A., and Przygoda, R.T., *J. Appl. Toxicol.* 15: 159-165, 1995.
- NTP. 1986. National toxicological program technical report series no. 310: Toxicology and carcinogenesis studies of marine diesel fuels and JP-5 navy fuel in B6C3F1 mice (dermal studies). Research Triangle Park, NC: National Toxicology Program/National Institute of Health. NIH publication no. 86-2566.
- Otson, R., and Peake, E. 1993. Characterization of bitumen upgrading and coprocessing products. In: P. Garrigues and M. Lamotte (eds.), *Polycyclic Aromatic Compounds. Synthesis, Properties, Analytical Measurements, Occurrence and Biological Effects*. PAH XIII, Gordon and Breach, Langhorn, PA.
- Peake, E. 1990. Characterization of coal coprocessing products. The toxicology of heavy distillates. A final report to the Health Protection Branch, Department of National Health and Welfare, Ottawa, Canada.
- Poon, R., Chu, I., Villeneuve, D.C., and Valli, V.E., *Fundam. Appl. Toxicol.* 23:237-250, 1994.
- Poon, R., Chu, I., Davis, H., Yagminas, A.P. and Valli, V.E., *Toxicology*. 109:129-146, 1996.
- Purde, M., and Etlin, S. 1980. Cancer cases among workers in the Estonian oil shale processing industry. In: Rom, W.N. and Archer, V.E.(eds.) *Health Implications of New Energy Technologies*, Ann Arbor Science, Ann Arbor, Michigan, pp. 527-528.
- Rao, T.K., Allen, B.E., Ramsey, D.W., Epler, J.L., Rubin, B., Guerin, M.R., and Clark, B.R., *Mutat.*

Res. 84:29-39, 1981.

Reilly, C.A., and Renne, R.A. 1988. Toxicological effects of coal-based synfuels. In: Gray, R.H., Drucker, H., Massey, M.J. (eds.). *Toxicology of Coal Conversion Processing*. John Wiley & Sons, New York, p.57-245.

Shepard, H., *J. Soc. Occup. Med.* 31:9-15, 1981.

Szczeklik, A., Szczeklik, J., Galuszka, Z., Musial, J., Kolarzyk, E., and Targosz, D., *Environ. Health Perspect.* 102:302-304, 1994.

Springer, D.L., Miller, R.A., Weimer, W.C., Ragan, H.A., Buschbom, R.L., and Mahlum, D.D., *Toxicol. Appl. Pharmacol.* 82:112-131, 1986.

Tomkins, B.A., Kubota, H., Griest, W.H., Caton, J.E., Clark, B.R., and Guerin, M.R., *Anal. Chem.* 52:1331-1334, 1980.

Tomkins, B.A., Reagan, R.R., Caton, J.E., and Griest, W.H., *Anal. Chem.* 53:1213-1217, 1981.

Tsien, A., Diaz-Sanchez, D., Ma, J., and Saxon, A., *Toxicol. Appl. Pharmacol.* 142:256-263, 1997.

Ward, E.C., Murray, M.J., and Dean, J.H. 1985. Immunotoxicity of nonhalogenated polycyclic aromatic hydrocarbons. In: *immunotoxicology and immunopharmacology* (J.H. Dean, M. I. Luster, A.E. Munson and H. Amos, Eds.). pp. 291-300. Raven Press, New York.

Winker, N., Tuschl, H., Kovac, R., and Weber, E., *J. Appl. Toxicol.* 17:23-29, 1996.

Yamaguchi, K., Near, R., Shneider, A., Cui, H., Ju, S-T., and Sherr, D.H., *Toxicol. Appl. Pharmacol.* 139:144-152, 1996.

Table 1. Mutagenicity (Salmonella test) of synthetic fuels.

Material tested	Without S-9	With S-9	Reference
<u>Coal Liquefaction Products</u>			
Hydrotreated naphtha (<200°C)	NT	-	McKee et al., 1995
EDS ¹ process, RS-I (200-427°C)	NT	+	McKee et al., 1995
EDS process, RS-II (200-427°C)	NT	+	McKee et al., 1995
Pittsburgh Energy Technology Center	NT	+	Ran et al., 1995
COED pyrolysis process	NT	+	Rao et al., 1995
<u>Coal Coprocessing Products</u>			
CANMET LGO (< 243°C)	-	-	Otson and Peake, 1993
CANMET HGO I (243-409°C)	-	+	Otson and Peake, 1993
CANMET HGO II (387-521°C)	+	+	Otson and Peake, 1993
<u>Bitumen Upgrading Products</u>			
CANMET LGO (200-315°C)	-	-	Otson and Peake, 1993
CANMET HGO I (315-415°C)	-	+	Otson and Peake, 1993
CANMET HGO II (415-525°C)	+	+	Otson and Peake, 1993

¹Abbreviations: EDS, a direct liquefaction process that utilizes an "in stream" catalytic hydrotreatment process; RS, recycle solvent; COED, Char-oil Energy Development liquid; CANMET, Canadian Centre for Mineral and Energy Technology; LGO, light gas oil; HGO, Heavy gas oil; NT (Not tested)

Table 2. Systemic toxicity of synthetic fuels via percutaneous administration.

Synthetic fuel	Animal/Length of Exposure	Target organ	NOAEL ^a (mg/kg/day)	Reference
<u>Gasoline (unleaded)</u>	Rabbits/2 weeks	Liver, blood, skin	590	Beck et al., 1983
<u>Fuel oil No. 1</u>	Mice/13 weeks	Blood	250	NTP 1986
<u>Clarified slurry oil</u>	Rats/13 weeks	Liver, thymus, bone marrow	<8	Cruzan et al., 1986
<u>Coal liquefaction products</u>				
CANMET HGO-I (154-378°C)	Rats/13 weeks	Liver, blood, bone marrow	<50	Chu et al., 1988
<u>Coal coprocessing products</u>				
CANMET HGO-II (387-521°C)	Rats/13 weeks	Liver, blood, thymus, thyroid, bone marrow	<8	Chu et al., 1992
<u>Bitumen upgrading products</u>				
CANMET LGO (200-315°C)	Rats/4 weeks	Bone marrow, skin	25	Poon et al., 1994
CANMET HGO-I (315-415°C)	Rats/4 weeks	Liver, blood, bone marrow, thymus	<25	
CANMET HGO-II (415-525°C)	Rats/4 weeks	Liver, blood, bone marrow, thymus	<25	
CANMET HGO-II (415-525°C)	Rats/13 weeks	Liver, blood, bone marrow, thymus, thyroid	<8	Poon et al., 1996

^a NOAEL = no-observed-adverse-effect-level

Table 3. Benzo(a)pyrene content in petroleum and synthetic fuels.

Synthetic fuel	Benzo(a)pyrene (µg/g)	Reference
<u>Jet Fuel JP5 (from shale oil)</u>	ND ¹	Griest et al., 1981
<u>Petroleum (crude)</u>	2.8-3.7	IARC 1985
<u>Shale oil (SRM 1580 certified)</u>	3.3-192	IARC 1985
<u>Coal liquefaction products</u>		
Coal derived fuel oil	82	Tomkins et al., 1980
NBS Coal liquid oil	179	Tomkins et al., 1981
Coal-II heavy distillate, 288-454°C	550	Springer et al., 1986
<u>Coal coprocessing products</u>		
HGO I, 315-435°C	211	Otson and Peake, 1993; Peak, 1990
<u>Bitumen upgrading products</u>		
LGO, 200-315°C	6.5	Otson and Peake, 1993; Peak, 1990
HGO I, 315-415°C	23	
HGO II, 415-525°C	590	

¹ ND - non-detectable